



Master's Degree in Environmental Engineering

**HYDRODYNAMIC MODELING OF THE FINAL REACH OF
THE MISA RIVER (SENIGALLIA, ITALY): THE ROLE OF
SEA ACTION AND BED FORMS**

Advisor:
Prof. Matteo Postacchini

Student:
Marco Ilari

Co-advisor:
Prof. Giovanna Darvini

Co-advisor:
PhD. Eleonora Perugini

A.Y. 2020/2021

INDEX

ABSTRACT	1
1 INTRODUCTION	2
1.1 Estuaries	3
1.2 River bars	6
1.2.1 Bars classification.....	6
1.3 The Misa River site.....	12
2 MATERIALS AND METHODS.....	15
2.1 HEC-RAS model construction	15
2.1.1 Data from the Civil Protection of the Marche Region	16
2.1.2 Field-survey data.....	19
2.1.3 Hydrodynamic data.....	22
2.2 Model validation	27
3 MODEL RESULTS	35
3.1 Description of the modeled events.....	35
3.2 Field campaign data validation within the EsCoSed project	38
3.3 River mouth bar implementation and H-ADCP data analysis.....	51
3.3.1 2019 events	63
3.3.2 2020 events	83
4 CONCLUSIONS	100
5 REFERENCES	101
6 ACKNOWLEDGMENTS.....	104

ABSTRACT

The work carried out within the framework of this thesis deals with the hydrodynamic modeling regarding the final stretch of the Misa River (Senigallia, Italy) using the HEC-RAS software with particular emphasis on the effect brought by the tidal action and some riverbed forms existing at the estuary. Initially, a characterization of the estuarine environments is performed, focusing successively on the description of the Misa River microtidal estuary. This is defined as a salt-wedge estuary marked by an upper freshwater layer that overrides the denser marine saltwater layer without mixing one another. Afterwards, an overall picture on the river bars is presented. Specifically, the river-mouth bars are taken into account given that an emerged bar intermittently shows up and moves close to the Misa River mouth, depending on the river discharge, tides and sea waves. Then, following a brief overview of the Misa River site, which is featured by a marked torrential regime, data from Marche Region Civil Protection, field surveys and hydrodynamic data regarding the final reach of the river are used with the aim of making unsteady simulations of the final reach of the Misa River extending for about 10km. The HEC-RAS modeling makes use of the data collected by two hydrometers (property of the Civil Protection), a river gauge (installed within the framework of the international MORSE project) and several surveys of the river bed. After the model calibration (carried out in a companion thesis work), unsteady simulations of events recorded in 2014, 2019, 2020 and 2021 are performed, with the main purpose of understanding the tide effect along the investigated river reach and the influence of the river-mouth bar on the water elevation along the river during different flow regimes.

1 INTRODUCTION

The impact of tides and bed forms on the hydrodynamics existing in the final reach of the Misa River (Senigallia, Marche Region, Italy) is studied in the present thesis through numerical simulations. The Misa River estuary is a microtidal environment, i.e., with a tidal excursion of less than 60 cm, and has been recently studied with the aim of figuring out river-sea interactions, from which it emerged that river action overwhelms the marine one especially during storms (Brocchini et al., 2017).

Estuarine environments are strongly dynamic regions, where hydrological and morphological processes occur simultaneously and affect one another. The sediment transport and related morphodynamics associated with such processes lead sometimes to the generation of interesting features, like river mouth bars, whose shape and size can vary over time depending on the incoming river discharge and sea waves. River mouth bars, like the one recurring in correspondence of the Misa River mouth, may lead the river flow to shift from subcritical (slow flow) to supercritical (fast flow) conditions passing through the critical state.

The current work thus analyzes the upriver propagation of the tidal constituents, also focusing on the role played by the mouth bar in such propagation. The thesis also compares the numerical results (with and without the mouth bar) with the in-situ measurements collected by a river gauge, located about 1.2 km from the Misa River mouth. A further comparison is that between the modeled river stage and the water-surface levels recorded by two pressure sensors during a field campaign dating back to January 2014, which was part of an international project.

1.1 Estuaries

In coastal environments, two types of river mouth, depending on the way the river flows into the sea, exist, i.e., river estuary and river delta. Focusing on the former classification, “an estuary is a partially enclosed coastal body of water that is either permanently or periodically open to the sea and which receives at least periodic discharge from a river(s), and thus, while its salinity is typically less than that of natural sea water and varies temporally and along its length, it can become hypersaline in regions when evaporative water loss is high and freshwater and tidal inputs are negligible” (Potter *et al.*, 2010). Figure 1 shows an example of an estuary, i.e., the Arno River estuary in this case.



Figure 1. The Arno River estuary top view

Estuarine environments are dynamically complex, with the hydrodynamics being triggered by many factors, e.g., nonlinear interactions between the bathymetry, the river current and many sea forcing actions. The sediment transport and related morphodynamics derive from such complexity and act in the estuarine region by shaping the riverbed and sometimes leading to interesting morphological features, like river mouth bars that after being generated, migrate, and evolve in proximity of the river mouth.

A classification of the estuaries can be made according to the water circulation, thus including:

- Salt-wedge estuaries
- Partially mixed estuaries
- Well-mixed estuaries
- Inverse estuaries
- Intermittent estuaries

For what concerns the salt wedge estuaries, river output greatly exceeds marine input and tidal effects have minor importance. Freshwater floats on top of the seawater in a layer that gradually thins as it moves seaward, whereas the denser seawater moves landward along the bottom of the estuary, thus forming a wedge-shaped layer that is thinner as it approaches land. As a velocity difference develops between the two layers, shear forces generate internal waves at the interface, mixing the seawater upward with the freshwater.

Partially mixed estuaries occur when the tidal forcing increases, hence the river output becomes less than the marine input. Therefore, the current turbulence causes the mixing of the whole water column such that the salinity varies more longitudinally rather than vertically, leading to a moderately stratified condition.

Well-mixed estuaries stand for river mouths where the tidal mixing forces exceed river output, resulting in a well-mixed water column and the disappearance of the vertical salinity gradient. The freshwater-seawater boundary is eliminated due to the intense turbulent mixing and eddy effects. Inverse estuaries occur in dry climates where evaporation greatly exceeds the inflow of freshwater. As a result, a salinity maximum zone is formed, and both riverine and oceanic water flow close to the surface towards this zone. This water is pushed downward and spreads along the bottom in both seaward and landward direction.

Intermittent estuaries change dramatically depending on freshwater input and are capable of changing from a wholly marine environment to any of the other estuary types.

Further, estuaries can be split out depending on the tidal range extent: in particular, micro-tidal (less than 2m), meso-tidal (between 2m and 4m), and macro-tidal (higher than 4m) may occur. Considering the latter, in Mediterranean climates, micro-tidal estuaries generally have narrow mouths, are poorly flushed and have relatively long water residence times, i.e., typically weeks to months, whereas macrotidal estuaries are generally funnel-shaped and well-flushed, with relatively short residence times, i.e., typically hours to days (*Uncles et al., 2002; Tweedley et al., 2016b*). In some microtidal estuaries, highly seasonal and/or low rainfall results in a sand bar forming at the

mouth of the estuary, which prevents the exchange of water with the ocean and further increases the residence time (*Ranasinghe and Pattiaratchi, 1998; Chuwen et al., 2009*). Such microtidal estuaries, having long residence times, are intrinsically less robust than better flushed estuaries, because they facilitate the accumulation of contaminants. Furthermore, even when there are no anthropogenic inputs, naturally-occurring dissolved and particulate organic materials from terrestrial sources accumulate in these systems and this can lead to a marked depletion in dissolved oxygen (*Nixon et al., 1996; Wolanski, 2007*). While the water column in macrotidal estuaries is well- or, at least, partially-mixed, driven by tidal action, microtidal estuaries are typically highly stratified, with little or no mixing between the fresh water on the surface and the salt water below (*Dyer, 1997*). Strong salinity stratification encourages high rates of sediment deposition (*Traykovski et al., 2004; Ralston et al., 2012*), thus enhancing nutrient recycling (*Hopkinson et al., 1999; Watanabe et al., 2014*).

Microtidal estuaries are likely to be more susceptible to the climate change effects, the longer-term effects of which are obvious and already manifesting themselves, while their causes are not being adequately addressed at a global scale. The estuaries of south-western Australia, for example, have been subjected to sustained warming and drying (*Hope et al., 2015; Hallett et al., 2018*). The ~15% decline in rainfall, which has occurred in south-western Australia since the mid-1970s, has led to a 70% reduction in runoff into reservoirs (*Petrone et al., 2010; McFarlane et al., 2012*). Similarly, the average annual freshwater flow into the Coorong in South Australia has been reduced by about 70% over recent decades and is highly variable (*Kingsford et al., 2011; Leblanc et al., 2012*). Decreased river flows resulted in an increase in residence time and the frequency of mouth closure, thereby producing stressful hypoxic and hypersaline (with salt concentrations higher than 40 g/l) conditions, with the maximum salinity approaching 200 g/l recorded in coastal lagoons of the Coorong (Australia), thus providing an increase of fish mortality (*Wedderburn et al., 2016*). Sea level rise is another feature of climate change that will potentially impact on estuaries. Rising sea levels will increase the susceptibility of estuaries to coastal flooding associated with extreme sea level and storm surge events (*Hallett et al., 2018*). Climate change impacts on microtidal estuaries will be exacerbated by their synergistic effects in combination with the anthropogenic and natural environmental stresses to which they are currently subjected. For example, many pollutants will exhibit increased toxicity at higher temperatures (*Ficke et al., 2007*), and decreasing rainfall will increase the concentration of nutrients arising from agricultural runoff.

1.2 River bars

Rivers are quite often characterized by bars, which are ridges of boulders, gravel, sand, and/or mud found along or in a stream channel at places where a decrease in flow velocity causes sediment deposition. The presence and dynamics of these deposits are at the heart of many river engineering problems, given that bars may block water intakes, hinder navigation, and reduce the water conveyance under bridges. Figure 2 exhibits the gravel bars under a bridge in a reach of the Tagliamento River (Italy).



Figure 2. Gravel bars under a bridge in the Tagliamento River (Italy)

Further, river bars are also associated with local scour and bank erosion, which can undermine bridge piers and hydraulic structures (e.g., groynes). Nevertheless, bars form important fluvial or riparian habitats, hence their restoration is a common objective in river rehabilitation projects.

1.2.1 Bars classification

River bars have horizontal sizes that scale with the width of the main river channel and heights that scale with the bankfull water depth.

River bars can be classified according to the location along the river where they may originate:

- Point bars (Figure 3a on the left)
- Central bars (Figure 3b on the right)
- Mouth bars (Figure 4)



Figure 3. a) Point bar inside a river bend (Rhine River, the Netherlands). b) Compound central bar forced by a local width expansion (Cauca River, Colombia).



Figure 4. Example of a river mouth bar

A point bar is an area of deposition typically originating on the inside of meander bends in meandering rivers. As the flow moves around the inside of the bend in the river, the water slows down because of the shallow flow and low shear stresses there reduce the amount of material that can be carried there. Point bars are usually crescent shaped and are typically found in the shallowest parts of rivers and streams, and are often parallel to the shore. At the deepest and fastest part of the stream there is the cut bank, the area of a meandering river channel that continuously undergoes erosion. The faster the water in a river channel, the better it is able to pick

up greater amounts of sediment, and larger pieces of sediment, which increases the river's bed load. Over a long enough period of time, the combination of deposition along point bars, and erosion along cut banks can lead to the formation of an oxbow lake.

A mid-channel bar (also referred to as a braid bar) is a river landform which originate from remnants of point bars or the growth of mid-channel unit bars in braided rivers. The latter is broad and shallow and are found in areas where sediment is easily eroded like at a glacial outwash. Braided rivers have complex and unpredictable channel patterns, and sediment size tends to vary among streams. It is these features that are responsible for the formation of braid bars. Braid bars are distinguished from point bars due to their presence in the middle of a flow channel, rather than along a bank of the river channel.

A mouth bar is an elevated region of sediment typically found out at a river delta. Sand deposits preferentially form near river mouths due to the high settling velocity of the river-discharged coarse sediment. Generally, river mouth bars are inaccessible most of the time, but when their subaerial portion is visible, they could be potentially visited. Further, as the gradual aggradation creates a portion of the river mouth bar that is not flooded by high tide, the river mouth bar evolves into an island, thus having the potential for farming, living, and engineering as shown in Figure 7. In river mouths characterized by shallow water (up to few meters), stratification effects are limited, and the river flow can be represented by a bounded, planar turbulent jet, which determines sediment particle flow paths and bed deposition patterns in front of the river mouth. Therefore, the evolving bed modifies the jet, giving rise to a coupled morphodynamic system.

Two important loci of deposition in the jet region exist, that are subaqueous levees that fringe the jet and river mouth bars (RMB, hereinafter) that form under the jet at some variable distance from the tip of the RMB. The RMBs take two end-member forms: a triangular "middle-ground" bar with two or more channels separating it from the subaqueous levees, and a crescentic, relatively unchanneled bar connecting the levee tips.

There are four stages in the formation of a RMB under stable jets expanding into a shallow, sloping basin [Edmonds and Slingerland, 2007] (Figure 5): initially, parallel subaqueous levees are deposited along the edges of the jet and a small RMB grows just basinward of the channel tip due to the decrease in jet momentum flux; then, the subaqueous levees continue to extend basinward and the RMB aggrades and progrades since its presence causes flow acceleration on streamlines over the bar, and subsequently, this acceleration changes the sediment transport gradient over the bar

triggering erosion on the upstream bar face and deposition in the downstream bar wake; afterwards, RMB progradation stops and the subaqueous levees continue extending and flare basinward around the stable river mouth bar; finally, as the levees continue to grow and spread due to the presence of the bar, increased water and sediment discharges around the bar cause widening and creation of the classic triangular RMB.

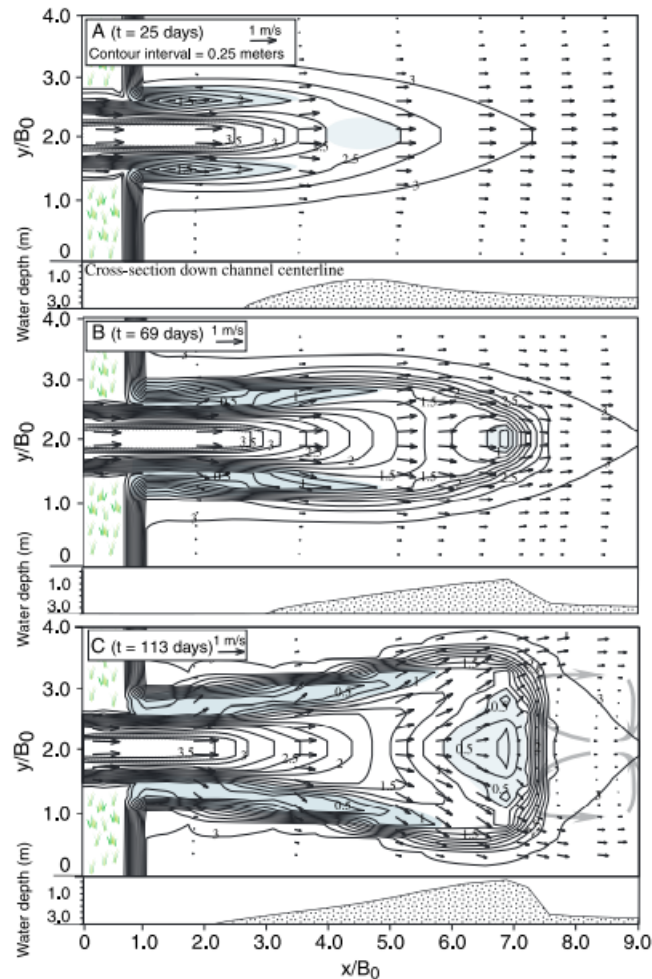


Figure 5. Serial bathymetric contour maps, longitudinal cross sections (B_0 stands for the river mouth width), and vertically integrated velocity vectors depicting the general evolution of a RMB system under a stable turbulent jet as predicted by the morphodynamic flow-sediment transport model Delft3D (Fagherazzi et al., 2015). A) RMB progrades to $x/B_0 = 5$. B) Levees continue to grow basinward but the RMB stops prograding. C) Levees begin to spread due to the presence of the RMB. The RMB aggrades vertically and widens.

Sediment erosion and deposition dynamics in estuarine regions, following the formation and growth of RMBs, are mainly affected by hydrodynamic factors, such as water runoff, discharge fluctuations of the rivers, sediment flux, sediment characteristics, river mouth geometry, vegetation, existence of tides and waves. For what concerns sediment characteristics, mass and cohesiveness play important

roles in RMBs evolution. Since coarser sediments are not well suspended by the jet, they are likely to deposit close to the river mouth and lead to RMB construction. On the other hand, since fine sediments are generally transported in a suspended form, they can be carried further and disperse widely, and most of the time, lead to levee construction. Moreover, both sediment cohesion and vegetation influence river mouth deposits by stabilizing the sediment surface. Cohesion stabilizes the sediment due to intermolecular forces among particles that make them harder to erode once they are deposited and aged [e.g., Black et al., 2002]. In the case of vegetation, stabilization arises from belowground roots that can withstand higher tensile stresses and increase material strength [van Eerd, 1985; Hey and Thorne, 1986; Huang and Nanson, 1997] and from dense aboveground biomass that diminishes turbulent kinetic energy in the flow [e.g., Nepf, 1999], thereby increasing deposition and reducing sediment erosion [Fagherazzi et al., 2012]. Grain size, which controls the settling velocity of the particles, also influences the location of the RMB basinward of the outlet.

Besides, the effects of waves and tides on river mouths are significant on the RMB evolution. Waves have a double effect on RMB growth: while small and locally generated waves favour the RMB formation by increasing the jet spreading, large, swell waves suppress bar development. The effect of tides on RMBs is a complex phenomenon due to the interaction between riverine and tidal flow [e.g., Cai et al., 2013; Lanzoni and Seminara, 1998]. Tides affect the hydrodynamics of the jet exiting the river mouth and therefore have important consequences from a morphodynamic point of view. When the tidal discharge is much higher with respect to the fluvial one, hydrodynamics of the jet exiting the RMB, dominating the sediment deposition, are highly affected, hence elongated deposits form due to tidally induced bidirectional sediment transport, parallel to the river outflow.

River bars can appear as single or periodic alternations of shoals, accompanied by deeper pools. Single bars form at geometrical features or discontinuities of the river channel causing a permanent flow perturbation or “forcing,” such as structures, exposed bedrock, confluences, bends, or bank line irregularities.

Periodic bars develop from an instability phenomenon that arises as a response to water flowing over loose material under certain hydraulic and sediment mobility conditions. They appear as double-harmonic waves of the riverbed surface, i.e., with transverse and longitudinal wavelengths, and are either steady or migrating. The periodic bars that form in straight channels without any forcing are indicated as “free bars” and are typically migrating in downstream or sometimes upstream direction (Figure 6). The presence of forcing, causing a permanent flow configuration at a

certain location, fixes the location of the bars, at least for a certain distance, which then become steady. These periodic bars are called “hybrid bars” (*Duró et al.*) because they depend on both morphodynamic instability and forcing.

Alluvial rivers present different bar patterns, ranging from alternate bars that alternately form at the left and the right bank, central bars that form in the middle of the channel, and multiple bars that appear as several bars within the cross-section.



Figure 6. Multiple free bars merging into large compound bars (the Tagliamento River, Italy)

Large amounts of organic matter and suspended particulate materials are delivered to coastal waters at the deltas of major river systems (*Milliman and Syvitski, 1992*). Additionally, the suspended sediments in the plumes increase fluid density and viscosity impacting local hydrodynamics. As rivers normally have both fine and coarse sand, studying the development and characteristics of bars should include both bed and suspended sediment processes. However, most theories for bar instability are based on bed load transport, assuming an immediate adaptation of sediment transport to the local flow conditions. On the other hand, only a few theoretical works focus on the effects of suspended sediment transport on bars: in particular, it emerged that when bed load transport is dominant, the bars fully develop, whereas the bars become damped in case of dominant suspended load transport. The wave action on the sea floor or up-current beaches may lead to the generation of river bars. At river mouths, breaking waves can cause intense mixing between river and sea waters

while wave-induced momentum flux and setup oppose outflow. Rapid deceleration and lateral expansion result, thus creating broad crescent-shaped bars near the outlets. Subaqueous levees assume the form of broad shoals surmounted by shoreward-migrating swash bars. Flocculation, in particular, complicates sediment dynamics in river-estuary-coastal systems. Flocculation affects particle size distributions in the water column, particle settling rates, and is an important process in the removal of both organic and inorganic materials from the water column. Flocculation processes play a key role in determining the strength, density, and cohesion of aggregates after deposition and accumulation in the sediments.

1.3 The Misa River site

The Misa River is a natural stream which rises in Colle Ameno Mountain (Arcevia, Ancona) at an altitude of approximately 793 above the sea level. It crosses the Marche region in SW-NE direction and runs for about 48 km from the “Appennino umbro-marchigiano” (central Italy) to Senigallia municipality (Ancona, Italy), one of the most important touristic towns of the Italian Middle Adriatic coast. The Misa River watershed has a narrow and elongated shape and is characterized by a clearly asymmetric hydrographic network, meaning that the left tributaries, which are more developed than the right ones, mainly feed the Misa River flow.

The watershed extension is about 383 km², with discharges of about 400, 450, and 600 m³/s for return periods of 100, 200, and 500 years, respectively (*Brocchini et al., 2017*). It is bounded by the Cesano river watershed north-westward, by the Esino river watershed south-eastward and by the Sentino stream (an Esino river tributary) sub-basin southward as shown in Figure 7.

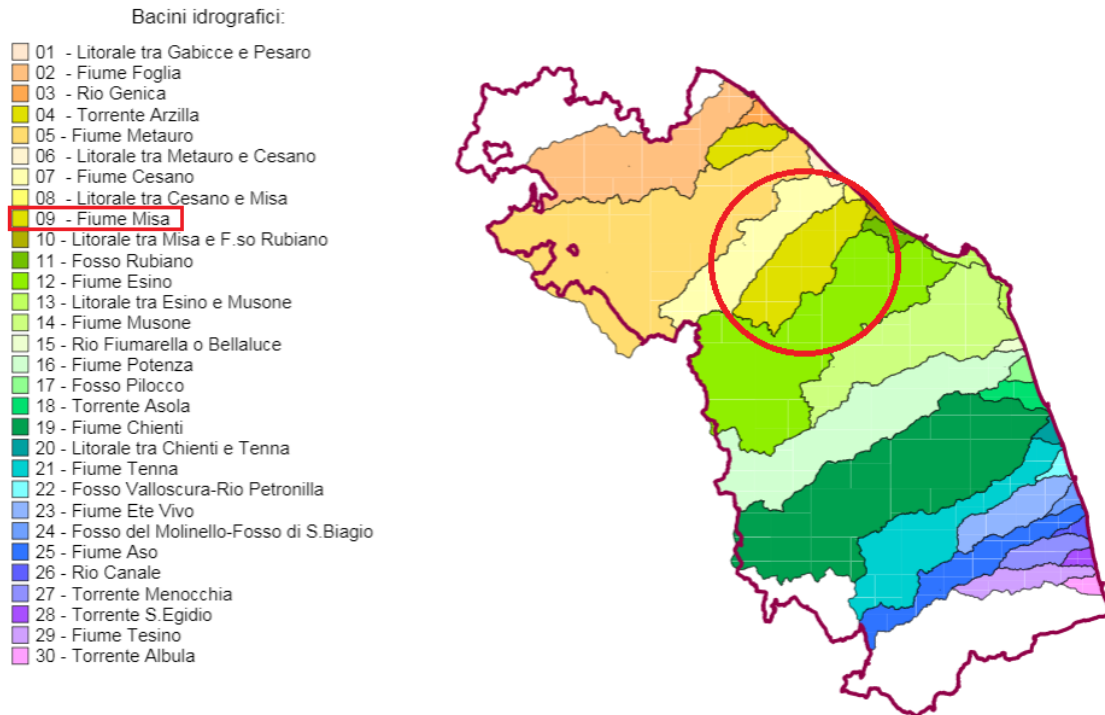


Figure 7. The Misa River watershed framework within the Marche region

The Misa River, as most of the Marche Region rivers, is characterized by a marked torrential regime, i.e., with poor or null flows during dry periods and very high flows (in the order of magnitude of hundreds of cubic meters of water) during rainy periods.

While the vast majority of the Misa River is characterized by natural levees, the final reach (from Ponte Garibaldi to the river mouth, crossing the Senigallia municipality) is delimited by reinforced concrete side walls with the aim at stabilizing the river banks from the erosion phenomena and floods. The Misa River flows to the sea by means of an estuary (Figure 8), which is oriented about 40° with respect to the North direction. Such an orientation has been decided since mainly the Bora (coming from the NNE) but also Scirocco (coming from the ESE) winds blow more frequently in this area throughout the year. As a result, sea storms generated by Bora winds are those impacting more in correspondence of the river mouth in terms of sediment transport. The Misa River estuary is classified as a salt-wedge estuary, where freshwater flows out to sea in the upper layer of the water column, while seawater intrusion occurs in the lower layer (Valle-Levinson, 2010). Saltwater intrusion is confirmed by salinity values larger than 10 psu 700 m upstream of the river mouth, and smaller, although non-zero values up to 1.5 km upstream of the mouth during summer (Brocchini et al., 2015). Small landward velocities in the lower part of the water column (up to 1–1.5 m above the bed) during salt wedge intrusion have been also detected 500 m upstream of the estuary

during winter (*Brocchini et al., 2017*). As typical for rivers originating in the Apennine Mountains, the Misa River is also characterized by large sediment transport rates in spite of its moderate discharge, which lead sometimes to the generation of a sediment accumulation and bars inside the river mouth, whose shape and size can vary over time depending on the incoming river discharge and sea waves. The intense sediment outflow has been postulated to have an influence on the evolution of morphological features of the unprotected beaches southward of the estuary (*Postacchini et al., 2017*).

Besides, the Misa River estuary is located in a microtidal environment, with semidiurnal tide, a mean tidal range rarely exceeding 0.6 m and negligible tidal currents.



Figure 8. The Misa River estuary satellite top view

Such a microtidal environment has been recently studied to understand river-sea interactions and so to better understand the wave propagation within the microtidal estuary. Inter alia, two experimental campaigns were undertaken in September 2013 and January 2014, aiming at characterizing the main forcing actions interacting in the estuarine region, and contrasting the general wintertime-summertime dynamics in the Misa River estuarine system. The data analysis showed that summertime is mainly characterized by calm periods and relatively mild storms, during which the wind continuously changes its direction and waves are relatively low. Furthermore, summertime conditions of the Misa River are provided with low freshwater discharge and net sediment deposition. Conversely, wintertime is featured by alternating calm and severe storm events characterized by almost constant wind directions and high waves, in which high

episodic freshwater discharge and net erosion and sediment transport occur. In addition, the river mouth acts as a low-pass filter, by letting low-frequency waves enter the channel, whereas higher frequency oscillations, like swell waves, are blocked. Infragravity waves have been observed to propagate upriver with velocities up to (3–5) m/s, according to the tidal excursion in the river (Melito et al., 2020). Such behaviour and seasonal differences underline a strong interaction between sea/swell waves, tide and river current during winter storms, which promotes large mixing and shear within the water column in the estuarine area.

2 MATERIALS AND METHODS

2.1 HEC-RAS model construction

The U.S Army Corps of Engineers' River Analysis System (HEC-RAS) is a software that was developed at the Hydraulic Engineering Center (HEC) as a part of the Hydrologic Engineering Center's "Next Generation" (NexGen) of hydrologic engineering software. HEC-RAS allows to perform one-dimensional steady flow, one and two-dimensional unsteady flow calculations, sediment transport/mobile bed computations, and water temperature/water quality. The main objective of this software is that of relating the discharge coming from the upstream basin with the velocities and the stage values obtained in the main channel and the floodplain areas of a river. The determination of the physical parameters that describe the water flow in a river cross-section is based on these hypotheses:

- One-dimensional flow
- Gradually varied flow
- Hydrostatic distribution of the pressures in each cross section, thus implying rectilinear and parallel flowlines)
- Gently steep channel ($i < 1:10$)
- On average constant continuous head losses between two adjacent cross-sections

The main rule of thumb in building up a HEC-RAS model is to insert good input data, hence this is considered the most important and tough part for hydraulic modelling. In order to do so, different data have been employed for this thesis including:

- Data from the Civil Protection of the Marche Region
- Data coming from field surveys
- Hydrodynamic data from two international projects, namely EsCoSed and MORSE (see section 2.1.3)

2.1.1 Data from the Civil Protection of the Marche Region

The Marche Region offers the opportunity to download meteorological and hydrological data of the regional watersheds by accessing to the Civil Protection Multirisk Functional Center online data extractor, called SIRMIP (Sistema Informativo Regionale Meteo-Idro-Pluviometrico). For this purpose, stage data recorded by both Bettollelle and Ponte Garibaldi hydrometric stations (indicated as RG2 and RG1, respectively, as shown in Figure 9) have been downloaded as shown in Figure 10. These data are provided by the SIRMIP online extractor each 30 minutes and they are referred to the local zero datum.



Figure 9. Location of Bettollelle (RG2) and Ponte Garibaldi (RG1) hydrometric stations within the Misa River (adapted from Melito et al., 2020)

SIRMIP ON-LINE
Regione Marche - Servizio Protezione Civile

Sistema Informativo Regionale Meteo-Idro-Pluviometrico

Esci [Modifica password](#) ilarimarco

Gestione dato: Idrometria [Torna alla pagina principale](#) [Torna alla selezione del bacino/provincia/comune/sensore](#)

Bacino: **Misa** Provincia: (Tutte) Comune: **Senigallia** 2 sensori trovati

Seleziona sensore, tipo dato, elaborazione e periodo.

Bettollele (RT-1112) Dati da 2000-05-31 a 2021-06-08 ▾

Tipo dato: Dato Validato Dato Originale

Elaborazione:

- Livello idrometrico [m]
- Livello idrometrico min/max [m]
- Livello idrometrico ore 12 [m]
- Portata massima [m³ s⁻¹]
- Portata media giornaliera [m³ s⁻¹]
- Scala di deflusso
- Portata media mensile [m³ s⁻¹]
- Portata media annuale [m³ s⁻¹]
- Portata [m³ s⁻¹]
- Presenza in Annali Idrologici 2
- Coordinate
- Afflussi meteorici mensili ed annuali
- Caratterizzazione idrologica

Data inizio (AAAA-MM-GG oo:mm) 2021-06-01 00:00 Data fine 2021-06-08 15:28

Premere un tasto per estrarre i dati:

NAVIGAZIONE

- [Esci](#)
- [Informazioni](#)
- [Manuale SIRMIP On-Line](#)
- [Contatti](#)
- [Modifica password](#)








Figure 10. SIRMIP window for stages downloading

Successively, given that the Bettollele hydrometer zero is known, the discharge values have been calculated by making use of the rating curve equations listed in Table 1, which stand for mathematical expressions that associate a stage value with a discharge one. On the other hand, Ponte Garibaldi rating curve equations are not available since they have never been calibrated.

Starting validity	Ending validity	Stage interval [m]	Rating curve equation
1/1/2011 00:01	1/3/2011 10:30	$0.77 \leq H \leq 9999$	$Q = 11.4929 \cdot [H - (0.76)]^{1.8516} + 0$
5/3/2011 00:01	23/5/2015 06:30	$0.55 \leq H \leq 4.39$	$Q = 6.195 \cdot [H - (0.517)]^{2.576} + 0$
5/3/2011 00:01	23/5/2015 06:30	$4.4 \leq H \leq 6.35$	$Q = 185.568 \cdot [H - (4.39)]^{1.138} + 202.776$
23/5/2015 00:01	7/3/2017 6:30	$0.2 \leq H \leq 1.51$	$Q = 5.9 \cdot [H - (0.148)]^{2.934} + 0$
23/5/2015 00:01	7/3/2017 6:30	$1.52 \leq H \leq 3.01$	$Q = 27.549 \cdot [H - (1.51)]^{1.188} + 14.609$
23/5/2015 00:01	7/3/2017 6:30	$3.02 \leq H \leq 6.5$	$Q = 101.284 \cdot [H - (3.01)]^{1.061} + 59.209$
7/3/2017 16:01	5/3/2018 00:00	$0.95 \leq H \leq 3.02$	$Q = 14.388 \cdot [H - (0.942)]^{1.974} + 0$
7/3/2017 16:01	5/3/2018 00:00	$3.03 \leq H \leq 6.5$	$Q = 100.396 \cdot [H - (3.02)]^{1.068} + 60.954$
15/12/2019 00:00	1/1/2030 00:00	$0.85 \leq H \leq 1.03$	$Q = 2.33 \cdot [H - (0.84)]^{0.79} + 0$
15/12/2019 00:00	1/1/2030 00:00	$1.04 \leq H \leq 2.1$	$Q = 19.68 \cdot [H - (1.03)]^{1.24} + 0.6$
15/12/2019 00:00	1/1/2030 00:00	$2.11 \leq H \leq 3.8$	$Q = 64.05 \cdot [H - (2.1)]^{1.26} + 22.01$
15/12/2019 00:00	1/1/2030 00:00	$3.81 \leq H \leq 5.5$	$Q = 155.87 \cdot [H - (3.8)]^{1.16} + 146.7$

Table 1. Employed rating curve equations list

Furthermore, precipitation data have been downloaded always within the SIRMIP online extractor. These data, which are recorded by Bettollelle rain gauge, are provided every 15 minutes and helps in the understanding of the peaks occurring in the used hydrographs. Although Senigallia river gauge is present within the Misa River watershed, precipitation data collected by this gauge have not been taken into consideration since the Bettollelle rain gauge better describes the rainfall affecting the considered watershed.

2.1.2 Field-survey data

Specific surveys were conducted in the Misa River over the past decades: specifically, in this thesis three different surveys have been taken into account.

In 2001 and 2002, the Marche region carried out topographic surveys regarding all the Marche region rivers, including the Misa River itself. As a result, Figure 11 displays some extrapolated cross-sections resulting from this survey.

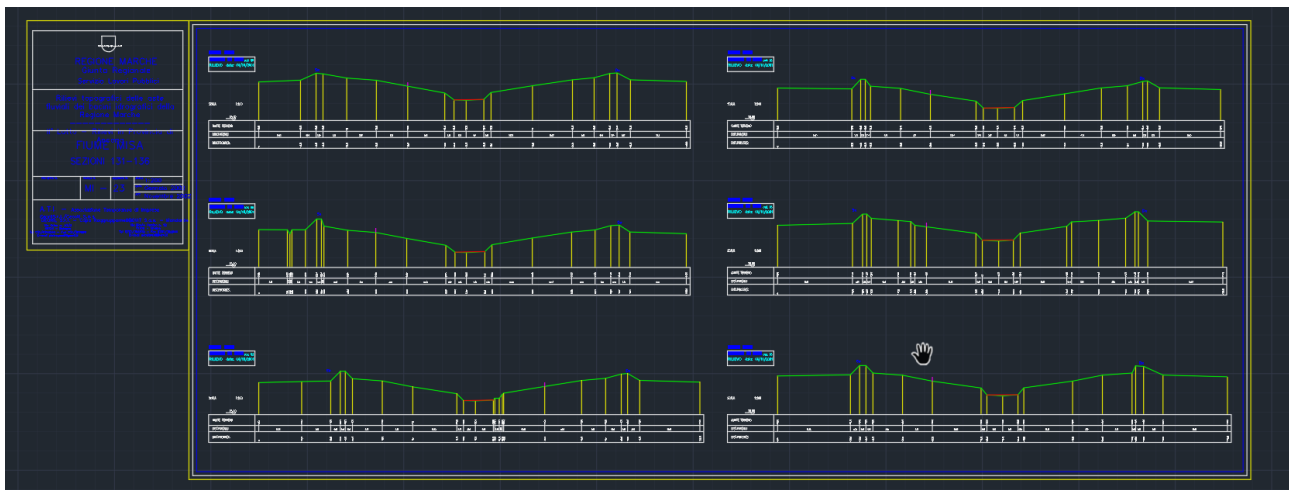


Figure 11. Example of the Misa River cross-sections dating back to 2001 topographic survey

In 2008 and 2009, the Ministry of Environment and Land launched a topographic survey campaign throughout Italy by exploiting the LIDAR (Light Detection And Ranging) remote sensing technique coupled with a GPS platform for points georeferencing. Therefore, thousands of DTM (Digital Terrain Model) tables, i.e., the representation of the elevation distribution of the bare earth (without considering both anthropic and vegetable elements) have been elaborated. In this thesis, 27 DTM tables of the study area (from Bettollelle to the river mouth) have been selected: these tables are WGS84 referenced raster data (.ASC format) and own a resolution of 1 or 2 meters, depending on where this topographic survey was conducted: all the tables including the Adriatic Sea shoreline own a resolution of 2 meters, whereas the remaining ones, that are located inland, have a resolution of 1 meter, as that presented in Figure 12. Such a low DTM table resolution has been chosen with the goal to properly develop an accurate geometry for the river analysis and thus have representative data concerning the main channel and the overbank areas.

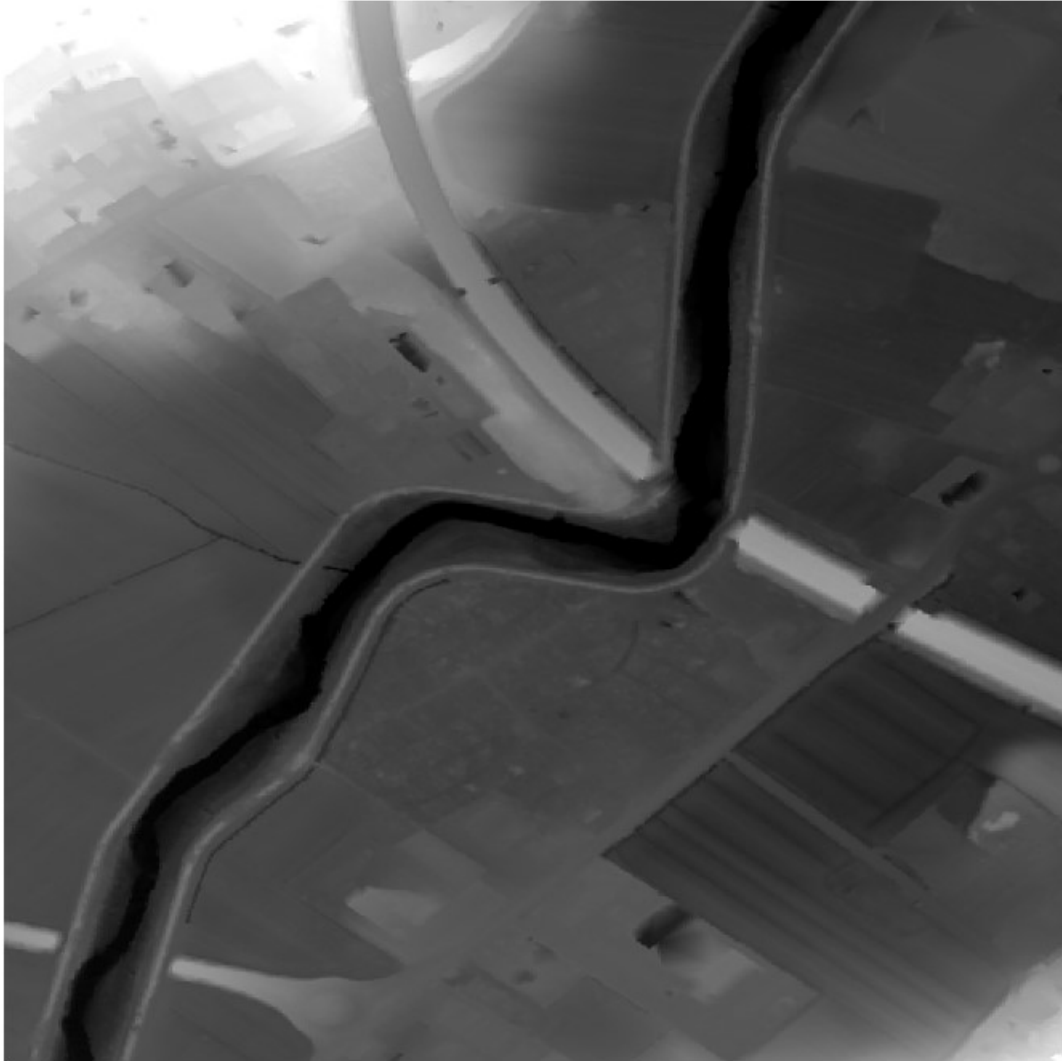


Figure 12. Example of a DTM table dating back to 2008-2009 topographic survey

More recently in 2019, another topographic survey was conducted from the Civil Protection of the Marche Region in the Bettolle area and nearby, and some cross-sections were extracted. Figure 13 shows an example of cross-section that was retrieved from this survey.

<i>REGIONE MARCHE</i>	
Sistema Regionale di Protezione Civile e Sicurezza Locale	
DEFINIZIONE SCALE DI DEFLUSSO DI QUATTRO SEZIONI IDROMETRICHE DELLA RETE METEO-IDRO-PLUVIO REGIONALE	
ELABORATO: Sezioni Trasversali e profili longitudinali	TAV.
Stazione di Misa a Bettollelle	scala 1:100
	CONTRATTO PROT.N°
	DATA: 2019
	REVISIONE
	DATA:

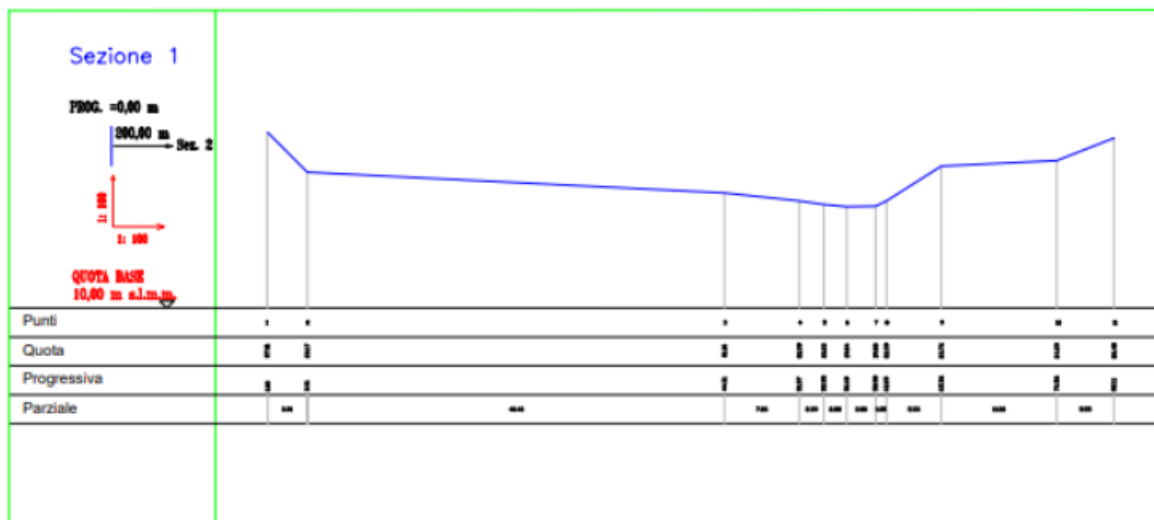


Figure 13. Example of cross-section extrapolated from the 2019 topographic survey

In addition to the previously described topographic surveys, even bathymetric survey campaigns were conducted by Socotec Italia company in 2015, 2018, and 2020 with the aim to characterize the final river reach and reconstruct the near coastal region. Such surveys have been carried out

between the Ponte della Ferrovia (about 700m from the mouth) location and the open Adriatic Sea, passing through the river estuary. Figure 14 illustrates an image depicting the 2020 bathymetric survey of the above-mentioned area.



Figure 14. The Misa River mouth 2020 bathymetry

2.1.3 Hydrodynamic data

In order to characterize the Misa River estuarine dynamics in summer and winter conditions as well as their differences (*Brocchini et al., 2017*), and study the physical-chemical properties of estuarine sediments, during the years 2013 and 2015, the EsCoSed (Estuarine Cohesive Sediments) project was carried out. To this purpose, specific equipment was used to measure the hydrodynamics in the lower reach of the Misa River and within the close nearshore area, including a series of quadpods, each equipped with several sensors and deployed in river and sea (QR1, QR2, QR3, QS1, and QS2 as shown in Figure 15) and two tide gauges. With reference to the wintertime campaign of January 2014 (specifically from 23rd to 31st January 2014), the surface level was collected by the tide gauges (TGdown and TGup, located in the river at about 280 m and 580 m, respectively, from the Misa River mouth as shown in Figure 14). Further details are also described in *Melito et al. (2020)*.



Figure 15. The Misa River mouth satellite top view showing the location of the two tide gauges

Always within the framework of the EsCoSed project, a SGS (Sena Gallica Speculator) video monitoring station coupled with four cameras was installed in 2015 in correspondence of the north jetty of the Senigallia harbour on the top of a pole (Figure 16a and 16b) with the purpose of acquiring information about both the Misa River mouth and part of Senigallia beach (which is not artificially protected) southward of the Senigallia harbour. Specifically, for this work the images taken by the four cameras have been used to evaluate the spatial variation of the sandbar located at the river mouth during different time periods.

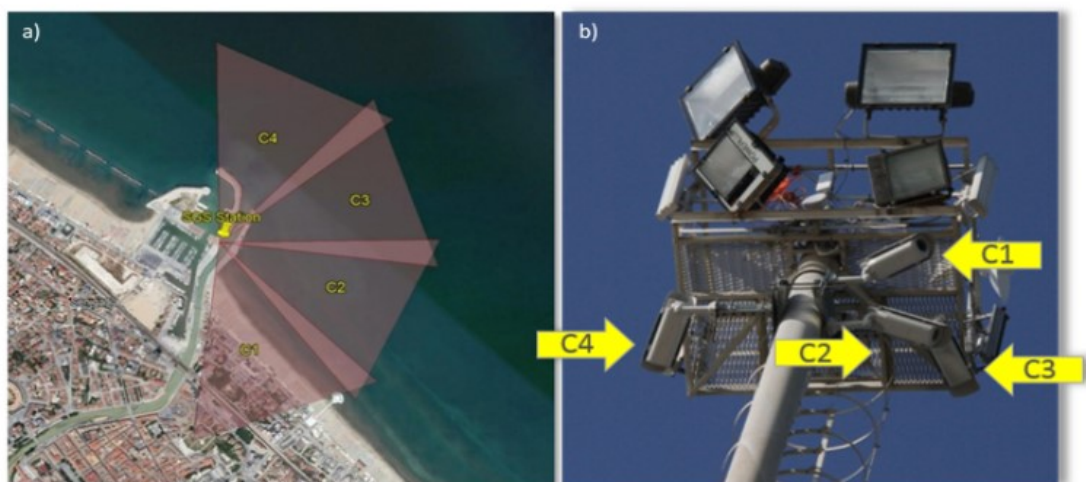


Figure 16. a) Satellite top view of the Misa River mouth with reference to the position of the SGS video monitoring station and the cameras field of view. b) Location of the four cameras installed on the top of the pole.

The MORSE (Modeling and Observation of River–Sea Exchanges) project can be seen as a natural continuation of the EsCoSed project; the difference is that while the latter focuses on the monitoring of a small area of the Misa River estuary (in the order of 1 km²) over a short period (in the order of days), the former concerns a wider area (in the order of 50-100 km²) over a longer duration (in the order of years). In fact, the MORSE study area is delimited inland by a H-ADCP (Horizontal Acoustic Doppler Current Profiler), i.e., a river gauge, placed in the Misa River left bank about 1.2km upstream of the river mouth and about 20m upstream of the Ponte Garibaldi hydrometer. This acoustic sensor is able to measure the river stage, the average flow velocity and subsequently the discharge value. To do so, the H-ADCP sends acoustic pulses from its transducer faces (Figure 17) into the water column, where they are reflected back by particles and return to the transducer face. Exploiting the Doppler principle, the total time is measured and used to infer the particles velocity, which corresponds to that of the water which transports the particles themselves. The measurements are related to Greenwich meridian and are supplied each 2 minutes. Since the Misa River is characterized by relatively low discharges especially during the summertime and wintertime and given that the river gauge height is about 0.63m above the average sea level (see Table 3), the instrument rarely results to be completely submerged by the water flow, which is a necessary condition for the proper functioning of the instrument, thus providing unreliable measurements.



Figure 17. H-ADCP river gauge

For what concerns the tides, the tide-gauge signal recorded at Ancona harbour have been taken into account for the 2014 and 2019 events, whereas Senigallia tidal stages have been employed for the 2020 events. The tide gauge of Ancona supplies tidal stages referred to the average sea level every 10 min; moreover, as the Figure 18 shows, these data have been downloaded by accessing the “Rete Mareografica Nazionale” website and then worked out to get data every 30 minutes. On the other hand, Senigallia tide gauge is installed at Senigallia harbour and records every 6 minutes (Table 2).

Ancona tidal elevations stages have been used since both Senigallia and Ancona tide gauges provide overlapping values, due to the reduced distance between the two instruments, and because the tide gauge of Senigallia operates just since 2018.



Figure 18. Mareografico website window for Ancona tidal stages downloading

SENIGALLIA TIDE	
Time	Stage [m]
'01-Jan-2020 00:30:00'	-0.104
'01-Jan-2020 00:36:00'	-0.163
'01-Jan-2020 00:42:00'	-0.052
'01-Jan-2020 00:48:00'	-0.121
'01-Jan-2020 00:54:00'	-0.091
'01-Jan-2020 01:00:00'	-0.127

Table 2. Example of Senigallia tidal stages series

Since the final reach of the Misa River crosses Senigallia municipality, the treated waters discharges by the Senigallia wastewater treatment plant (WWTP) into the Misa River must be taken into account as well. This WWTP is located close to the A14 highway bridge (Figure 19), and it treats wastewaters having a capacity of 100,000 population equivalent. Both inlet and bypass effluent discharges have been provided by Viva Servizi S.p.A. in order to check the wastewater contribution when comparing the HEC-RAS simulated stages in Ponte Garibaldi with those measured by Ponte Garibaldi hydrometer.



Figure 19. Satellite top of view of a reach of the Misa River with focus on the Senigallia WWTP (red circle) and the point where WWTP effluent discharges are discharged inside the river (red arrow)

2.2 Model validation

An existing HEC-RAS project characterizing the Misa River stretch going from about 2 km upstream of Bettollelle area (cross-section 52 in Figure 20) to the river mouth (cross-section 0.8 in Figure 20) has been initially employed with the aim to carry out steady-state simulations and check potential instability problems arising from the simulations themselves. This project is composed of 52 cross-sections extracted following the topographic surveys dating back to 2001 and 2002. Some issues came out after looking into both the river profile and its cross-sections, e.g., the location of the Bettollelle bridge about 400m upstream with respect to its real position.

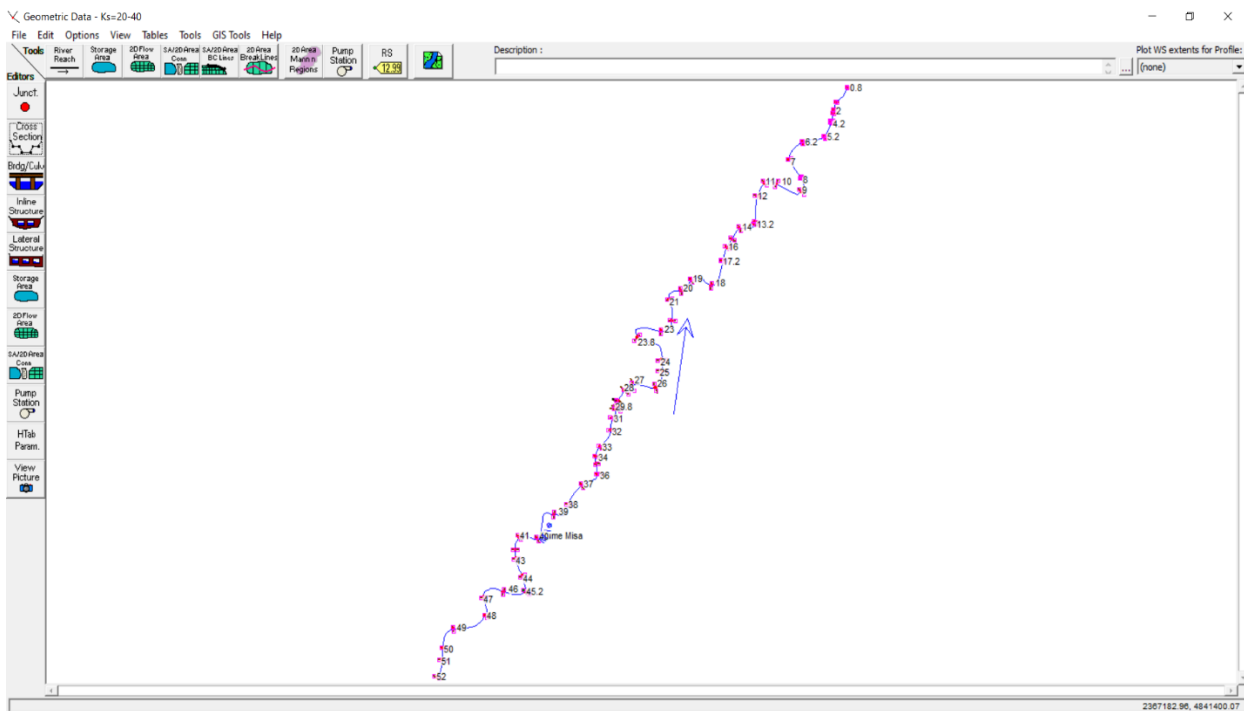


Figure 20. HEC-RAS first project river profile

Another HEC-RAS project has been built up by modifying the geometry of the previously mentioned project, including the reduction of the cross-sections number so that the first cross-section of the reach corresponds to the Bettollelle one, and the replacement of the 2001 Bettollelle and Ponte Garibaldi cross-sections with the ones provided by the Civil Protection (Figure 21) and the Metis Company (Figure 22), respectively.

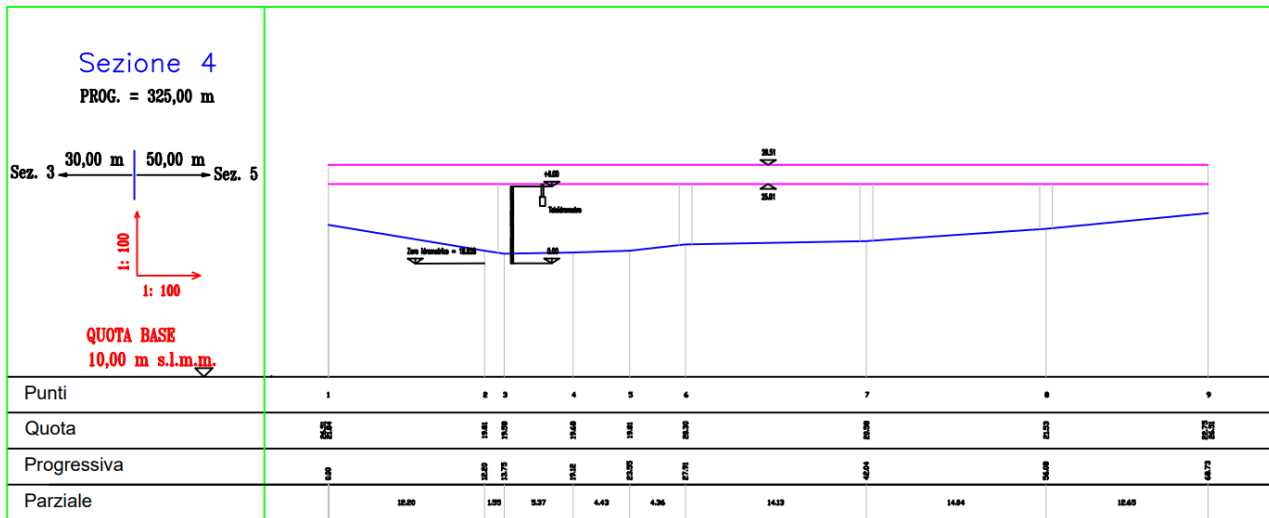


Figure 21. 2019 Bettolle cross-section

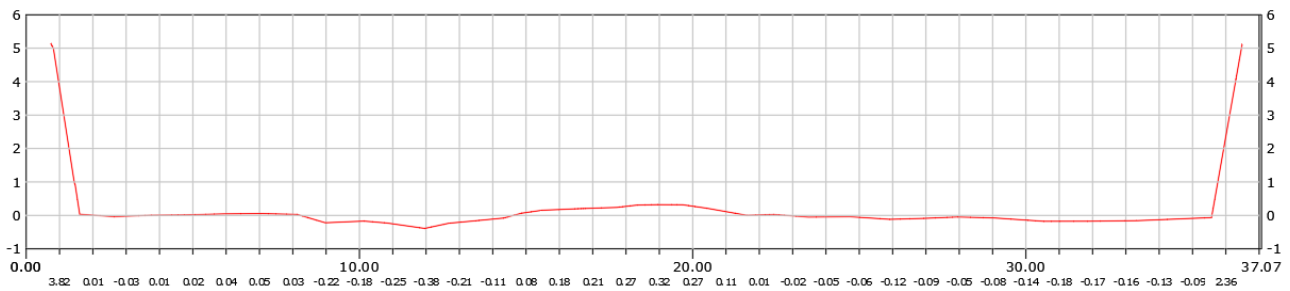


Figure 22. 2019 Ponte Garibaldi cross-section

Once the new geometry has been fixed, unsteady-state simulations have been implemented for the following events:

- 20th January - 30th January 2014
- 7th October - 31st December 2016
- 26th January - 3rd February 2017
- 4th February - 18th February 2017
- 3rd March - 24th April 2017
- 18th November - 22nd December 2017
- 18th February - 5th March 2018
- 10th January - 13rd January 2021

For each simulated period, both the discharge values obtained through the rating curve equations and the tide stages have been employed as upstream and downstream boundary conditions of the

system, respectively. This model has not been validated since the model comprising of the DTM tables would then be chosen as the benchmark one for calibration purposes.

Afterwards, a third HEC-RAS model involving the 2019 Bettolle and Ponte Garibaldi cross-sections, the cross-sections belonging to the final reach of the Misa River retrieved from the 2020 bathymetric survey (Socotec Italia srl), as well as the cross-sections extracted from the DTM tables following the 2008-2009 topographic survey has been constructed. HEC-RAS allows to make use of DTM tables by exploiting the HEC-RAS Mapper module in order to build up a 2D model and perform 2D unsteady simulations. After importing the DTM tables of the study area and establishing the project spatial reference system, a geometry group including the definition of layers concerning the river centerline (blue line), the bank lines (red line), the floodplain (light blue line) and the cross-sections (green line) has been built up as shown in Figure 23.

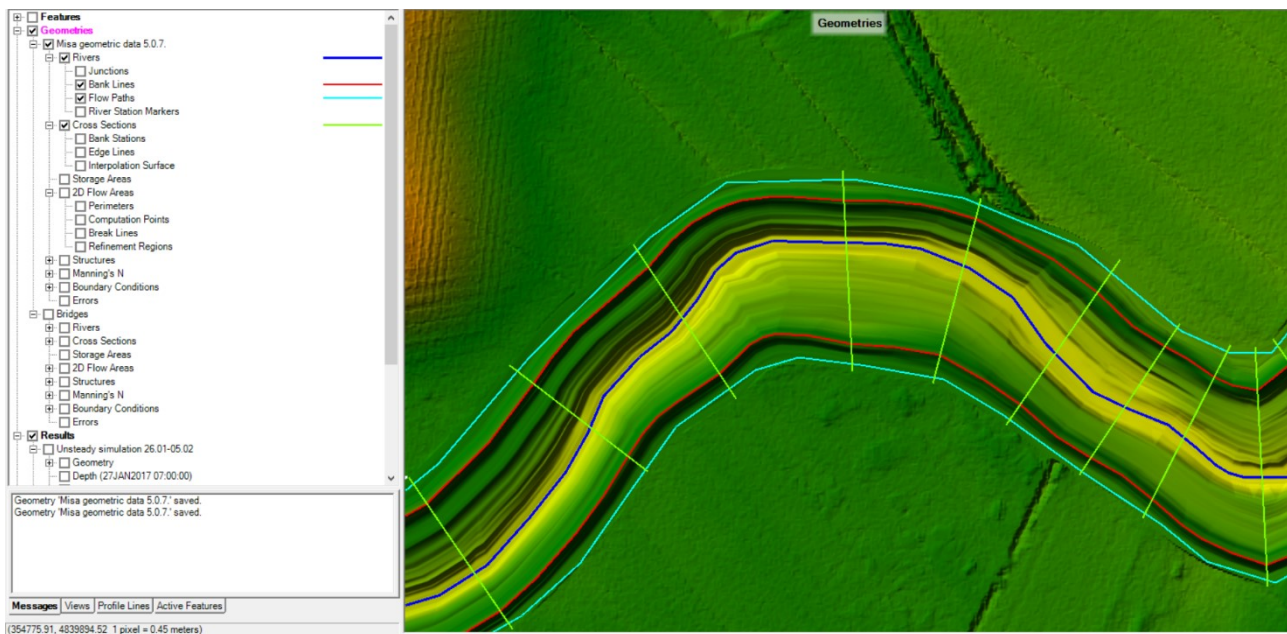


Figure 23. HEC-RAS Mapper geometry group displaying the river centerline (blue line), the bank lines (red line), the floodplain (light blue line) and the cross-sections (green line) for a Misa River reach

A problem occurring in the extrapolation of cross-sections from the DTM has regarded the ending part of the Misa River, specifically from Ponte Garibaldi area to the river mouth. In fact, both left and right walls delimiting the river, have been cut with respect to the reality. Therefore, the walls heights have been changed and replaced with those found in the first HEC-RAS project.

Moreover, the same number of bridges and associated geometric characteristics included in the previous two projects have been added, except for the Via Urbana bridge where the piers have been removed, since from a recent survey it turned out that the bridge piers were no longer there. Further, the cross-section in correspondence of the H-ADCP river gauge (Figure 24), which was surveyed by the Metis company in 2019, has been inserted.

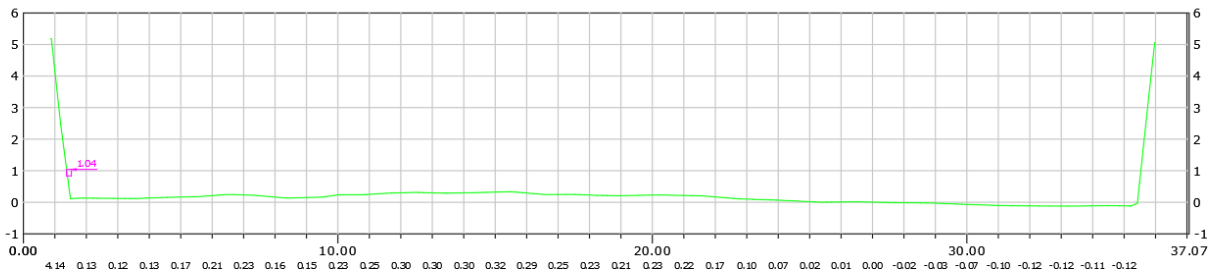


Figure 24. 2019 H-ADCP cross-section

Whenever a new element has been added, it has been necessary to interpolate, based on the position of the bank stations, the hydraulic properties between cross-sections, thus obtaining interpolating hydraulic results from cross-section to cross-section.

Unsteady simulations likewise have been carried out in the third project for the considered events:

- 20th January - 30th January 2014
- 1st November - 30th November 2016
- 26th January - 3rd February 2017
- 4th February - 18th February 2017
- 3rd March - 24th April 2017
- 18th November - 22nd December 2017
- 18th February - 5th March 2018
- 26th May - 1st June 2019
- 9th November - 15th November 2019
- 22nd December - 24th December 2019
- 27th March - 29th March 2020
- 27th December - 31st December 2020
- 10th January - 13rd January 2021

This HEC-RAS model has been properly validated in another work (Martinelli, 2021) by exploiting Manning coefficients range from 0.025 to 0.2. The results of the calibration are shown for the second, third and fourth events of the above list and concern the comparison in terms of stages between the SIRMIP measured stages (solid black line) and the HEC-RAS simulated stages (solid green line). The precipitation depth (solid blue line) is relative to Bettollele rainfall station and it gives an idea of the precipitation falling within the watershed during the considered events. The tidal excursion (solid red line) has been displayed only at the Ponte Garibaldi cross-section, given that its contribution at Bettollele cross-section can be taken as negligible.

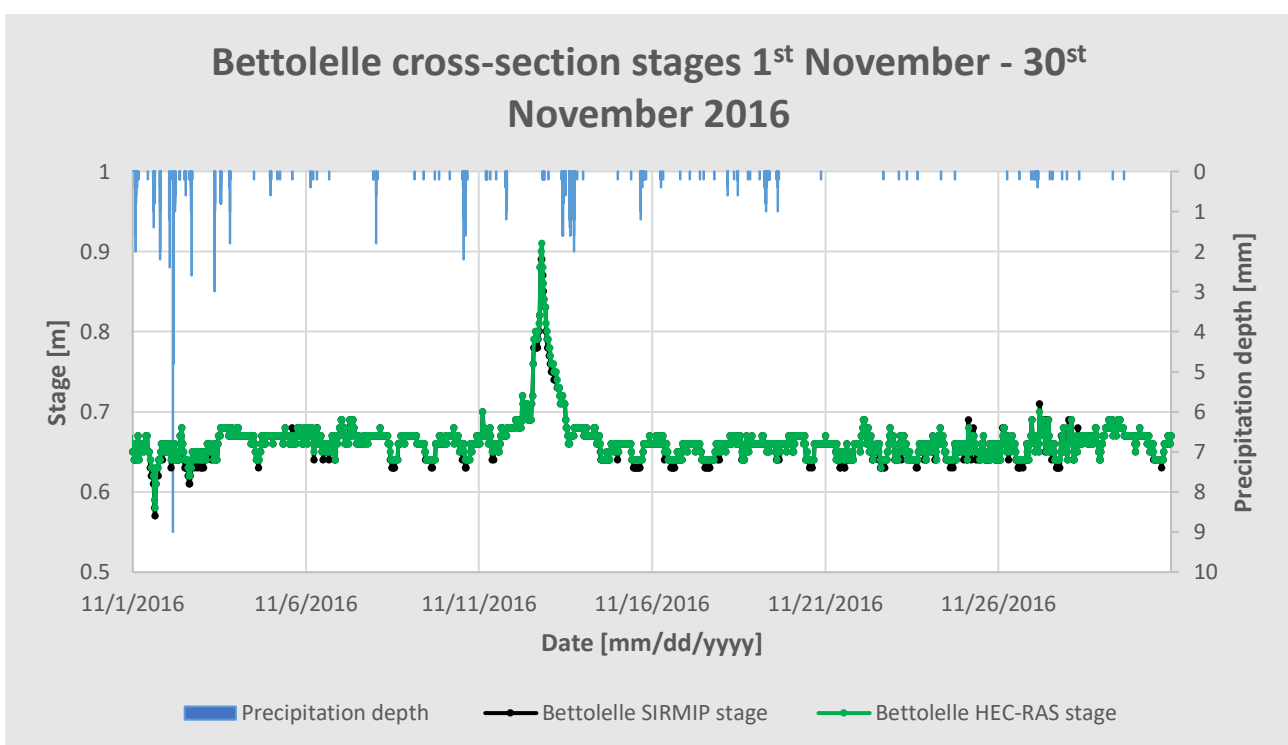


Figure 25. Simulation results at Bettollele cross-section for the 1st November – 30th November 2016 event

Ponte Garibaldi cross-section stages 1st November - 30th November 2016

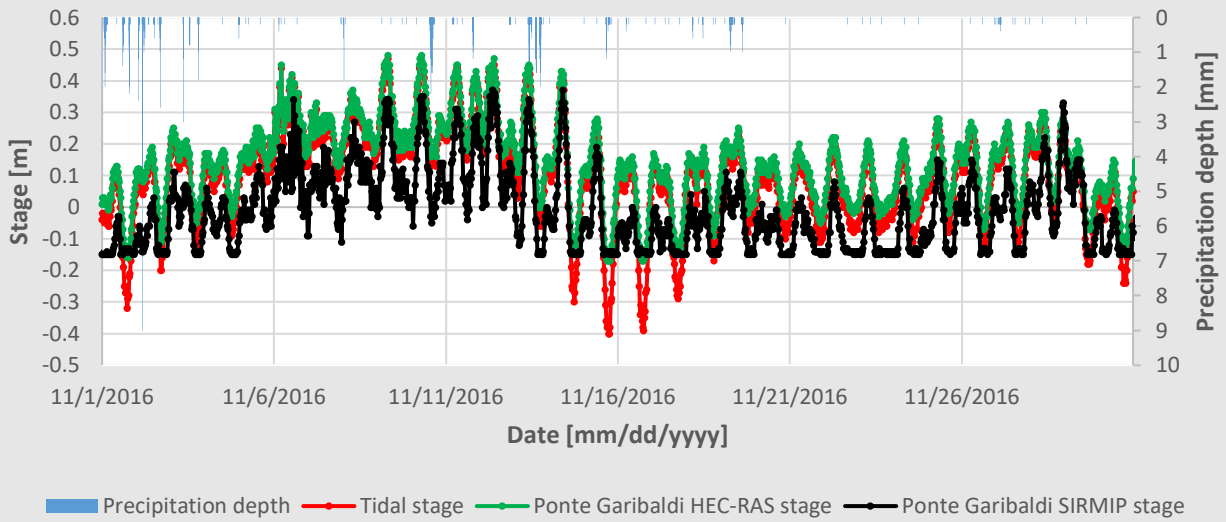


Figure 26. Simulation results at Ponte Garibaldi cross-section for the 1st November – 30th November 2016 event

Bettolelle cross-section stages 26th January - 3rd February 2017

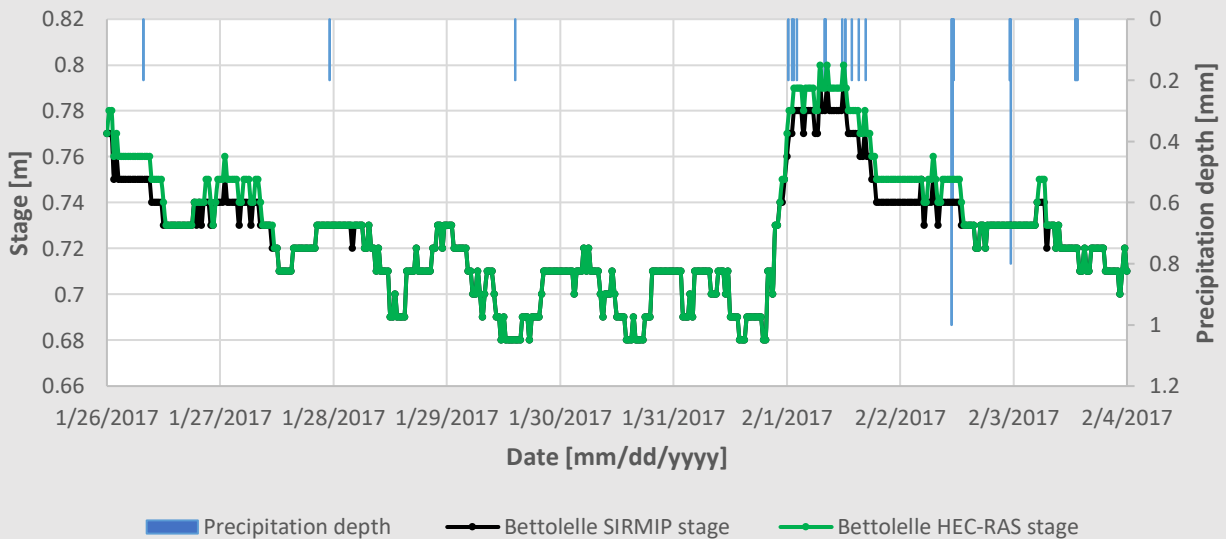


Figure 27. Simulation results at Bettollelle cross-section for the 26th January – 3rd February 2017 event

Ponte Garibaldi cross-section stages 26th January - 3rd February 2017

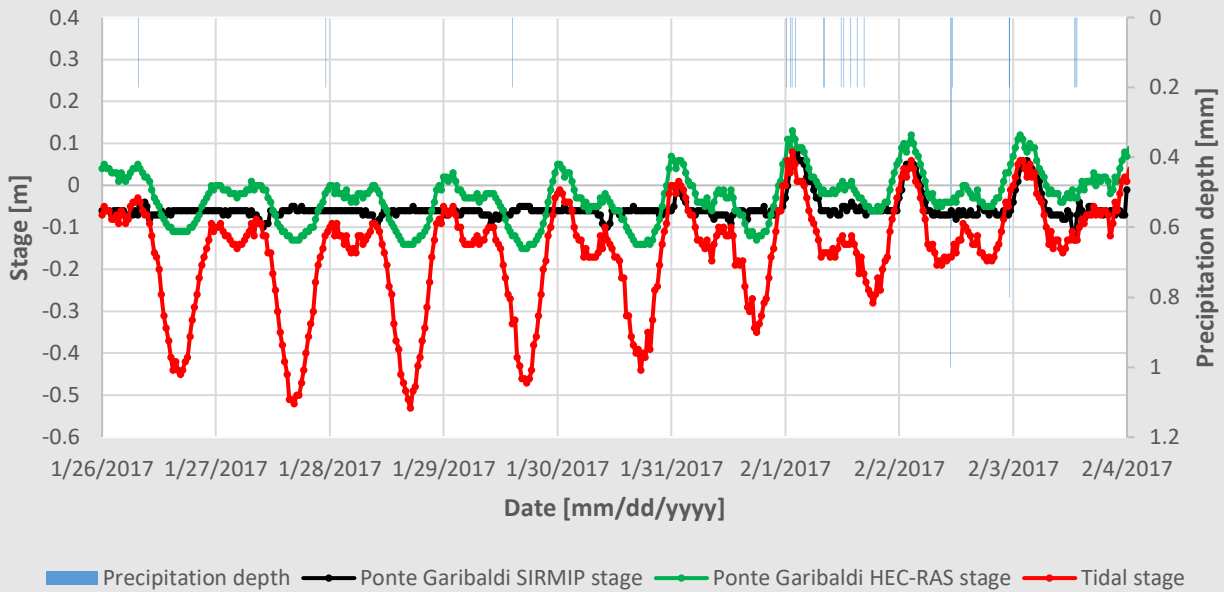


Figure 28. Simulation results at Ponte Garibaldi cross-section for the 26th January – 3rd February 2017 event

Bettollelle cross-section stages 4th February - 18th February 2017

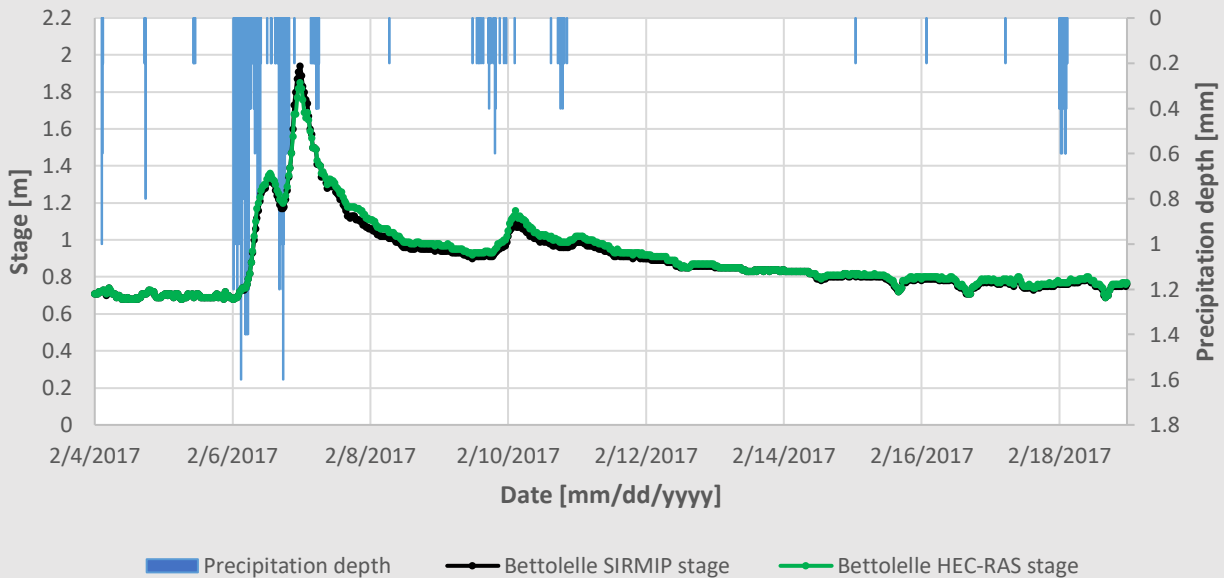


Figure 29. Simulation results at Bettollelle cross-section for the 4th February – 18th February 2017 event

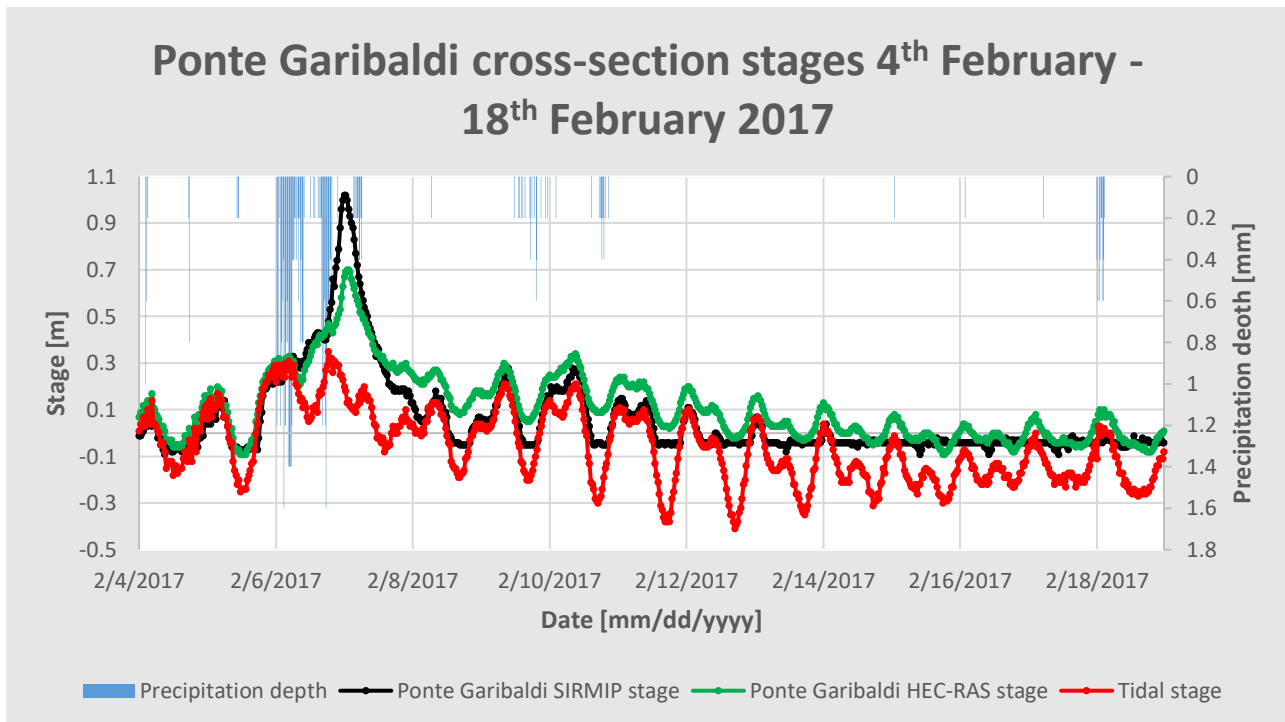


Figure 30. Simulation results at Ponte Garibaldi cross-section for the 4th February – 18th February 2017 event

The results observed at Bettollele cross-section highlight a good matching between the measured SIRMIP stage values and the HEC-RAS ones as shown in Figure 25, 27 and 29.

On the other hand, for what concerns Ponte Garibaldi cross-section, the simulation results are not fully in line with the measured ones. Specifically, in the 1st November to 30th November 2016 event, the SIRMIP stages are always below the HEC-RAS stages and even lower than the tidal stages for the vast majority of the time (Figure 26), thus implying probably cross-section local variations in correspondence of the hydrometer.

As regards the 26th January to 3th February 2017 event, the HEC-RAS stage series own a similar trend to the tidal stages one, even though the latter present a reduced excursion because of the river discharge contribution (Figure 28). SIRMIP stages have a flat shape whenever negative tides occur, whereas for tidal excursions greater than -0.05m, they follow the trend of both the HEC-RAS stages and the tidal one. The flat trend may likewise be addressed to the occurrence of a low flow detection limit of the instrument.

The 4th to 18th February 2017 event displays a good agreement between the measured and the simulated stages, with the exception of the SIRMIP flat trend and the peak (Figure 30). Basically, it emerged that the river forcing prevails on the tidal motion when high discharge values occur, thus confirming what expressed in Brocchini et al. (2017). The gap existing in the peak zone may be

addressed to the runoff contribution existing between Bettollelle and Ponte Garibaldi, the uncertain validity of the rating curve employed at Bettollelle for large discharges, as well as the uncontrolled sewer outflow occurring during flood conditions, since in dry periods this difference in water elevation does not exist.

3 MODEL RESULTS

3.1 Description of the modeled events

Once the model has been calibrated, the following events have been considered, i.e.,

- 20th January - 30th January 2014
- 26th May - 1st June 2019
- 9th November - 15th November 2019
- 22nd December - 24th December 2019
- 27th March - 29th March 2020
- 27th December - 31st December 2020
- 10th January - 13rd January 2021

The first event (20th January - 30th January 2014) has been chosen with the aim at comparing the EsCoSed tide levels recorded by the pressure sensors called TGup and TGdown (see Melito et al., 2020) with those simulated by HEC-RAS. The remainder of the events have been selected with the goal to understand the effects of the different river mouth bar morphologies with regard to the comparison between the measured and simulated stages at Bettollelle, H-ADCP, and Ponte Garibaldi cross-sections.

In order to allow for the comparison between the stages, a datum for the stages have been selected for each of the three considered cross-sections. For what concerns the Bettollelle cross-section, the measured stages have been referred to the thalweg level: therefore, since the HEC-RAS output data are always referred to the average sea level, they have been reduced by 19.58m, which stands for the difference between the cross-section thalweg and the average sea level. For what concerns the SIRMIP stage values, being the hydrometric zero located at 19.18m above the sea

level for the period prior to 2019 and 18.828m above the sea level from the 2019 onward, they have been reduced by a quantity of 0.4m and 0.75m, respectively.

Conversely, the average sea level has been chosen as datum for the measured stages of both Ponte Garibaldi and H-ADCP cross-sections. As a result, the stages outcoming from the HEC-RAS software have been left as they were, whereas both the 2019 bathymetric survey and 2020 H-ADCP survey (Figure 31 and Table 3) have been considered in order to compute how much the measured stage values needed to be reduced. Considering that the H-ADCP river gauge uppermost part is located at 0.630m above the average sea level (see Table 3) and that the SIRMIP measured stages are relative to the Metis survey cross-section zero (see section 2.2), the Ponte Garibaldi SIRMIP stages have been reduced of 0.41m in order to be reconducted to the average sea level.

Name	ID code	UTM Coordinate North	UTM Coordinate East	Elevation [m]
4012	River gauge	4841784.770	356078.424	0.630
4002	River gauge red eye lower part	4841784.688	356078.410	0.482
4003	River gauge red eye upper part	4841784.687	356078.411	0.605

Table 3. H-ADCP elevations with respect to the average sea level

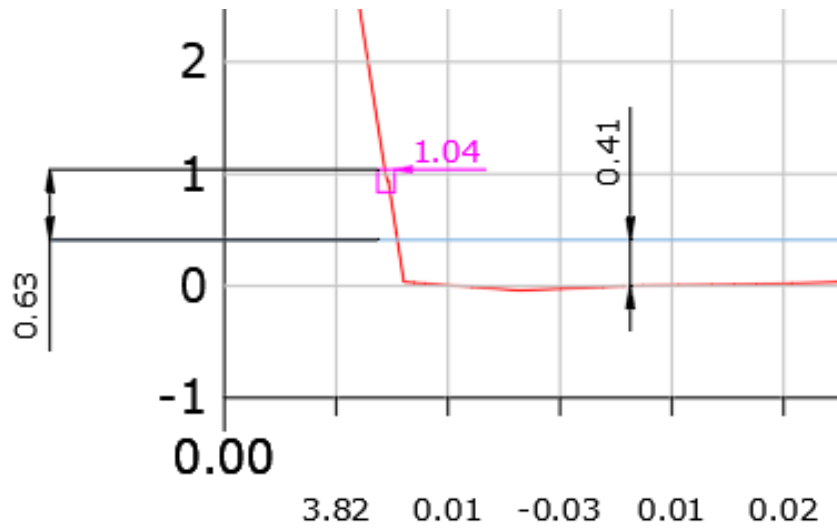


Figure 31. Selection of the Ponte Garibaldi reference system

On the other way round, given that the H-ADCP measured stages are referred to the cross-section bed in correspondence of the instrument, H-ADCP stages have been reduced of 0.29m in order to be reconducted to the average sea level (Figure 32).

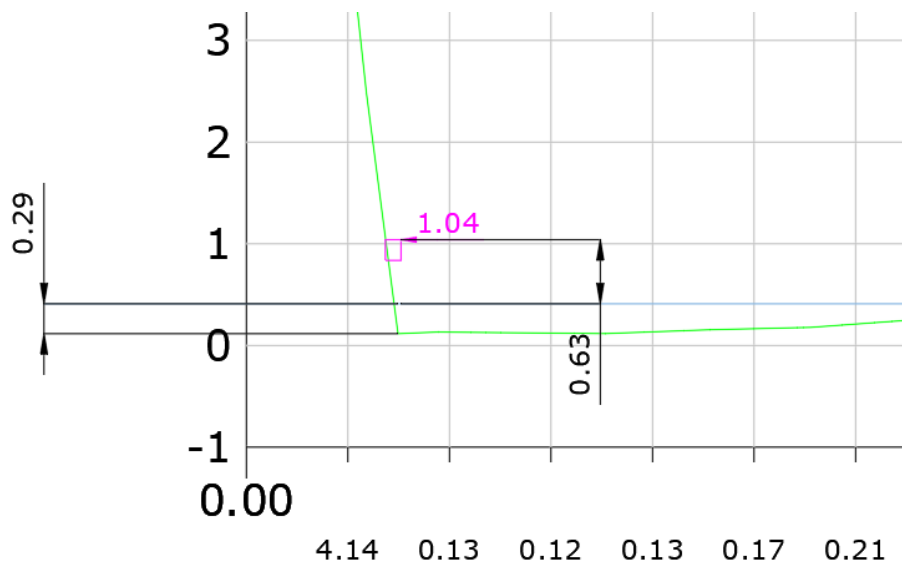


Figure 32. Selection of the H-ADCP reference system

Furthermore, during flood conditions, both the H-ADCP river gauge and Ponte Garibaldi hydrometer seem to measure the same water depth with a good approximation. Considering that both H-ADCP and Ponte Garibaldi zeros are found at different elevations, with a difference of around 9 cm (that is also equal to the bed slope), the water profile turns out to have a slope equal to the bed one (Figure 33).

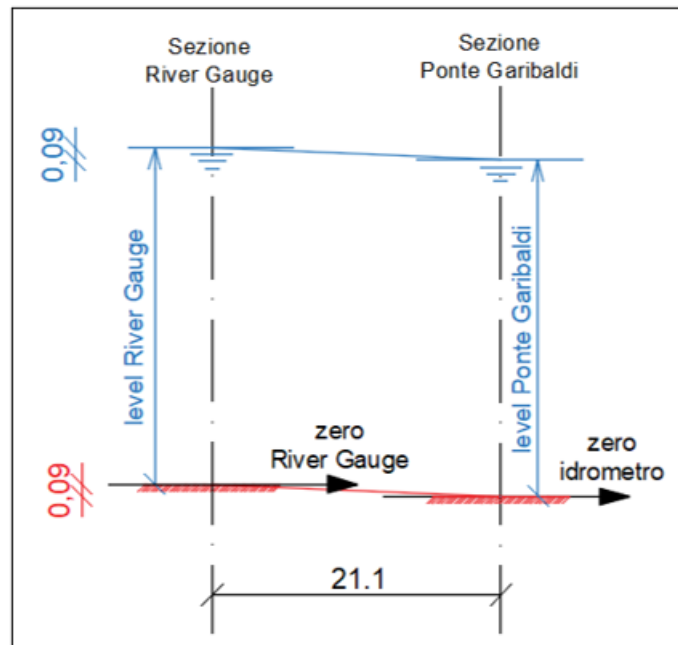


Figure 33. Schematization of the longitudinal profile between the H-ADCP cross-section and the Ponte Garibaldi cross-section

3.2 Field campaign data validation within the EsCoSed project

The event that goes from 20th to 30th January 2014 has been investigated in order to compare the water-surface level recorded by the two tide gauges (TGup and TGdown) during the EsCoSed project and that provided by HEC-RAS. Moreover, since the analyzed event is prior to the 30th June 2016, that is the date after which Ponte Garibaldi stages are provided by the SIRMIP online extractor, only Bettollelle measured stages have been compared with those simulated by HEC-RAS. Table 4 displays the Bettollelle discharge values (fourth column in table), measured stages, which are provided with respect to the Bettollelle hydrometer zero (fifth column in table) and to the cross-section thalweg (sixth column in table), as well as the difference between thalweg and Bettollelle hydrometer zero (seventh column in table) for the beginning of the considered event.

Bettollelle SIRMIP 20th January - 30th January 2014						
Date	Time	Stage series	Discharge [m³/s]	Stage w.r.t. hydrometer zero [m]	Stage w.r.t. thalweg [m]	Difference between thalweg and hydrometer zero [m]
2014/1/20	0:0	41659	2.69	1.24	0.84	0.4
2014/1/20	0:30	41659.02083	2.69	1.24	0.84	
2014/1/20	1:0	41659.04167	2.50	1.22	0.82	
2014/1/20	1:30	41659.0625	2.41	1.21	0.81	
2014/1/20	2:0	41659.08333	2.50	1.22	0.82	
2014/1/20	2:30	41659.10417	2.50	1.22	0.82	

Table 4. Bettollelle discharge and stage time series for the 20th January – 30th January 2014 event

Moreover, water-surface elevation provided with respect to average sea level from Ancona harbour as well as precipitation depth recorded at Bettollelle rain gauge each 15 minutes have been displayed in table 5 and 6, respectively, for the beginning of the considered event.

Ancona water-surface elevation 20th January - 30th January 2014			
Date	Time	Stage series	Stage [m]
2014/1/20	0:0	41659	0.44
2014/1/20	0:30	41659.02083	0.45
2014/1/20	1:0	41659.04167	0.45
2014/1/20	1:30	41659.0625	0.4
2014/1/20	2:0	41659.08333	0.45
2014/1/20	2:30	41659.10417	0.41

Table 5. Bettollelle water-surface elevation time series for the 20th January – 30th January 2014 event

Bettolelle precipitation 20th January - 30th January 2014			
Date	Hour	Precipitation series	Bettolelle precipitation depth [mm]
2014/1/20	0:0	41659	0
2014/1/20	0:15	41659.01042	0
2014/1/20	0:30	41659.02083	0
2014/1/20	0:45	41659.03125	0
2014/1/20	1:00	41659.04167	0
2014/1/20	1:15	41659.05208	0

Table 6. Bettollelle precipitation time series for the 20th January – 30th January 2014 event

Table 7 shows the HEC-RAS simulated stages at Bettollelle cross-section: in particular, the first column represents the Bettollelle simulated stages relative to the average sea level, whereas the third column illustrates the stage values reduced by the hydrometric zero to refer them to the thalweg level.

HEC-RAS Bettollelle cross-section 20th January - 30th January 2014		
Stage w.r.t. the average sea level [m]	Hydrometer zero [m]	Stage with respect to the thalweg [m]
20.38	19.58	0.8
20.38		0.8
20.36		0.78
20.34		0.76
20.35		0.77
20.35		0.77

Table 7. Bettollelle HEC-RAS stage time series for the 20th January – 30th January 2014 event

Table 8 displays the HEC-RAS output stages at Ponte Garibaldi cross-section. Stage data in the first and the third column in table are the same since the both HEC-RAS output data and Ponte Garibaldi datum are relative to the average sea level.

HEC-RAS Ponte Garibaldi cross-section 20 th January - 30 th January 2014		
Stage w.r.t. the average sea level [m]		Stage w.r.t. the average sea level [m]
0.45	0	0.45
0.46		0.46
0.46		0.46
0.41		0.41
0.46		0.46
0.42		0.42

Table 8. Ponte Garibaldi HEC-RAS stage time series for the 20th January – 30th January 2014 event

The results of the comparison between modelled and observed data at Bettollele cross-section are shown in Figure 34.

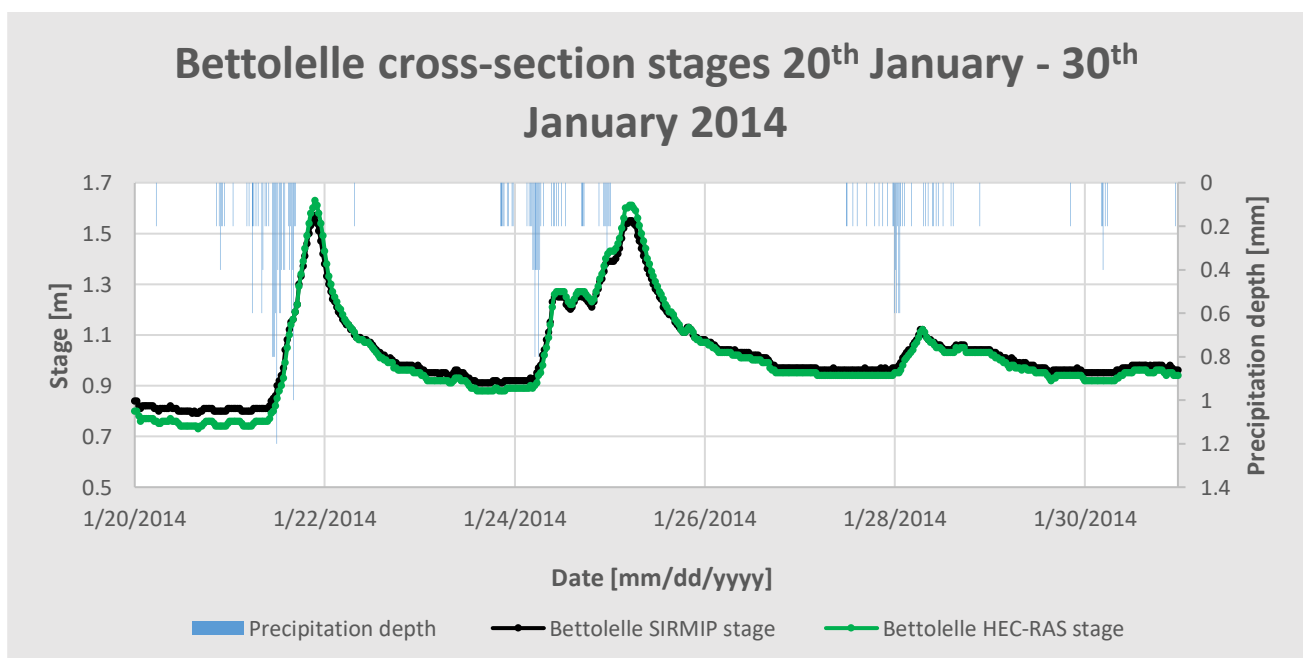


Figure 34. Simulation results at Bettollele cross-section for the 20th January – 30th January 2014 event

Figure 34 is structured in such a way that the stages series is associated with the primary axis (on the left), whereas the precipitation depth series, which is related to a secondary axis (on the right), have been implemented with the aim at checking their contribution in the increase of the stage values at Bettollelle. Looking at the graph, there is an almost perfect overlapping between stages, thus suggesting that the cross-section used at the upstream boundary is correct.

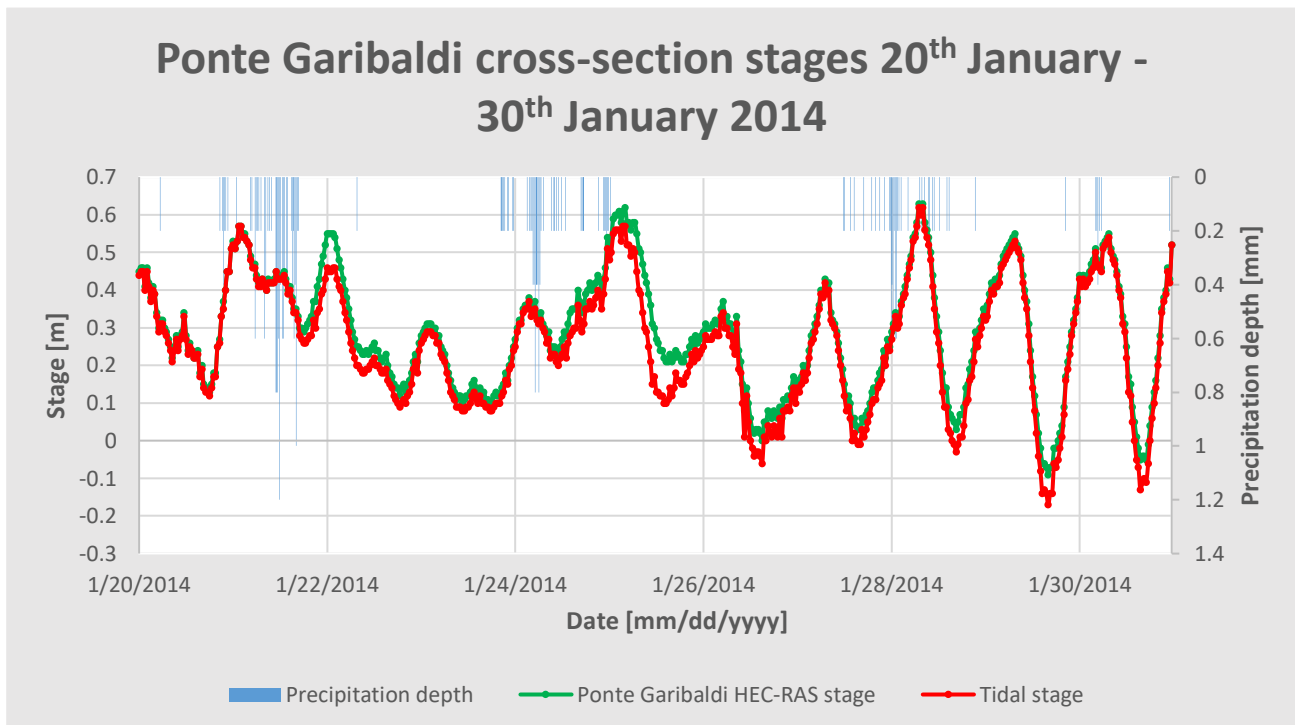


Figure 35. Simulation results at Ponte Garibaldi cross-section for the 20th January – 30th January 2014 event

Figure 35 shows, likewise, a quite good correspondence between the stage simulated in Ponte Garibaldi and that recorded by the tide gauge at Ancona harbour (linked to the primary axis). This is in line with what expressed in Brocchini et al., (2017), which states that tide effects are felt even 1.5 km upriver from the river mouth.

Considering the EsCoSed measurements, TGup (from 23rd January 2014 17:42:11 to 31st January 2014 15:24:00) and TGdown (from 23rd January 2014 17:18:51 to 31st January 2014 15:44:48) stages relative to the tidal gauges elevation are shown in Table 9 and 10.

TGup measured stages			
Date	Time	TGup series	Stage [m]
2014/1/23	17:42:11	41662.73763	0.0716
2014/1/23	17:43:11	41662.73832	0.0686
2014/1/23	17:44:11	41662.73902	0.0638
2014/1/23	17:45:11	41662.73971	0.074
2014/1/23	17:46:11	41662.74041	0.0574
2014/1/23	17:47:11	41662.7411	0.0625

Table 9. TGup measured stages

TGdown measured stages			
Date	Time	TGdown series	Stage [m]
2014/1/23	17:18:51	41662.721	0.5907
2014/1/23	17:19:51	41662.722	0.5965
2014/1/23	17:20:51	41662.723	0.5822
2014/1/23	17:21:51	41662.724	0.5869
2014/1/23	17:22:51	41662.724	0.5733
2014/1/23	17:23:51	41662.725	0.5778

Table 10. TGdown measured stages

Knowing the location of the TGup and TGdown within the Misa River mouth, the cross-sections 1912 e 908 (which are close to the tide gauge locations), respectively, have been chosen within the HEC-RAS study reach to retrieve the stages from the HEC-RAS output table. In both table 11 and 12, stages are referred to the average sea level.

HEC-RAS TGup cross-section		
Stage [m]		Stage [m]
0.44	0	0.44
0.45		0.45
0.45		0.45
0.4		0.4
0.45		0.45
0.41		0.41

Table 11. TGup HEC-RAS stages

HEC-RAS TGdown cross-section		
Stage [m]		Stage [m]
0.44	0	0.44
0.45		0.45
0.45		0.45
0.4		0.4
0.45		0.45
0.41		0.41

Table 12. TGdown HEC-RAS stages

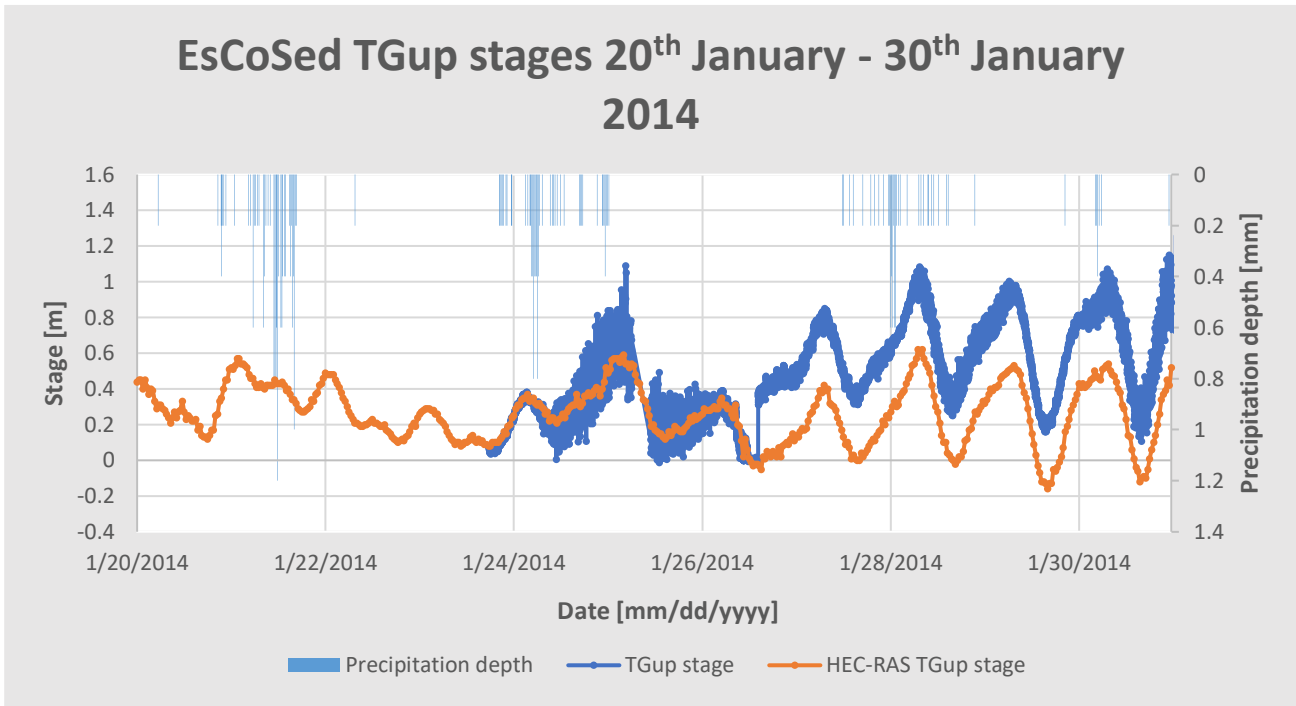


Figure 36. Simulation results prior at TGup cross-section prior to the gauge shifting for the 20th January – 30th January 2014 event

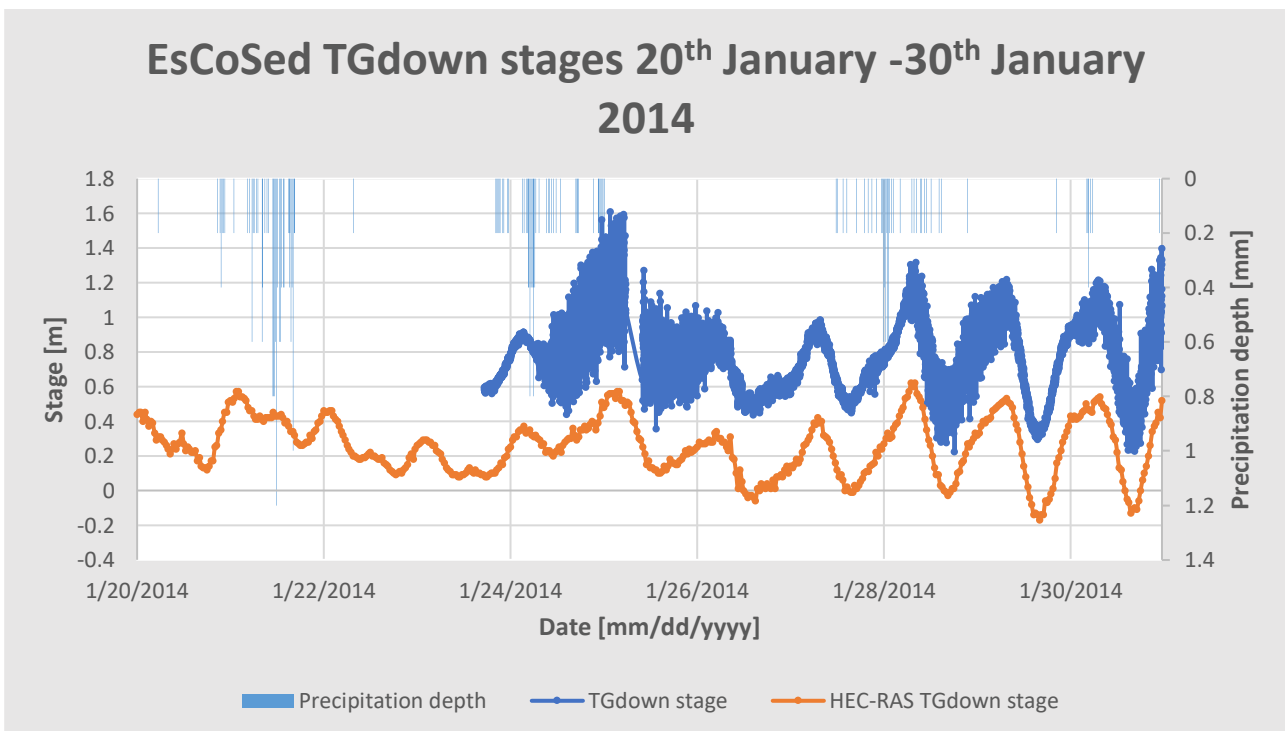


Figure 37. Simulation results at TGdown cross-section prior to the gauge shifting for the 20th January – 30th January 2014 event

The peculiarity of both graphs (Figure 36 and 37) lies on the fact, albeit the measured stages trend seems to follow the HEC-RAS stages one, they are translated upward due to the different reference system: in particular, TGup stages shifted upward on 26th January 14:14:50 onward, when the pressure sensor was physically lowered of some centimetres to allow the data recording even during low tide conditions, whereas the entire TGdown series is shifted with respect to the simulated series, as it was installed at a certain depth since the beginning. The sensor positioning was thus due to the need to capture the wave oscillations, even during low tide conditions. Because of this reason, TGup and TGdown stages have been translated downward of 0.37m and 0.53m, respectively, in order to be more or less overlapped with the HEC-RAS simulated stages (see Figure 38 and 39).

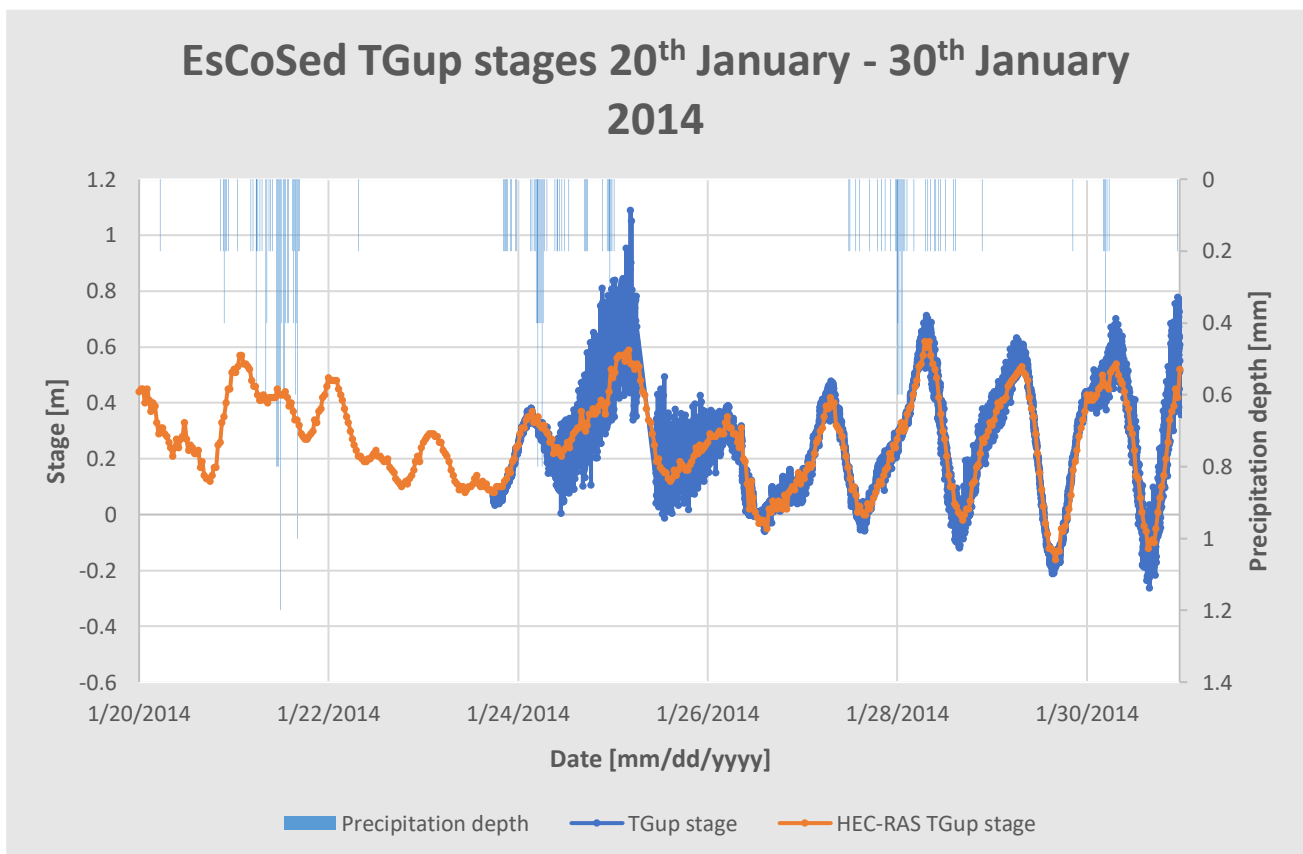


Figure 38. Simulation results TGup cross-section following the gauge shifting for the 20th January – 30th January 2014 event

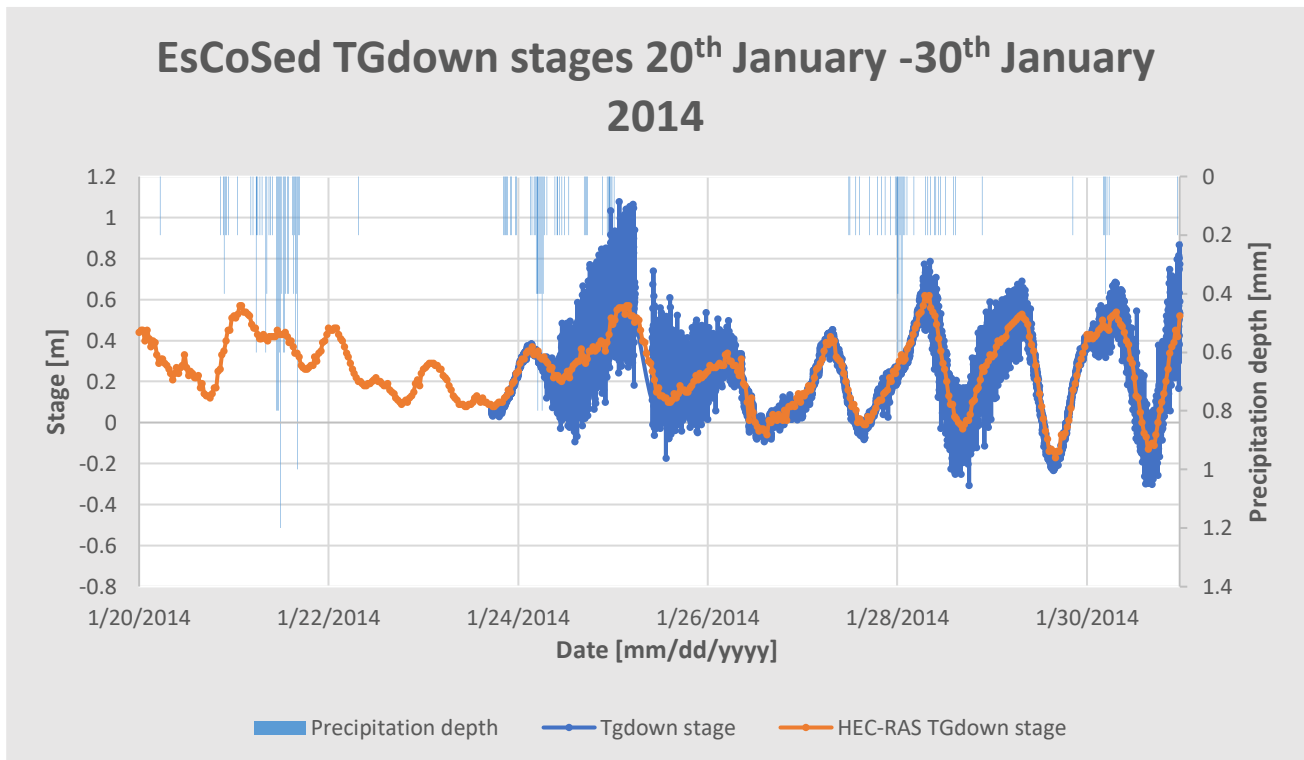


Figure 39. Simulation results at TGdown cross-section following the gauge shifting for the 20th January – 30th January 2014 event

Despite pronounced water level oscillations have been recorded by both the TGup and TGdown gauges due to a storm event, in calm conditions it is possible to notice a match between the water levels coming from both the Senigallia harbour and HEC-RAS ones.

Moreover, in order to understand at which point of the ending reach of the Misa River the tidal effect can be considered negligible, HEC-RAS stages belonged to Ponte Garibaldi cross-section and some cross-sections located upstream of it have been plotted for the 20th January – 30th January event (Figure 39). Additionally, water-surface elevation (solid red line) measured by the tide gauge placed in Ancona harbour and the Bettolle discharge values (solid black line), related to a secondary axis, have been considered. Considering the initial part of the hydrograph prior to the peak characterized by an almost flat trend, it emerged that from the cross-section 5655 (located about 1.7 km upstream of the river mouth) moving downstream, the tidal effect is relevant, whereas moving from the cross-section 6052 (placed about 1.8 km upstream of the river mouth, close to the Via Urbana bridge) upriver, the tidal effect is negligible. However, the higher the discharge values, the lower the tidal contribution is as shown in correspondence of the peaks in Figure 40. For the sake of completeness, HEC-RAS river profiles regarding the three flood events corresponding to 25th January 2014 at 4:00, 28th January 2014 at 8:00, 29th January 2014 at 7:30

(Figure 41, 43 and 44) and the calm event of the 27th January 2014 at 11:00 (Figure 42) are presented.

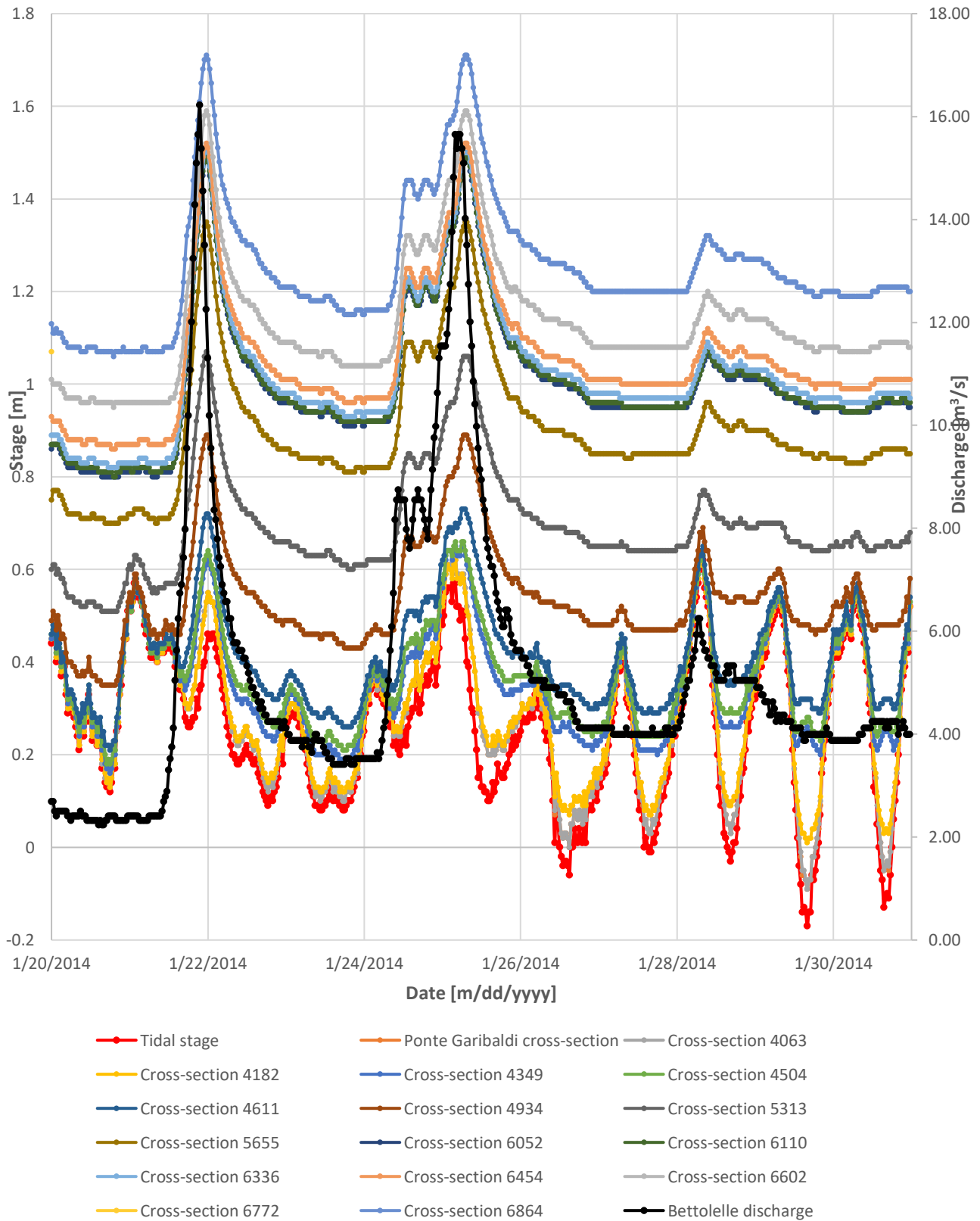


Figure 40. Influence of tides on cross-sections upstream of Ponte Garibaldi

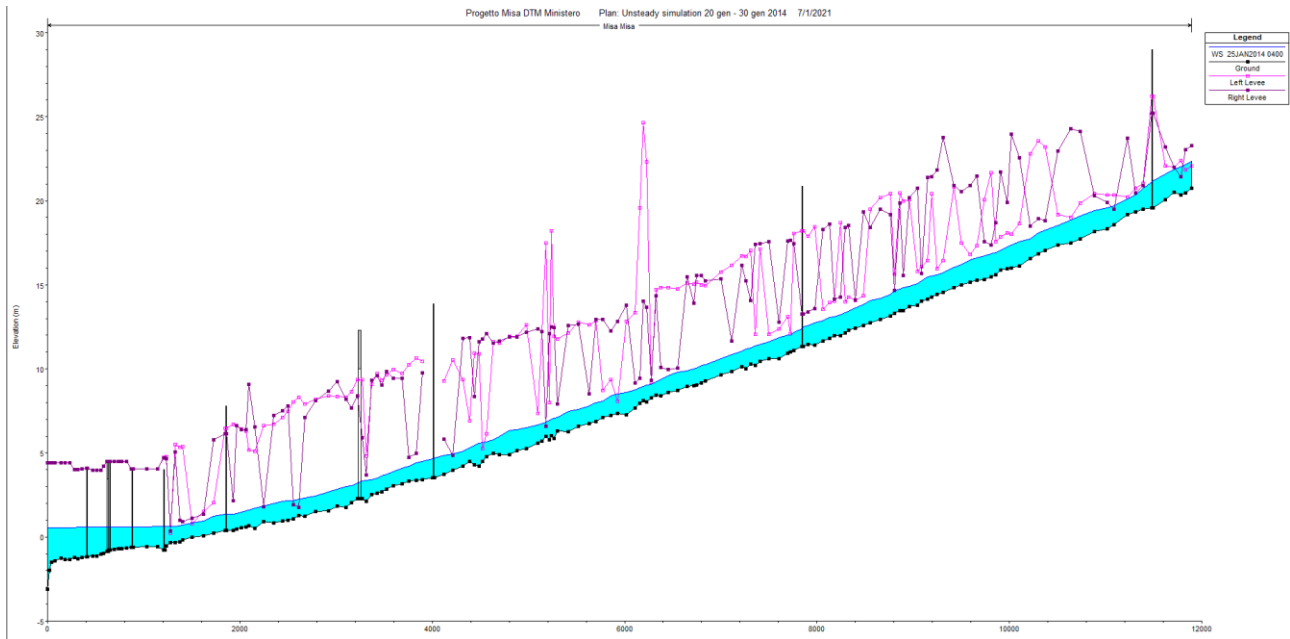


Figure 41. HEC-RAS river profile on 25th January 2014 at 4:00. The black squares represent the thalweg points of each cross-section; the light and dark purple lines stand for the left and right levee, respectively; the vertical black lines display the bridges along the river profile; the light blue area represents the water-surface elevation

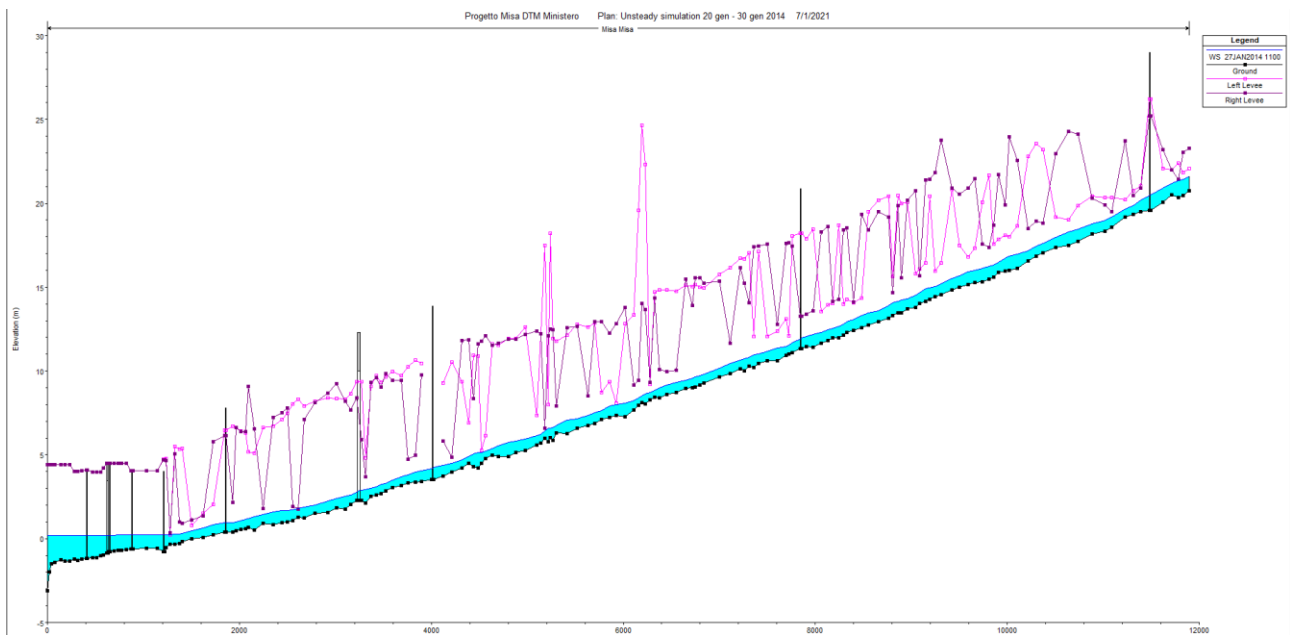


Figure 42. HEC-RAS river profile on 27th January 2014 at 11:00 under low flow conditions. The black squares represent the thalweg points of each cross-section; the light and dark purple lines stand for the left and right levee, respectively; the vertical black lines display the bridges along the river profile; the light blue area represents the water-surface elevation

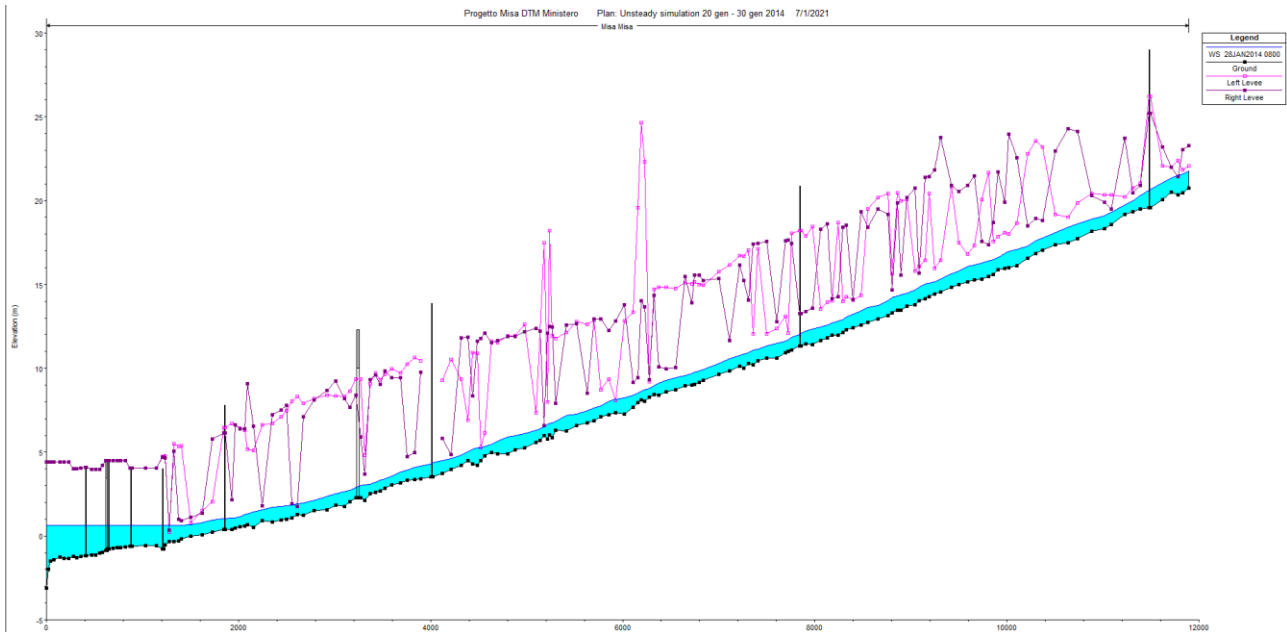


Figure 43. HEC-RAS river profile on 28th January 2014 at 8:00. The black squares represent the thalweg points of each cross-section; the light and dark purple lines stand for the left and right levee, respectively; the vertical black lines display the bridges along the river profile; the light blue area represents the water-surface elevation

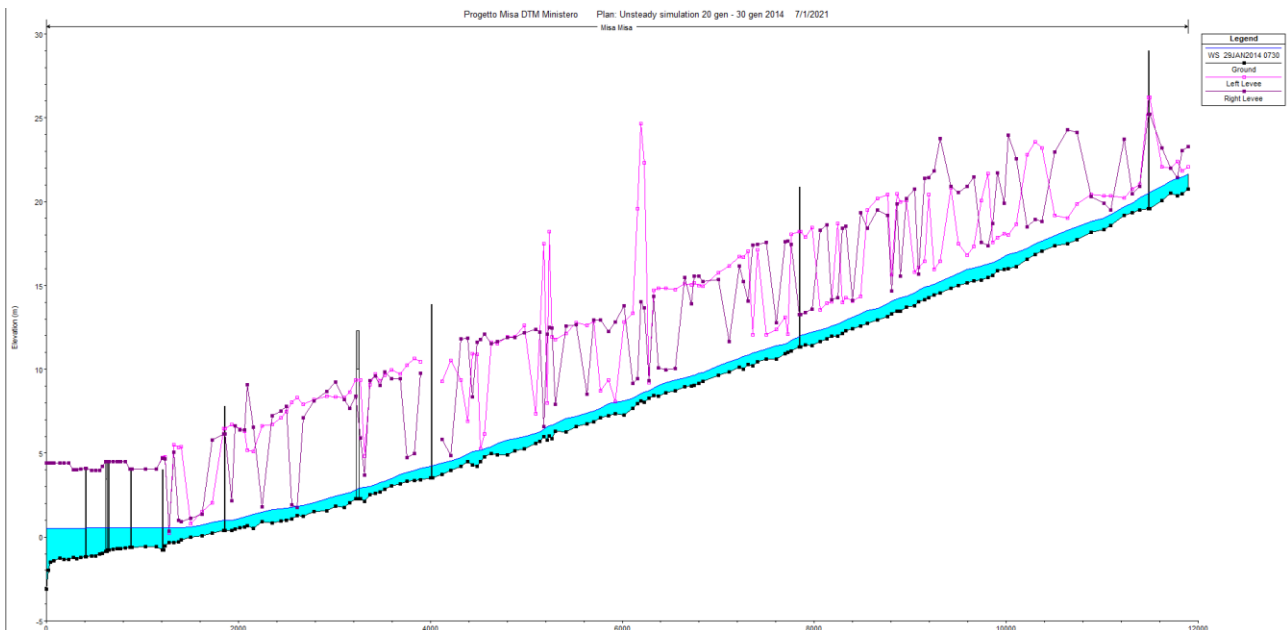


Figure 44. HEC-RAS river profile on 29th January 2014 at 7:30. The black squares represent the thalweg points of each cross-section; the light and dark purple lines stand for the left and right levee, respectively; the vertical black lines display the bridges along the river profile; the light blue area represents the water-surface elevation

3.3 River mouth bar implementation and H-ADCP data analysis

The remaining events that have been simulated through HEC-RAS are characterized by the presence of a sandbar close to the Misa River mouth. In order to get adequate results in terms of stage values, thus allowing the comparison between measured and simulated stages, the sandbar has been modelled through HEC-RAS.

Before all, additional cross-sections have been introduced in the Misa River reach near the sandbar (Figure 45 and 46) with the aim at reproducing a gradual and slow change in terms of bar extension and channel shrinkage, thus reducing the simulation instability.

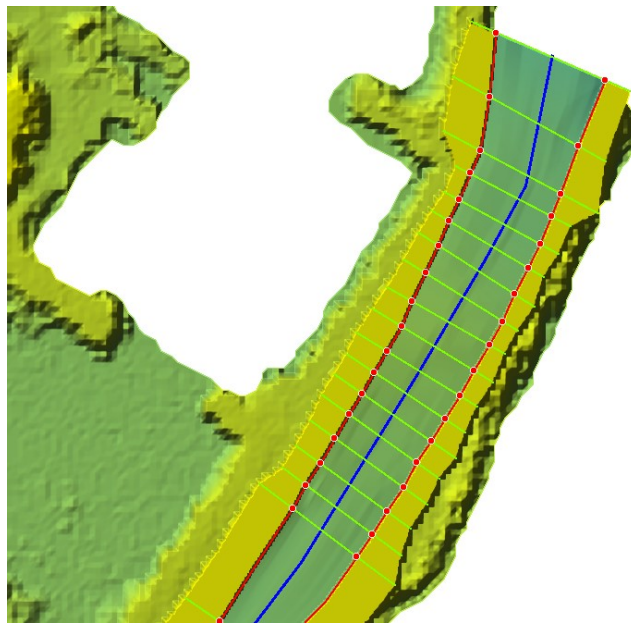


Figure 45. Addition of cross-sections in correspondence of the bar in HEC-RAS Mapper



Figure 46. Addition of cross-sections in correspondence of the bar in HEC-RAS Mapper along with Google Earth overlay

Sandbars can be modelled in different manners, including the possibility to:

- modify the HEC-RAS cross-sections located in correspondence of the sandbar;
- insert a physical obstruction;
- add an inline structure.

The first option has been selected among the three previously mentioned and consist in modifying the original cross-sections placed in correspondence and in the proximity of the sandbar. Since the bar has changed in shape throughout the considered events, this operation has been carried out twice to account for the 2019 and 2020/2021 events.

To properly characterize the sandbar cross-sections for the 2019 events, a photograph of the Misa River mouth dating back to 18th October 2019 at 15:42 has been taken as reference (Figure 47).



Figure 47. Lateral view of the river mouth bar dating back to 18th October 2019 at 15:42

Further, in order to provide an estimation of the sandbar height, it has been necessary to retrieve the tidal stage occurring at that time, that is around -0.04 m with respect to the average sea level.

Figure 48, 49 and 50 show three cross-sections depicting the upstream, central, and downstream portions of the bar for the 2019 events after carrying out several sandbar sensitivity analyses. This analysis has been conducted starting, as a first trial, by implementing the same river bar geometry of the figure; afterwards, the bar geometry has been modified in a way that the HEC-RAS simulated stages get as close as possible to the measured ones. In particular, the change in the bar characteristics has involved not only the HEC-RAS cross-sections where the bar was emerged, but also different bed forms have been applied in both neighbouring upstream and downstream cross-sections in order to ensure a gradual variation of the river bar as in reality.

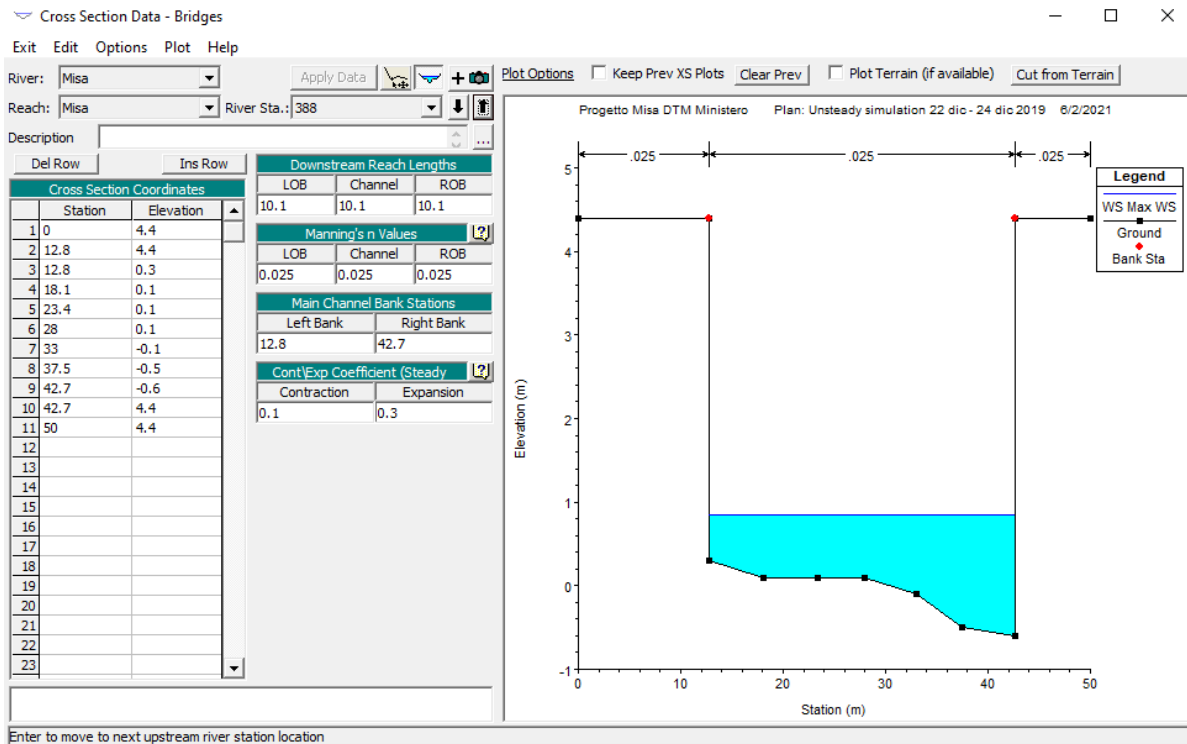


Figure 48. HEC-RAS cross-section representing the upstream portion of the river mouth bar for the 2019 events

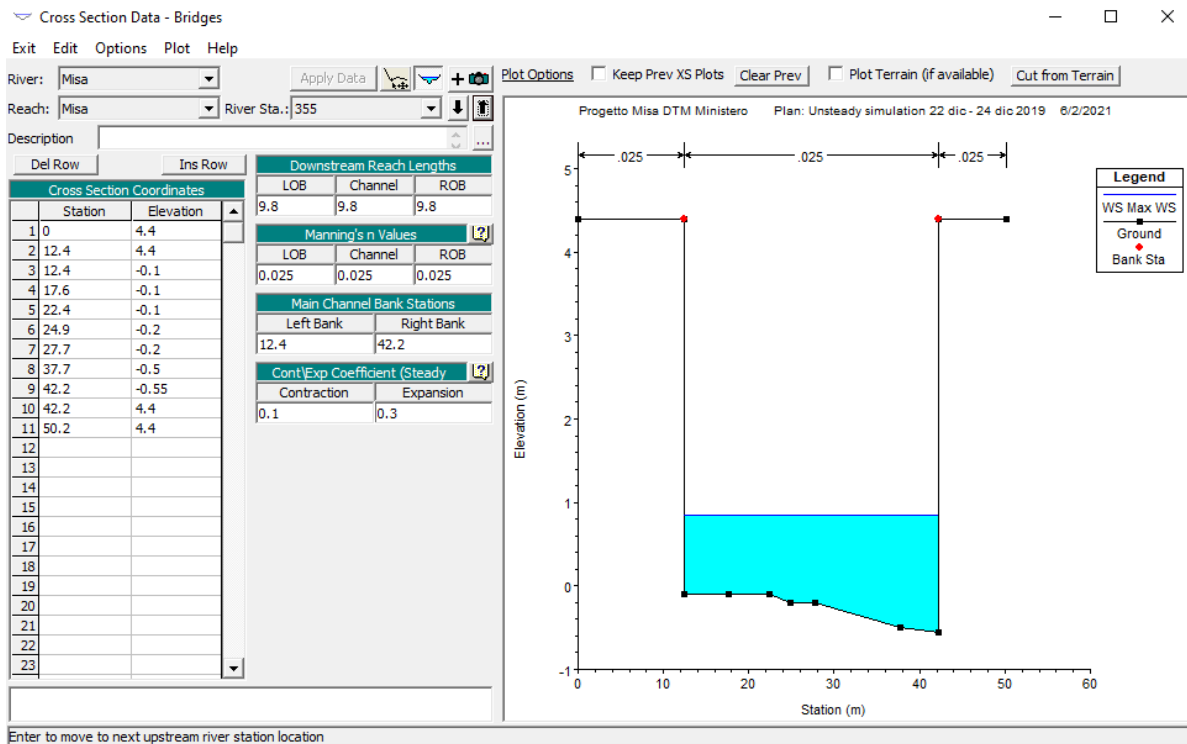


Figure 49. HEC-RAS cross-section representing the central portion of the river mouth bar for the 2019 events

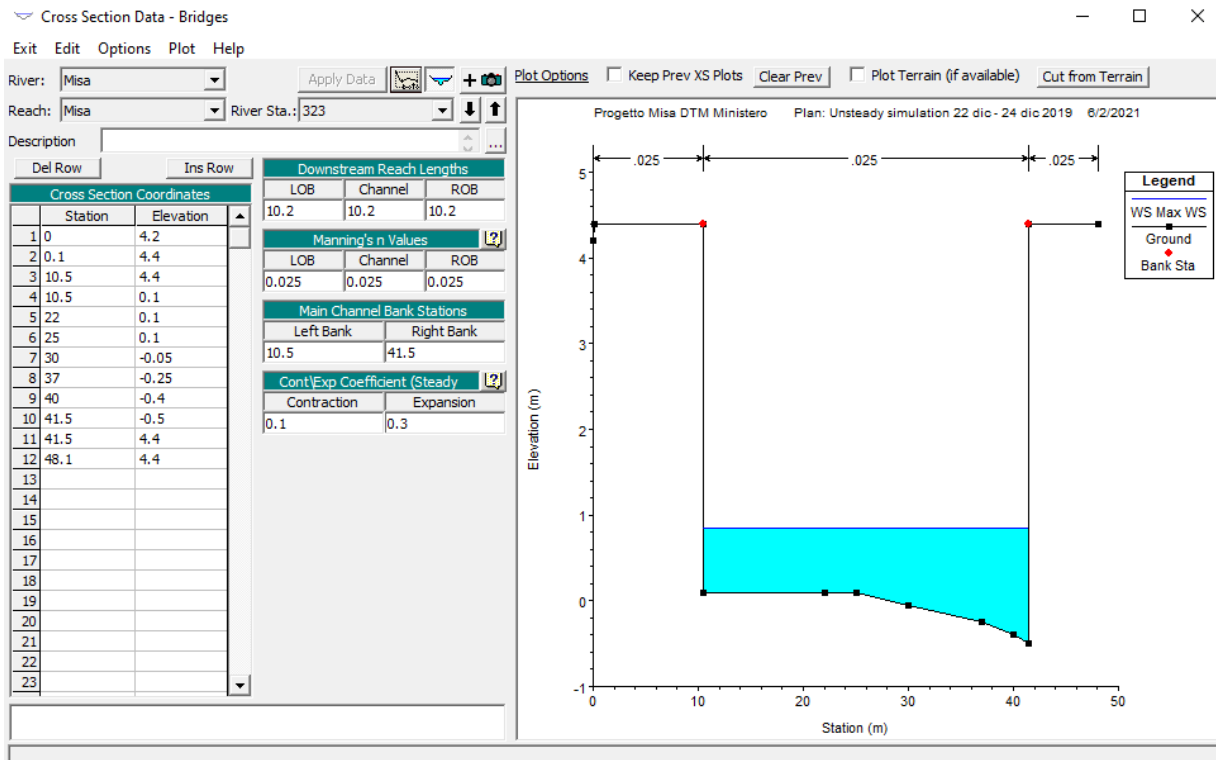


Figure 50. HEC-RAS cross-section representing the downstream portion of the river mouth bar for the 2019 events

As regards the 2020 events, a photograph of the Misa River mouth dating from 16th February 2020 at 16:09 has been taken as reference (Figure 51).



Figure 51. Lateral view of the river mouth bar dating back to 16th February 2020 at 16:09

A tidal stage of -0.28m has been measured likewise at the time the above photograph was taken, so, following the sandbar sensitivity analysis, the upstream, central, and downstream portions of the bar for the 2020 events have been represented as shown in Figure 52, 53 and 54, respectively.

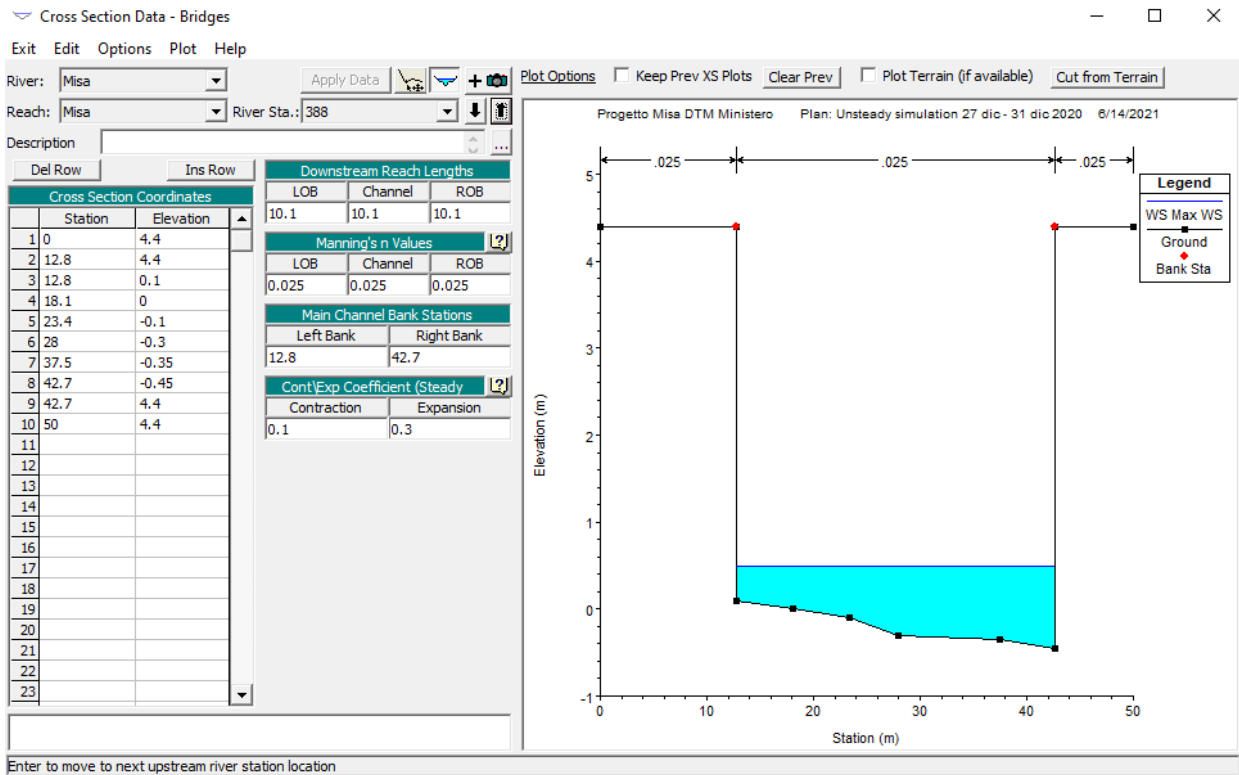


Figure 52. HEC-RAS cross-section representing the upstream portion of the river mouth bar for the 2020 events

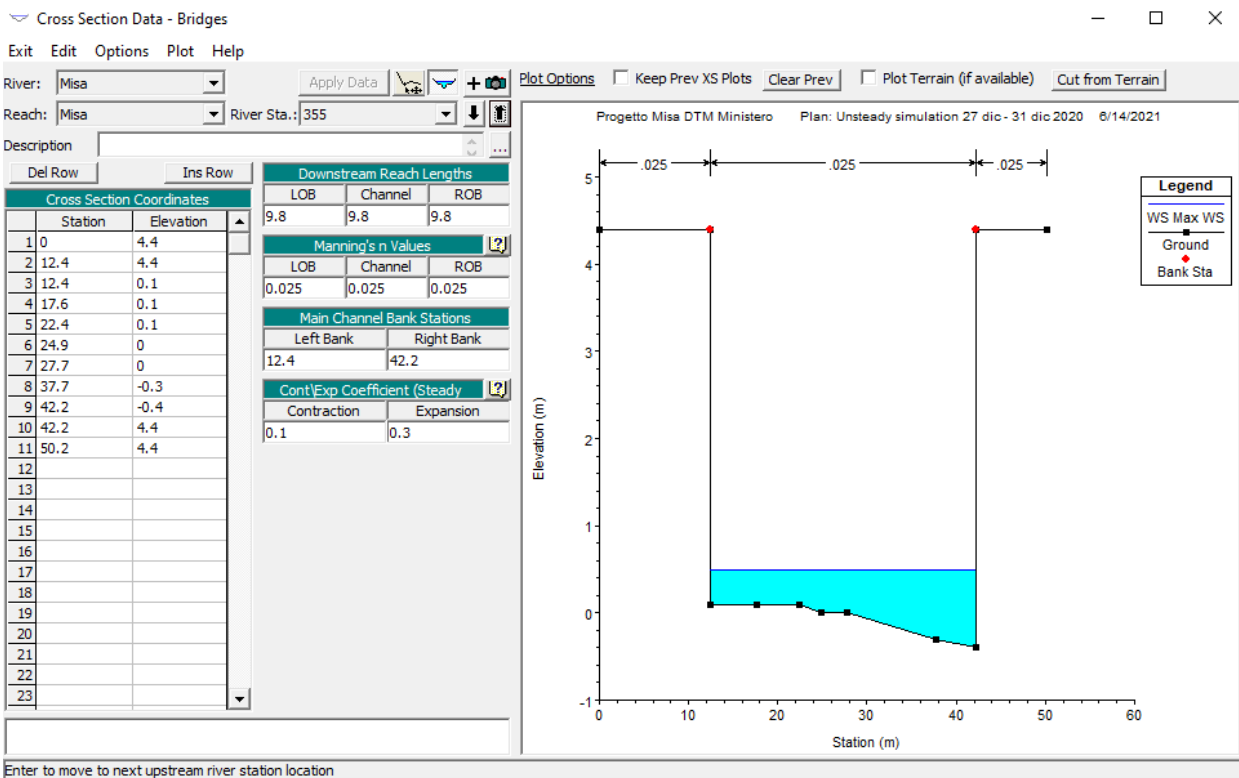


Figure 53. HEC-RAS cross-section representing the central portion of the river mouth bar for the 2020 events

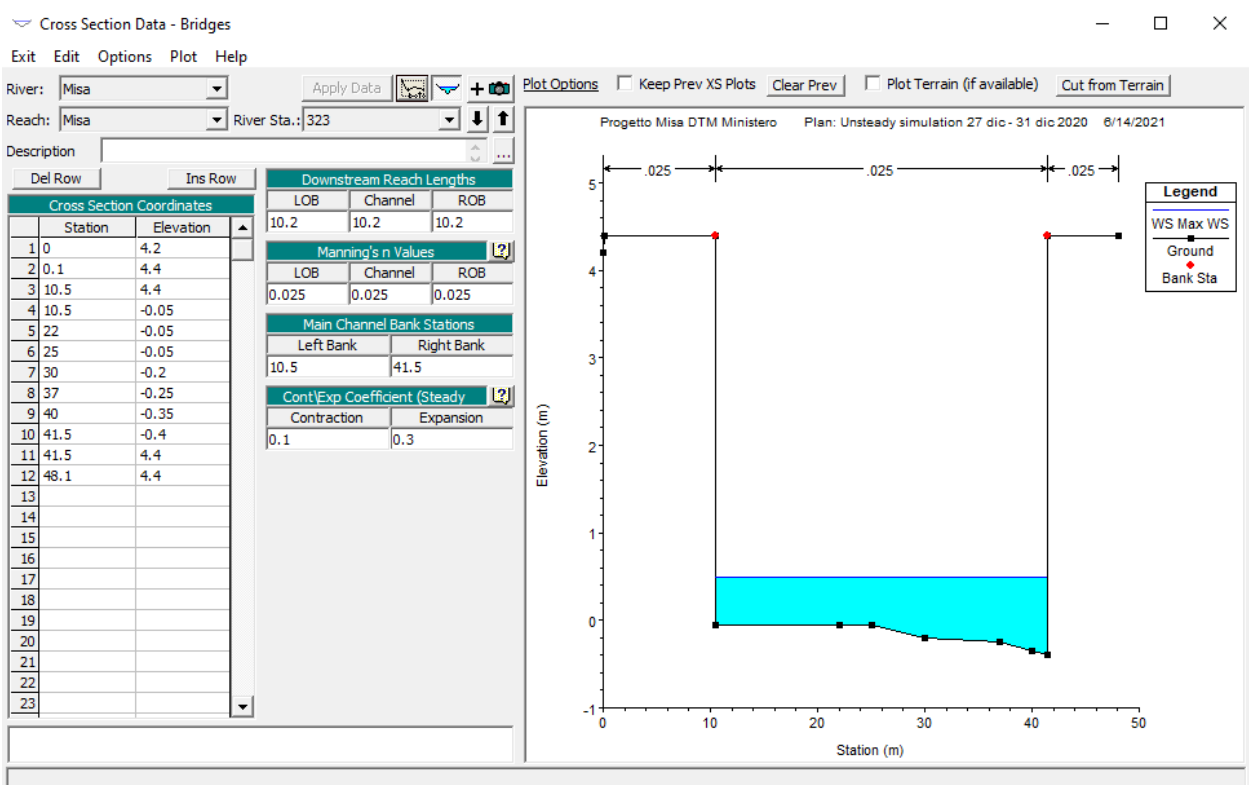


Figure 54. HEC-RAS cross-section representing the downstream portion of the river mouth bar for the 2019 events

The presence of a sandbar can be easily approximated to an obstacle located in the bottom of the channel. So, the transition of the flow over the sandbar depends, given a certain hydrograph, on the type of flow (slow or fast), and on the sandbar size. Therefore, the passage from subcritical (slow-speed flow) conditions upstream of the bar to supercritical (high-speed flow) conditions downstream of the bar occurs. To better handle this situation, the “Mixed Flow Regime” option has been selected. Figure 55 shows the Misa River ending part profile without enabling that option: as a result, a significant increase of the stages values upstream of the sandbar itself occurs because in this way HEC-RAS considers the flow as either fast or slow in its entirety.

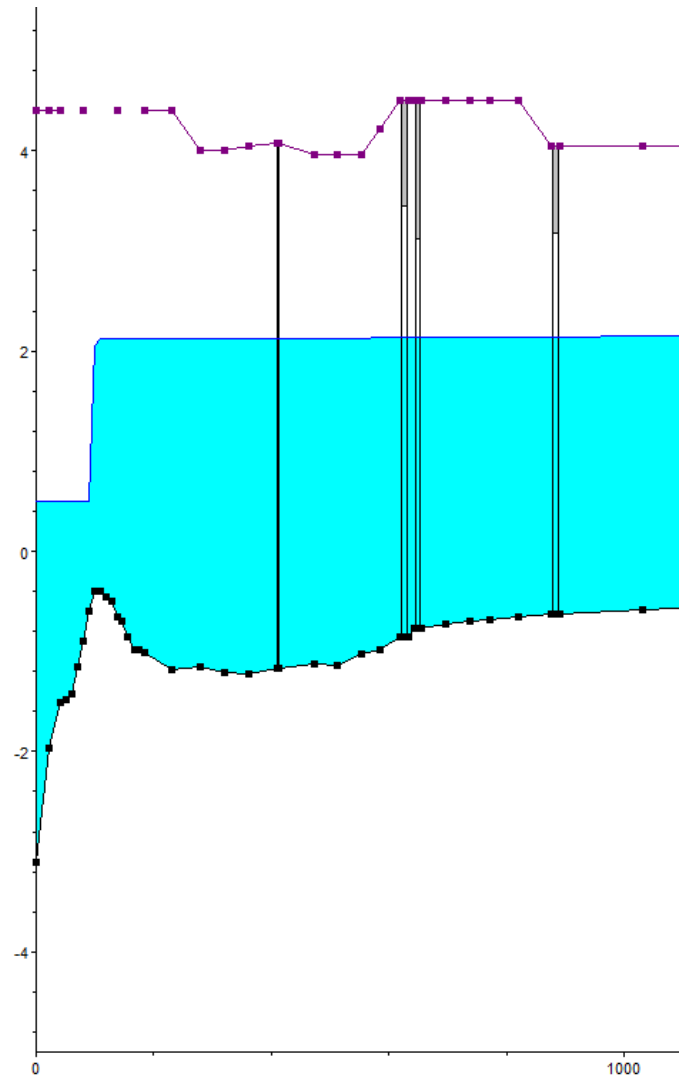


Figure 55. HEC-RAS final reach of the Misa River without the activation of the “Mixed Flow Regime” option

Figures 56 and 57 illustrate the Misa River ending part profile, respectively, two among the 2019 and 2020 events in the case of activation of the “Mixed Flow Regime” option, combined to the adjustment of the sandbar neighbouring thalweg points, to avoid a sudden variation of the hydraulic properties between cross-sections, which may bring to instability. In the Figure 54, the y-axis corresponds to the water-surface elevation, whereas the x-axis stands for the main channel distance (both expressed in meters). Moreover, the black squares represent the thalweg points for each extracted cross-section, while the light and dark purple lines identify the left and right levees, respectively, of each cross-section. Besides, the vertical lines refer to the location of the bridges along the river profile, whereas the light blue area displays the water-surface elevation.

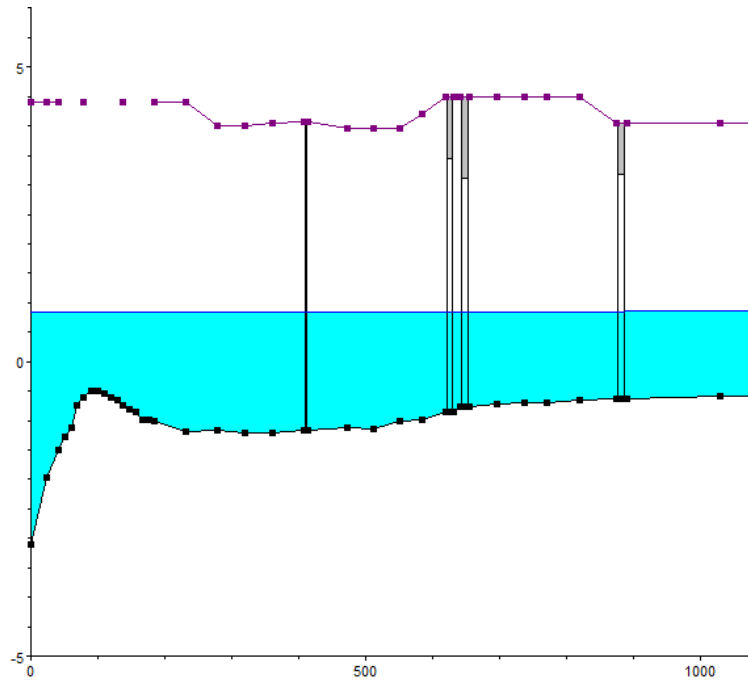


Figure 56. HEC-RAS final reach of the Misa River for one of the 2019 events with the activation of the "Mixed Flow Regime" option

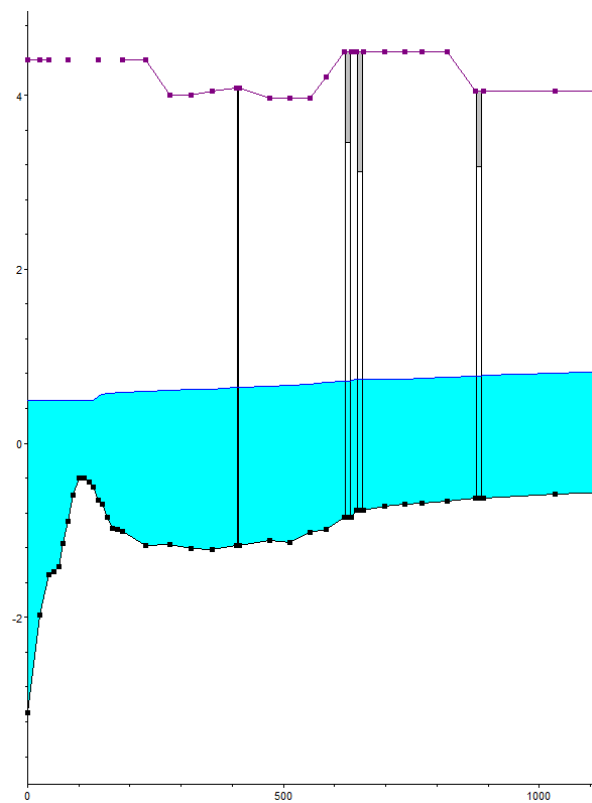


Figure 57. HEC-RAS final reach of the Misa River for one of the 2020 events with the activation of the "Mixed Flow Regime" option

Figure 58 shows an example of a HEC-RAS Mapper simulation results where the sandbar is quite emerged under low flow conditions. On the other hand, the high flow conditions promote the complete submergence of the sandbar, which retains the sea water (Figure 59), followed by the sandbar shape modification.

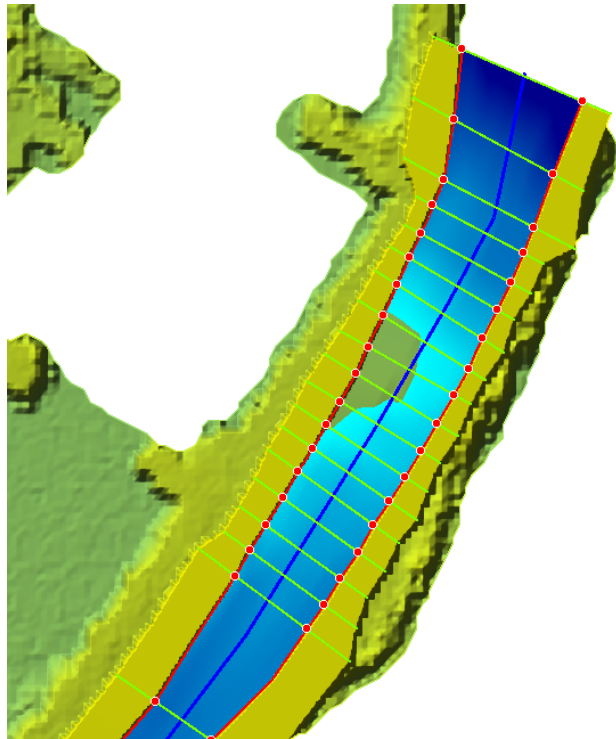


Figure 58. HEC-RAS Mapper simulation results displaying the river mouth bar under low flow conditions

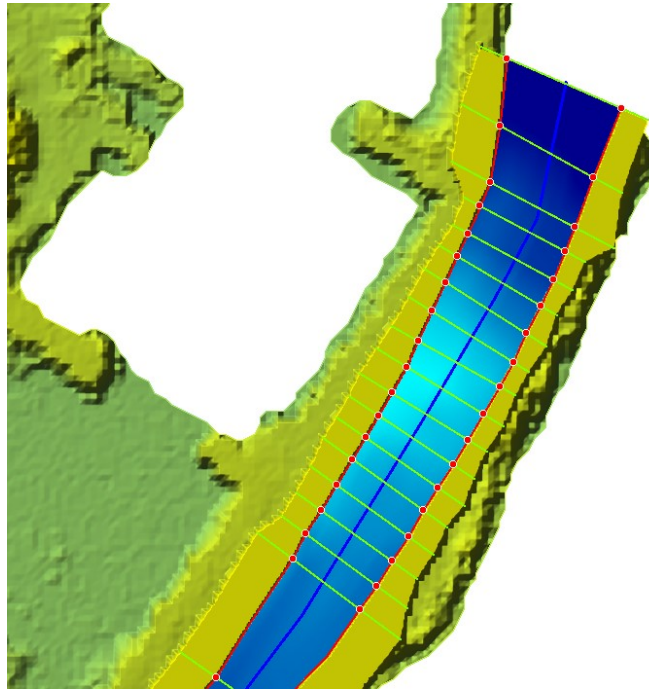


Figure 59. HEC-RAS Mapper simulation results displaying the river mouth bar under high flow conditions

The remaining events have been simulated with and without the presence of the sandbar because of the uncertainty in terms of the sandbar shape and geometry. For each event, the configuration that better provides a correspondence between the measured and the simulated stages has been chosen. Besides, the H-ADCP recorded stages and discharges have been included in all the remaining events except for the 10th – 13th January event, due to the lack of enough reliable data with the purpose of checking the reliability of the H-ADCP river gauge measurements.

3.3.1 2019 events

The first event that has been looked into involves a time period that goes from 26th May 2019 at 00:00 to 1st of June 2019 at 23:30.

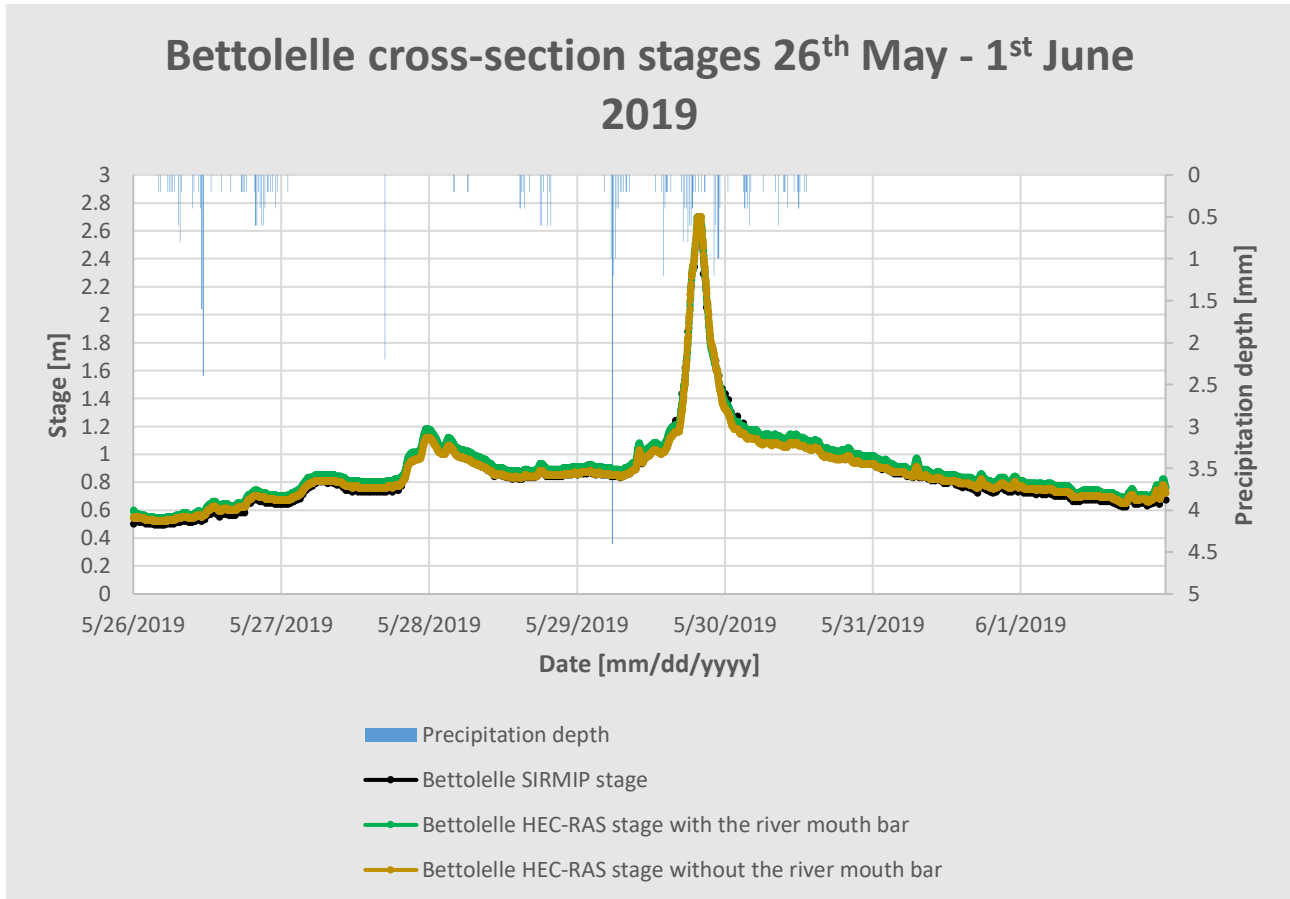


Figure 60. Simulation results at Bettollele cross-section for the 26th May – 1st June 2019 event

Figure 60 shows the comparison between SIRMIP stages and HEC-RAS stages at Bettollele cross-section.

Observing both Bettollele HEC-RAS stage with and without the presence of the sandbar, the latter graph is the one which gets closer to the SIRMIP stage series except for the peak zone.

Conversely, the unsteady simulation, performed with the addition of the bar, has provided results with a perfect matching in the peak zone and slightly higher differences far from it (either way less than 10 cm). This is due to the fact that the sandbar effect is felt less moving upriver. However, both HEC-RAS series are very similar, thus implying a negligible influence of the bar at Bettollele.

In correspondence of the H-ADCP cross-section, the H-ADCP data measured from 29th May 2019 17:32 to 30th May 2019 03:16 have been added to provide a comparison with HEC-RAS simulated stages. In particular, both HEC-RAS series turns out to be similar to the SIRMIP one in correspondence of the peak (Figure 61), with a slight overestimation by the HEC-RAS stages characterized by the presence of the bar (solid green line) with respect to the SIRMIP values, and a little underestimation by the HEC-RAS stages characterized by the absence of the bar (solid brown line). Additionally, in correspondence of the decreasing limb of the stage hydrograph and immediately before the ending of H-ADCP data recording, the solid green line appears to better fit the SIRMIP line. The HEC-RAS stage lines comprising of the bar is always higher than the SIRMIP measured stage line since, being the Misa River study reach mild sloped and slow, the presence of a quite high sandbar together with the significant shrinkage associated with it leads the upstream flow to increase its minimum energy in order to overcome it, and to do so, an increase of the stages upstream of the sandbar comes out. The minimum energy is reached when the critical condition is established in correspondence of the sandbar; finally, the flow accelerates, thus becoming fast flow downstream of the sandbar itself. Moreover, the presence of the bar induces a reduction in terms of tides effect on the associated stage series, especially when higher discharges occur, whereas a greater correspondence of trends is observed in the case without the river mouth bar.

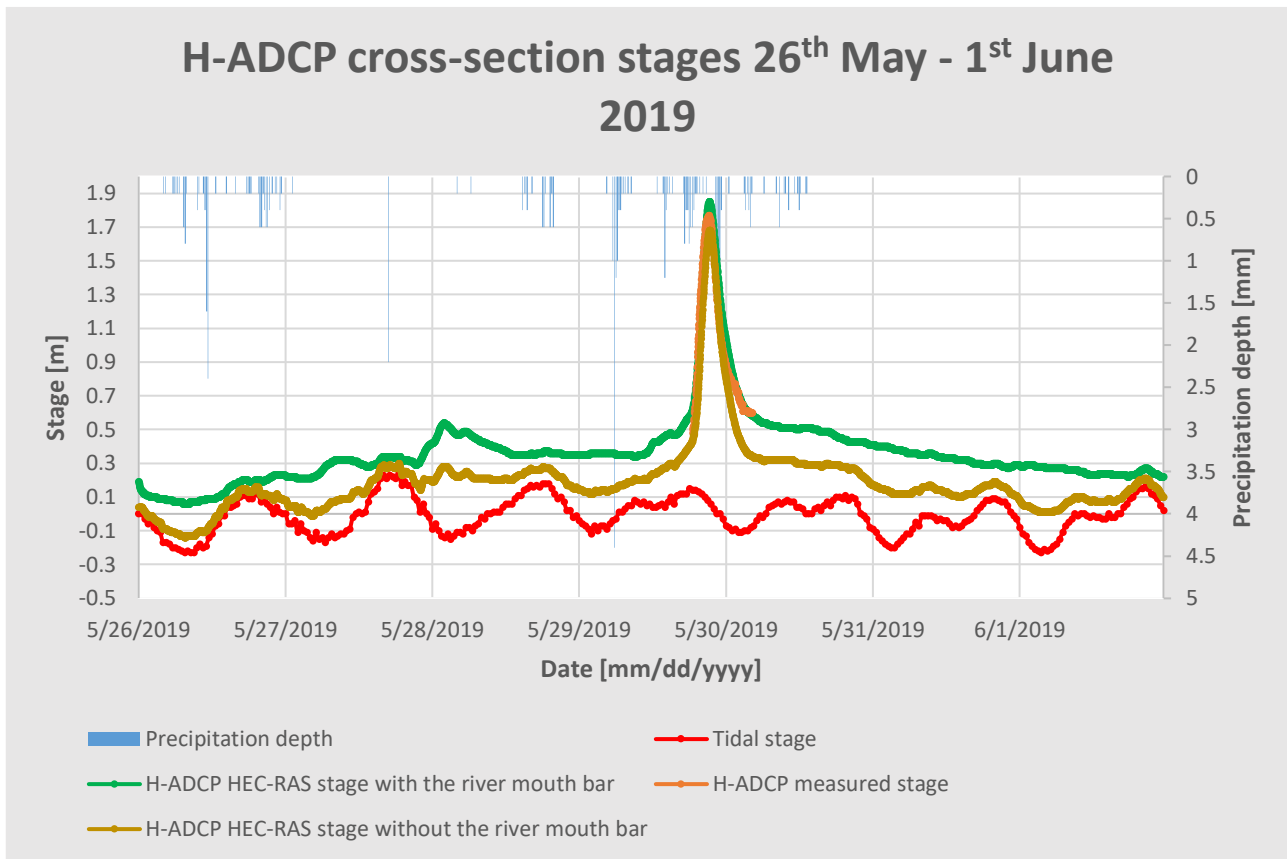


Figure 61. Simulation results at H-ADCP cross-section for the 26th May – 1st June 2019 event

The same comparison has been carried out in correspondence of Ponte Garibaldi cross-section as well (Figure 62). Specifically, as in the previous plot, the simulated stage which is the closest to SIRMIP stage is the one that does not include the presence of the river mouth bar, while an overestimation of the stages and a minor effect of tides are looking at when the bar is present in the model.

Ponte Garibaldi cross-section stages 26th May - 1st June 2019

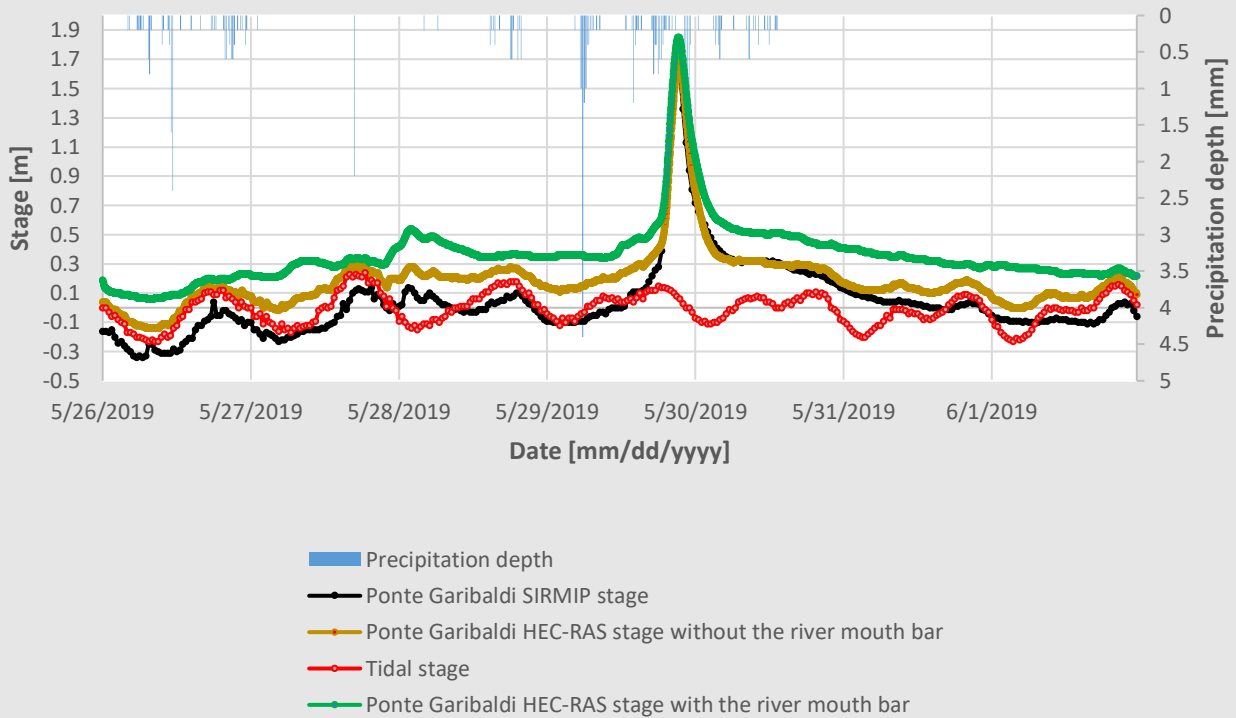


Figure 62. Simulation results at Ponte Garibaldi cross-section for the 26th May – 1st June 2019 event

The H-ADCP measured discharge data have been compared to the HEC-RAS one retrieved from the H-ADCP cross-section (Figure 63) with the goal of checking the robustness of the H-ADCP river gauge. Firstly, discharge values outliers have been filtered, resulting in the figure. In particular, the H-ADCP measured data trend seems to follow the HEC-RAS one, even though the recorded data looks larger than those predicted by the model. The reason why this discrepancy exists lies probably on the fact that the HEC-RAS curve does not include the runoff contribution between Bettolle and Ponte Garibaldi. Another reason could be the partial recording of the H-ADCP, this only accounting for the leftmost portion of the cross-section (i.e., included within about 8m from the left bank, where the instrument is installed). Negligible differences in terms of HEC-RAS discharge values are noticed whether or not the river mouth bar is considered.

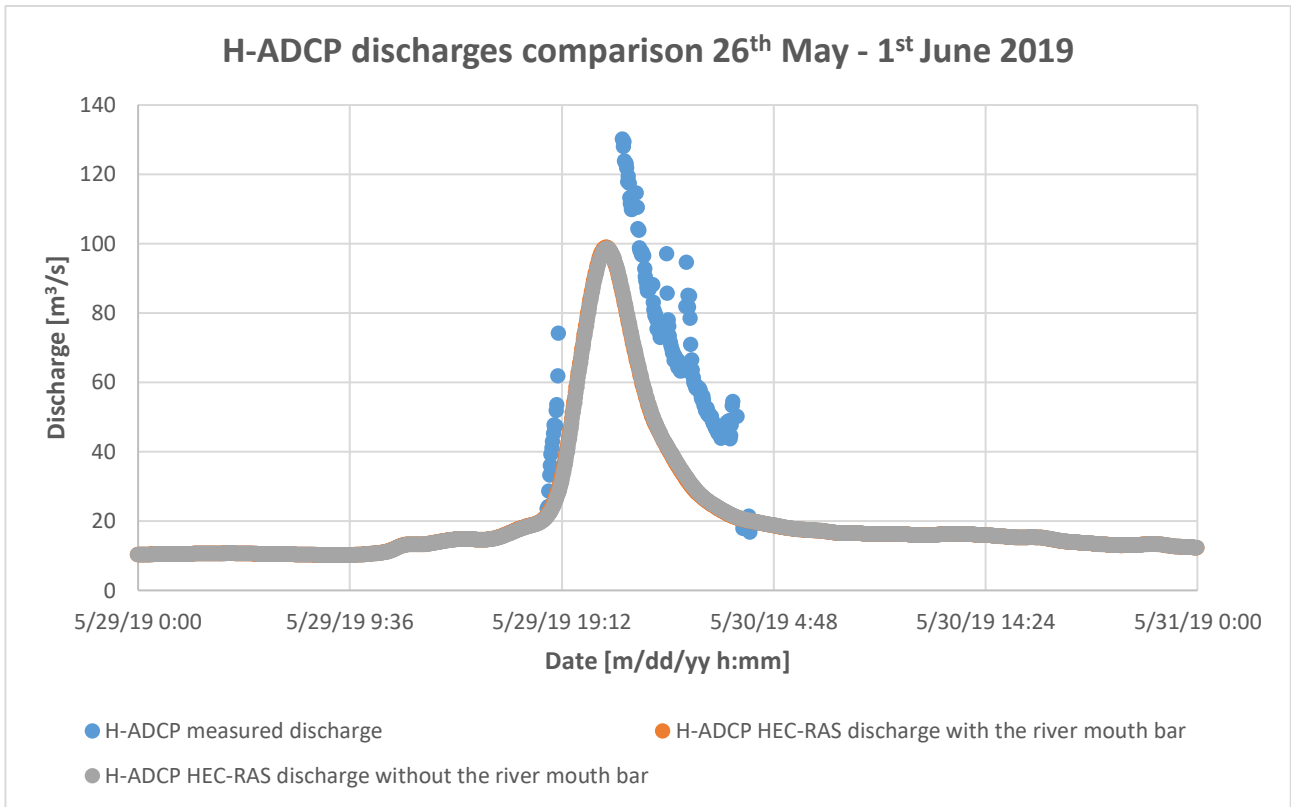


Figure 63. H-ADCP discharges comparison for the 26th May – 1st June 2019 event

Figures 64 and 65 show the H-ADCP discharges scatter plot in case of the presence and the absence of the bar.

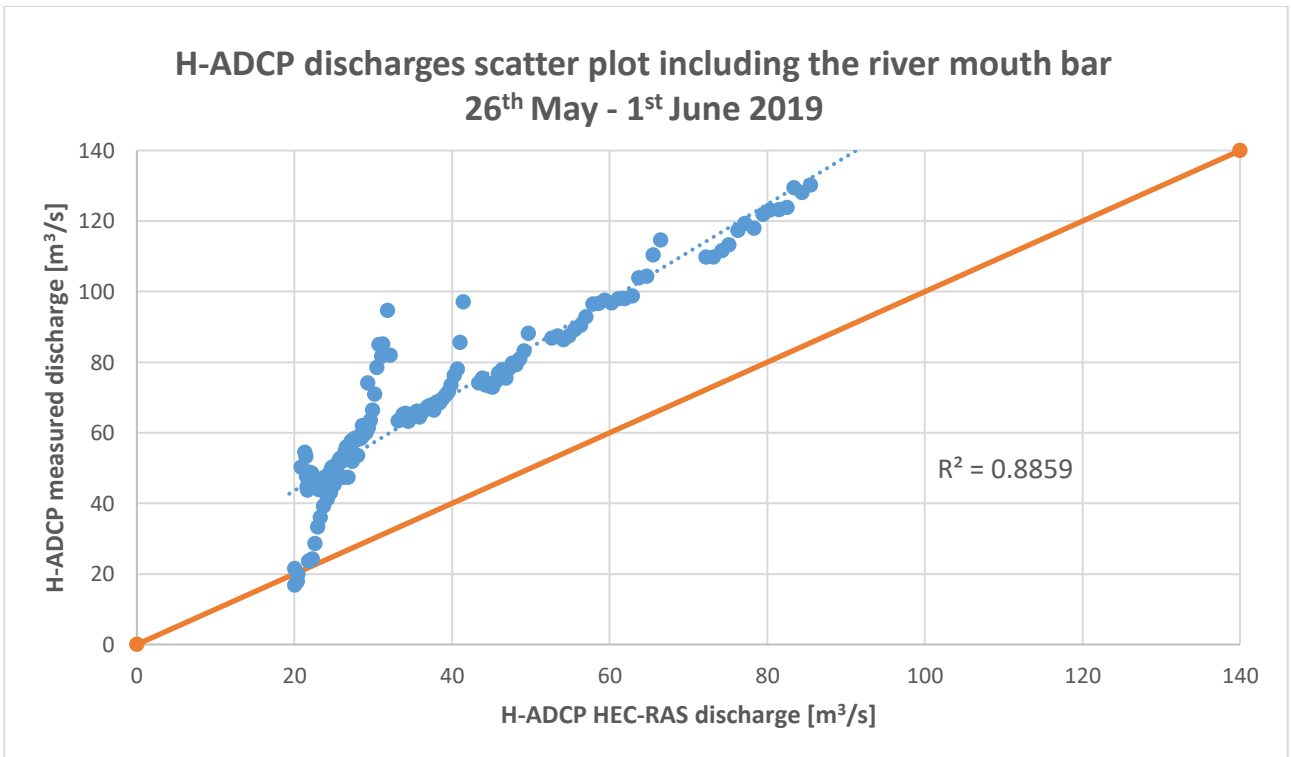


Figure 64. H-ADCP discharges scatter plot including the river mouth bar for the 26th May – 1st June 2019 event

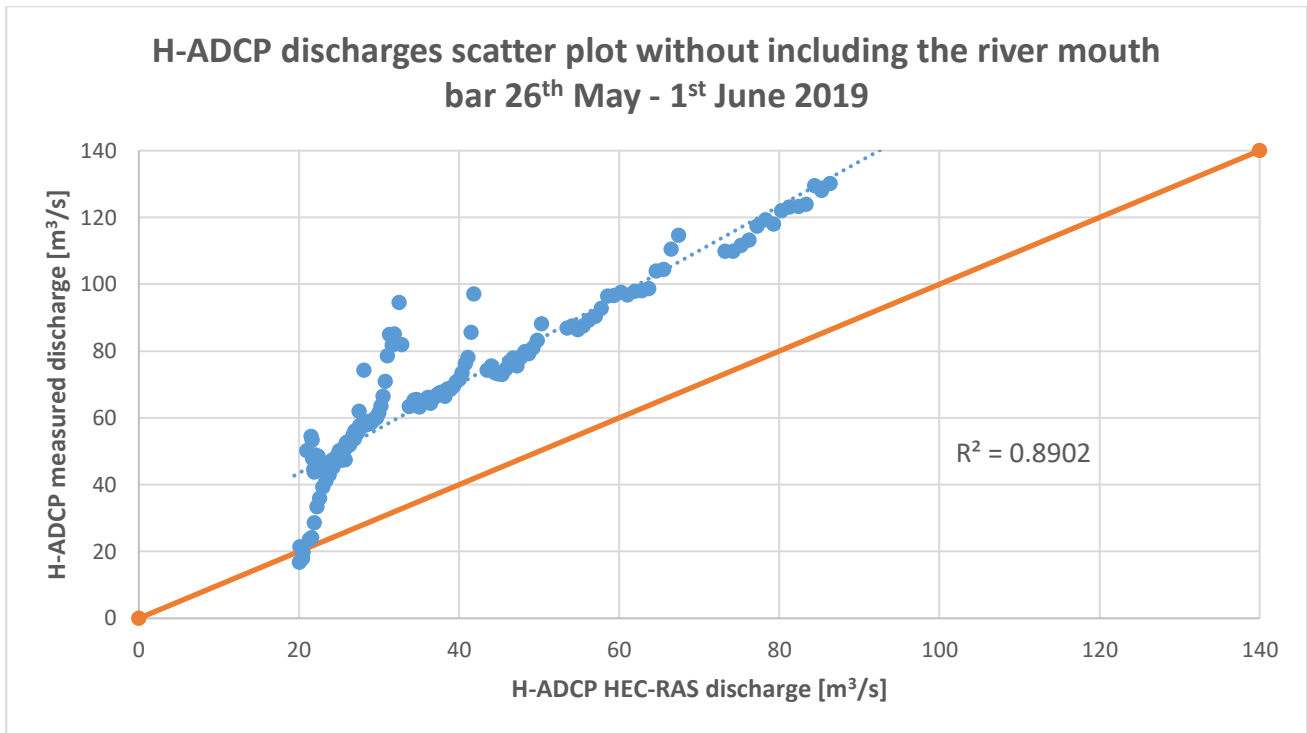


Figure 65. H-ADCP discharges scatter plot without including the river mouth bar for the 26th May – 1st June 2019 event

In both cases, as seen in the previous graph, the H-ADCP discharge points are nearly all above the bisector line, which states the perfect matching between the two variables. Consequently, a quite relevant overestimation of the H-ADCP measured data towards the HEC-RAS simulated ones is present. Moreover, the determination coefficients R^2 related to a linear regression of the data are quite high and almost similar, thus indicating that, albeit the discrepancy between collected and simulated data, an almost linear trend exists between the H-ADCP measured data and the HEC-RAS ones.

No information about the sandbar characteristics is available for the considered period. Anyway, two photographs taken by the SGS station are available to try to understand the bar geometry, i.e., one before the event dating back to 16th May 2019 (Figure 66) and other one following the event dating back to 11st June 2019 (Figure 67).



Figure 66. The Misa River mouth photograph taken by the SGS station on 16th May 2019



Figure 67. The Misa River mouth photograph taken by the SGS station on 11st June 2019

These images illustrate that, the sandbar was not emerged during the chosen period, even though a remarkable submerged accumulation of sediment was present.

Moreover, while the beige curve seems to follow the tidal stage trend, this does not occur in the case of the green curve where the dam effect exerted by the sandbar over the tides is felt.

Figure 68 shows the shape of the sandbar under minimum flow conditions following the unsteady simulation of the considered event in HEC-RAS Mapper.

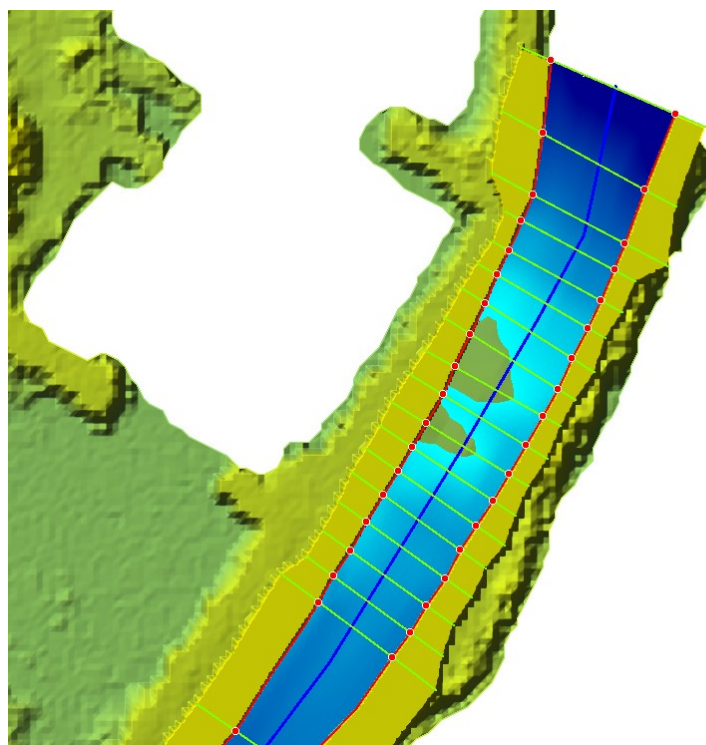


Figure 68. HEC-RAS Mapper simulation results displaying the river mouth bar under minimum flow conditions for the 26th May – 1st June 2019 event

The next event that has been analysed goes from 9th November 2019 at 00:00 to 15th November 2019 at 23:30.

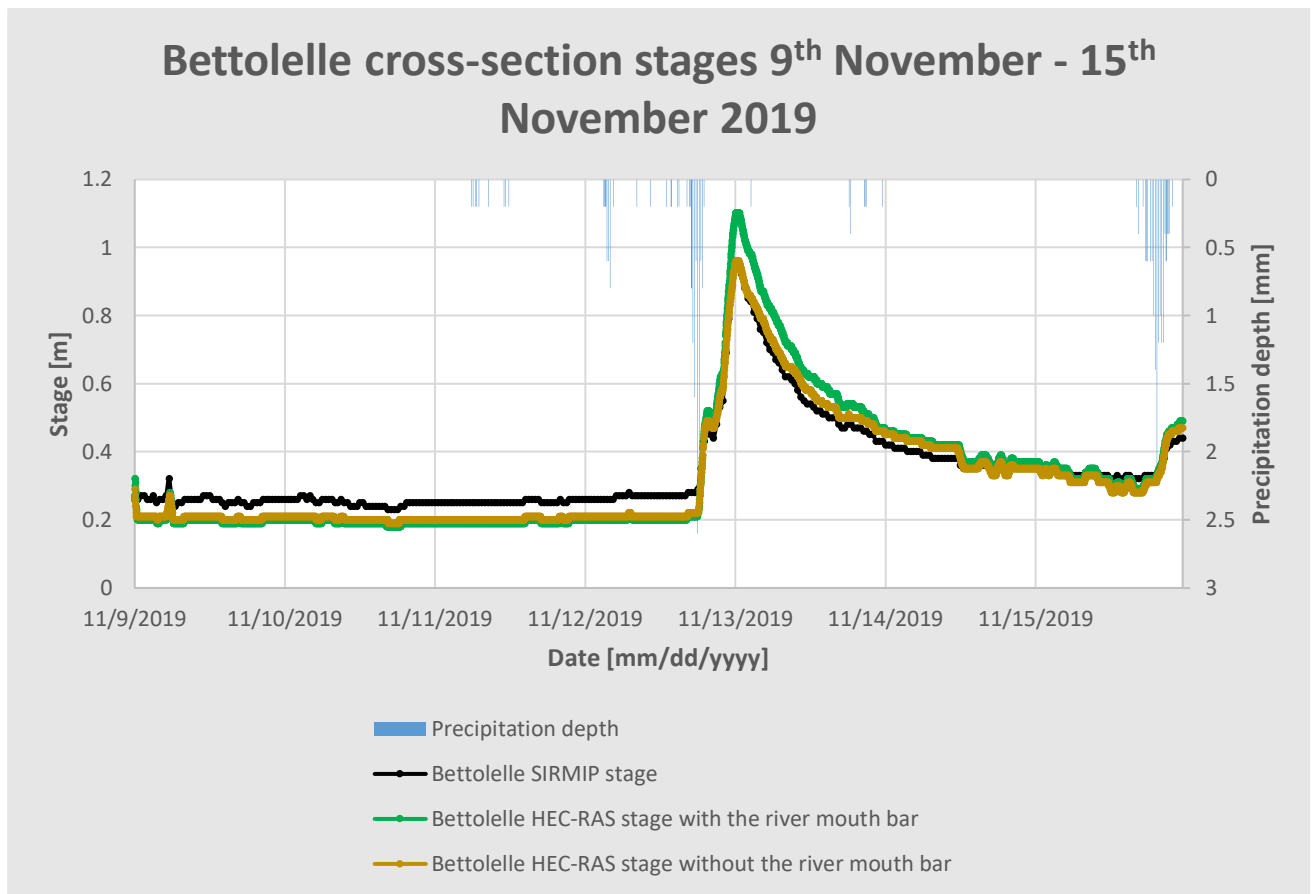


Figure 70. Simulation results at Bettollelle cross-section for the 9th November – 15th November 2019 event

As regards Bettollelle cross-section, the HEC-RAS stages without the addition of the bar has a better matching than the curve associated with the bar presence, especially from the main peak occurrence onward (Figure 70).

A particularity is observed in Figure 71 where both H-ADCP HEC-RAS simulated stage curves are almost overlapped. In fact, since the event was characterized by quite low discharge values (less than 12 m³/s) at Bettollelle location, the sandbar exerts a sort of barrier against the river flow, which does not manage to cross the bar itself. As a result, the increase of the upriver stages results to be limited or negligible. Furthermore, the event is marked by positive tides, which makes both the HEC-RAS curves to overlap with the tide (solid red line).

Furthermore, the H-ADCP measured stages seem to follow both the HEC-RAS curves for most of the time with a good approximation.

H-ADCP cross-section stages 9th November - 15th November 2019

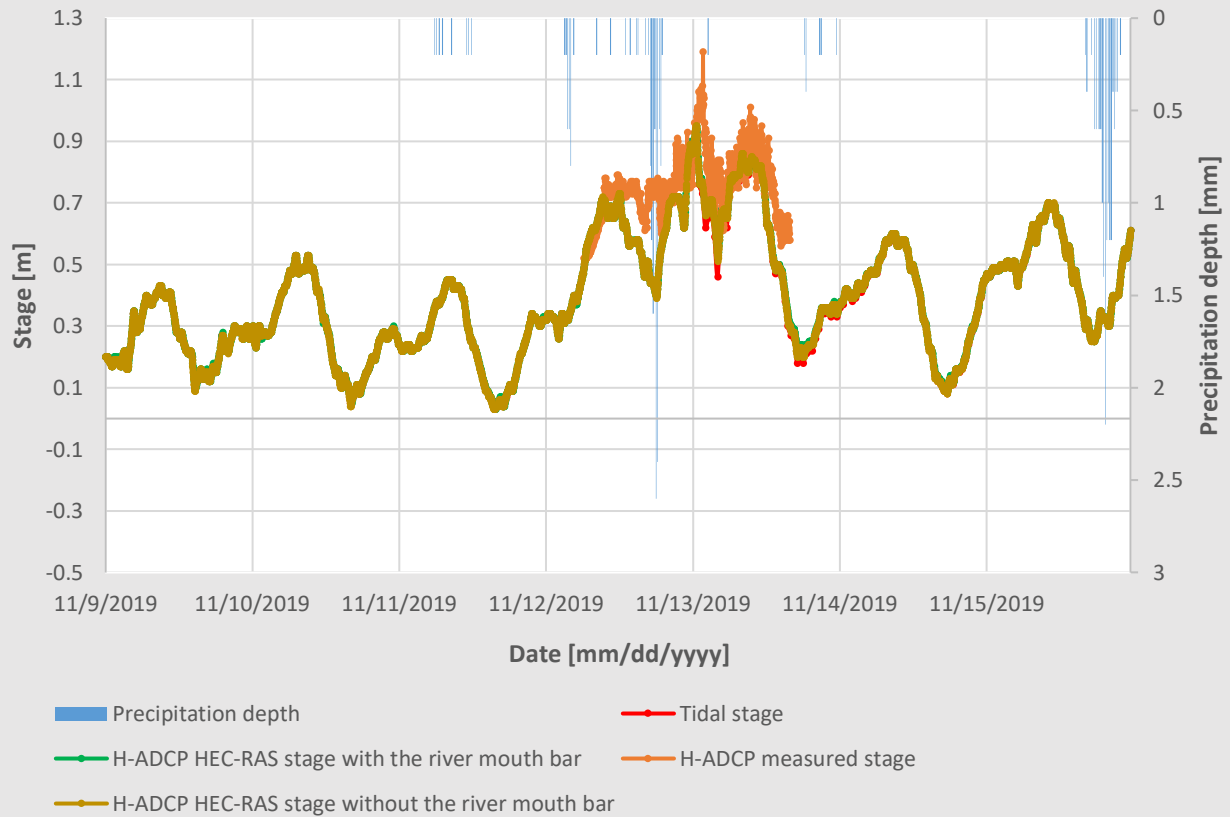


Figure 71. Simulation results at H-ADCP cross-section for the 9th November – 15th November 2019 event

The same behaviour in terms of HEC-RAS stages arises also at Ponte Garibaldi cross-section (Figure 72); in addition, both HEC-RAS stages series result to be a little bit translated upward, thus highlighting the existence of an emerged bar, which surface is not particularly wide. Further, the SIRMIP stages (solid black line) seems to be less influenced by the tide.

Ponte Garibaldi cross-section stages 9th November - 15th November 2019

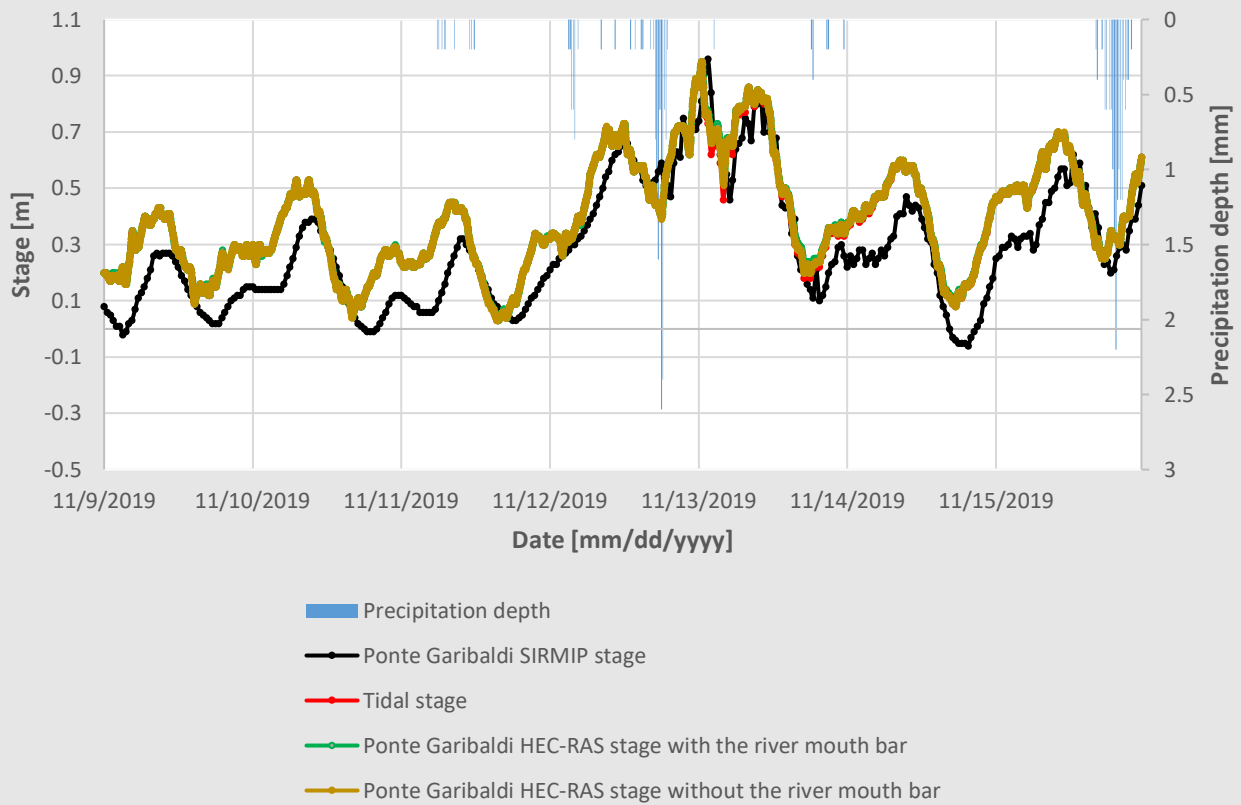


Figure 72. Simulation results at Ponte Garibaldi cross-section for the 9th November – 15th November 2019 event

In this event, a better matching between discharges exists, especially in the initial part of the hydrograph, probably because of the lower runoff contribution caused by lower discharges (figure 73).

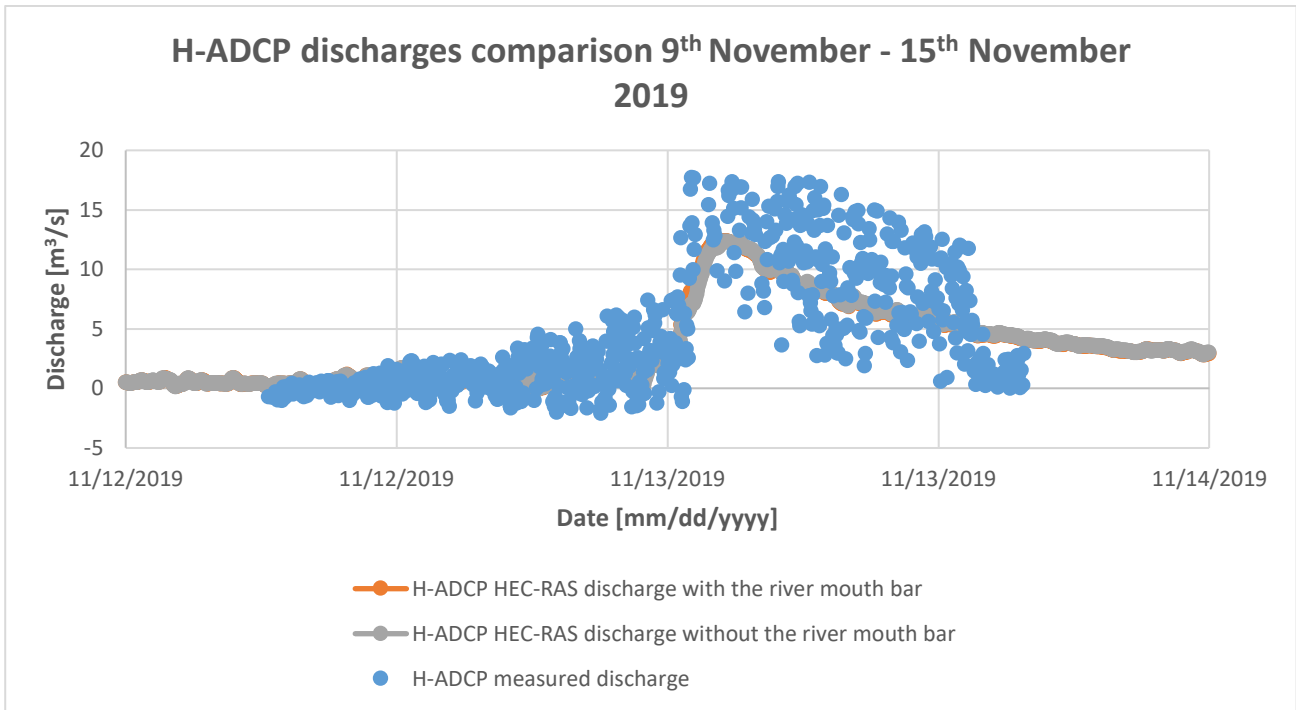


Figure 73. H-ADCP discharges comparison for the 9th November – 15th November 2019 event

This is confirmed by looking at both the scatter plots including whether or not the river bar (Figure 74 and 75): inter alia, although the R^2 coefficient turns out to be smaller than the one of the previous event, the simulated results are displaced all around the bisector and better represent the recorded data.

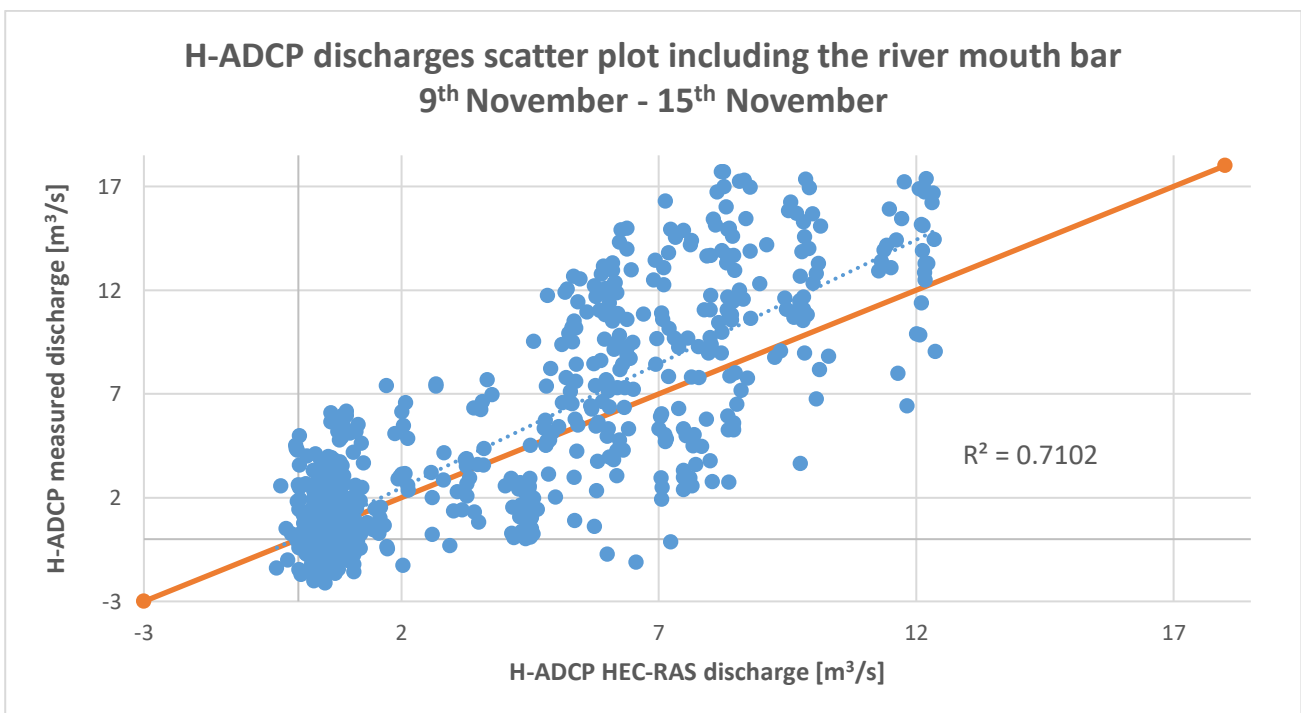


Figure 74. H-ADCP discharges scatter plot including the river mouth bar for the 9th November – 15th November 2019 event

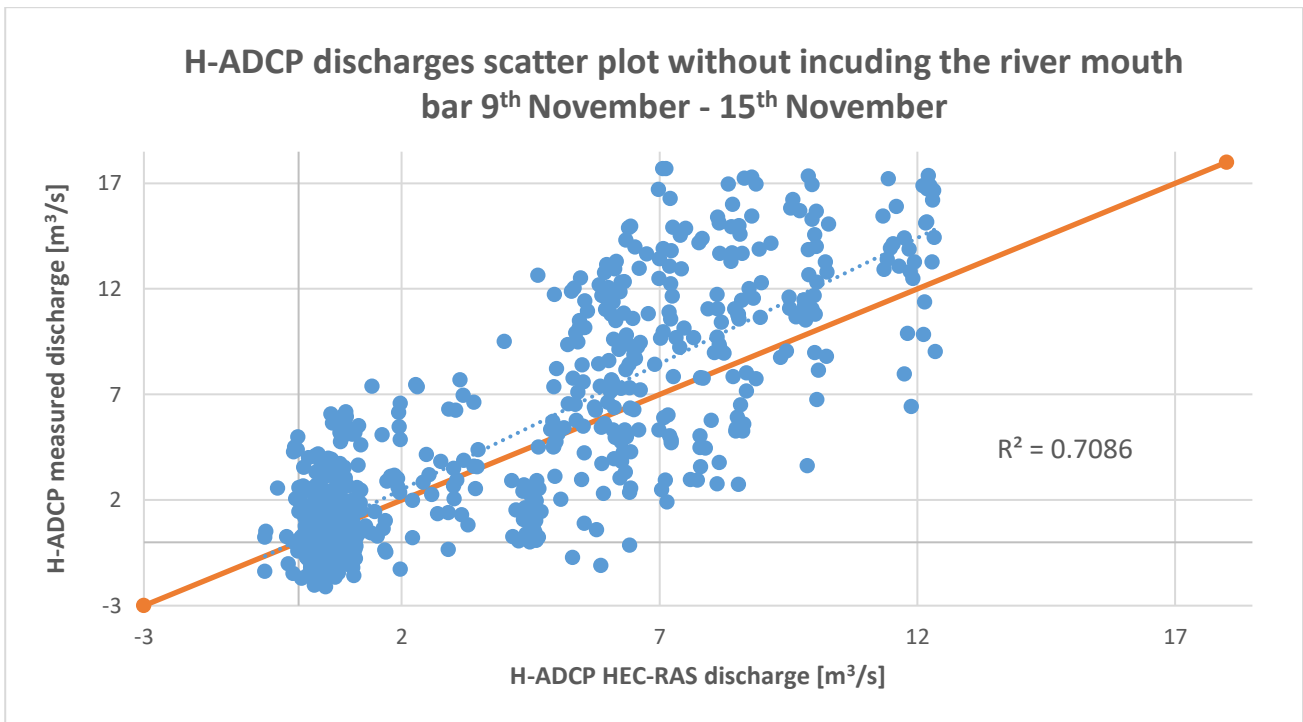


Figure 75. H-ADCP discharges scatter plot without including the river mouth bar for the 9th November – 15th November 2019 event

To have an idea about the river mouth bar morphology and to confirm what has been said above, a photograph taken by the SGS the 9th of November 2019 (Figure 76) has been taken into account.



Figure 76. The Misa River mouth photograph taken by the SGS station on 9th November 2019

Figure 77 shows the emerging part of the sandbar in HEC-RAS mapper under the minimum water level conditions after carrying the event simulation.

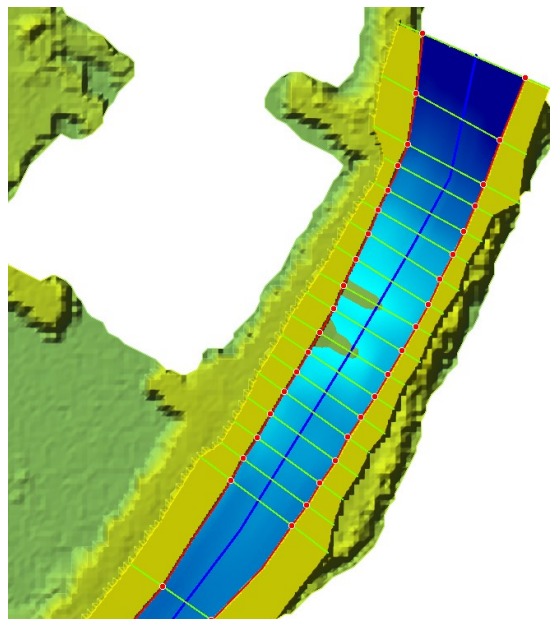


Figure 77. HEC-RAS Mapper simulation results displaying the river mouth bar under minimum flow conditions for the 9th November –15th November 2019 event

The third event that has been investigated deals with a time interval which ranges from 22nd December 2019 at 00:00 to 24th December 2019 at 23:30.

As in the previous event, at Bettollelle cross-section, the difference between the two HEC-RAS stages curves (Figure 78) is not significant meaning that the bar effect is felt less far from the river mouth. Further, there is not a significant gap between the SIRMIP measured and HEC-RAS simulated stages.

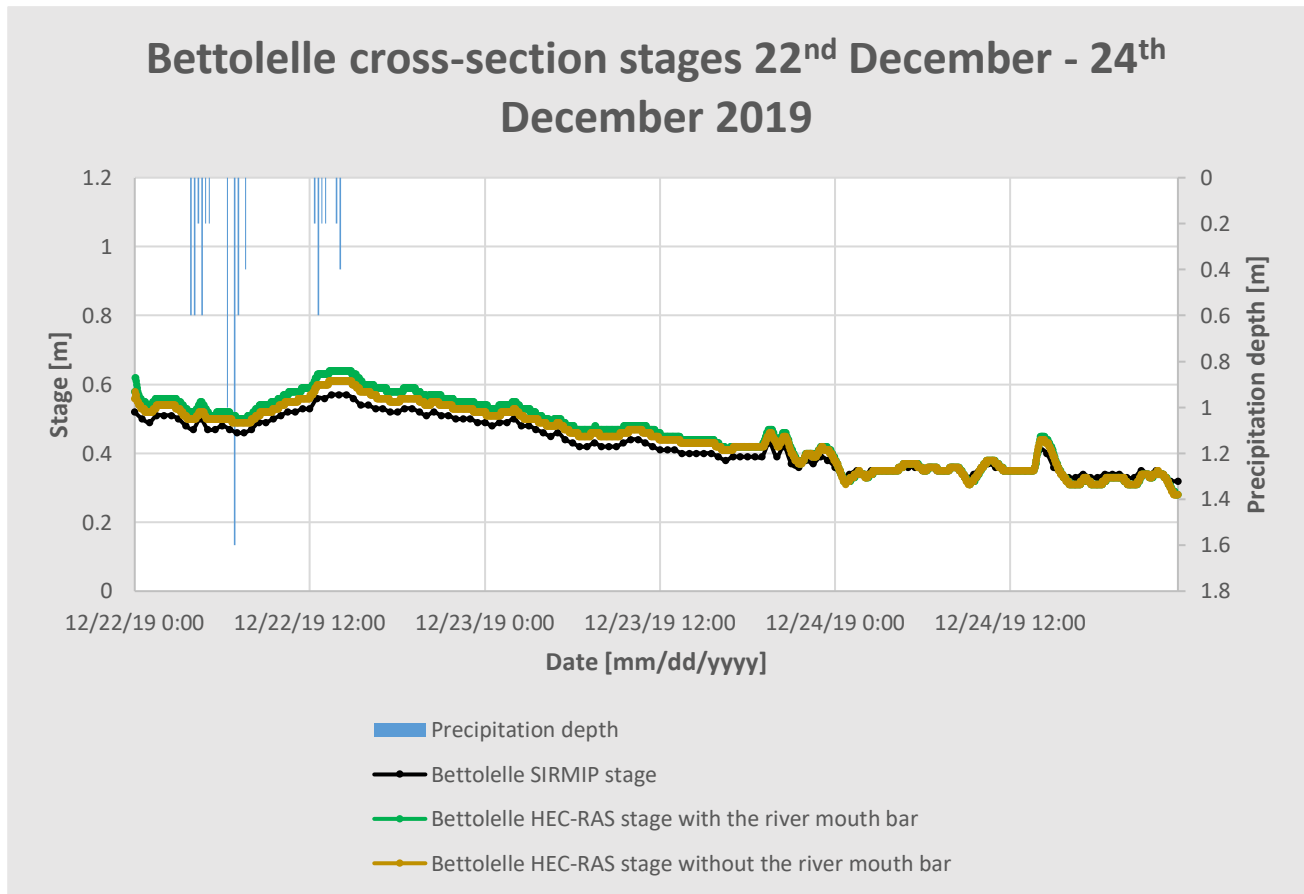


Figure 78. Simulation results at Bettollelle cross-section for the 22nd December – 24th December 2019 event

In the Figure 79, the H-ADCP curve seems to be quite shifted rightward with respect to both HEC-RAS curves. This event is characterized by even lower discharge values than the previously described one and by remarkable tidal oscillations. As regards the configuration without the river mouth bar, stages are perfectly aligned with the tidal ones, hence, the tides overwhelm the incoming river discharge.

Focusing on the case comprising of the bar, at high tides occurrence, there is a perfect matching in terms of stages, meaning that the river mouth bar does not lead to an increase of the upstream

stages. On the other way around, in correspondence of the lowest tide peaks, the effect of the bar over the tide is felt in a major way: namely, the more negative the tidal stages are, the higher the discrepancy between the HEC-RAS stage curves will be.

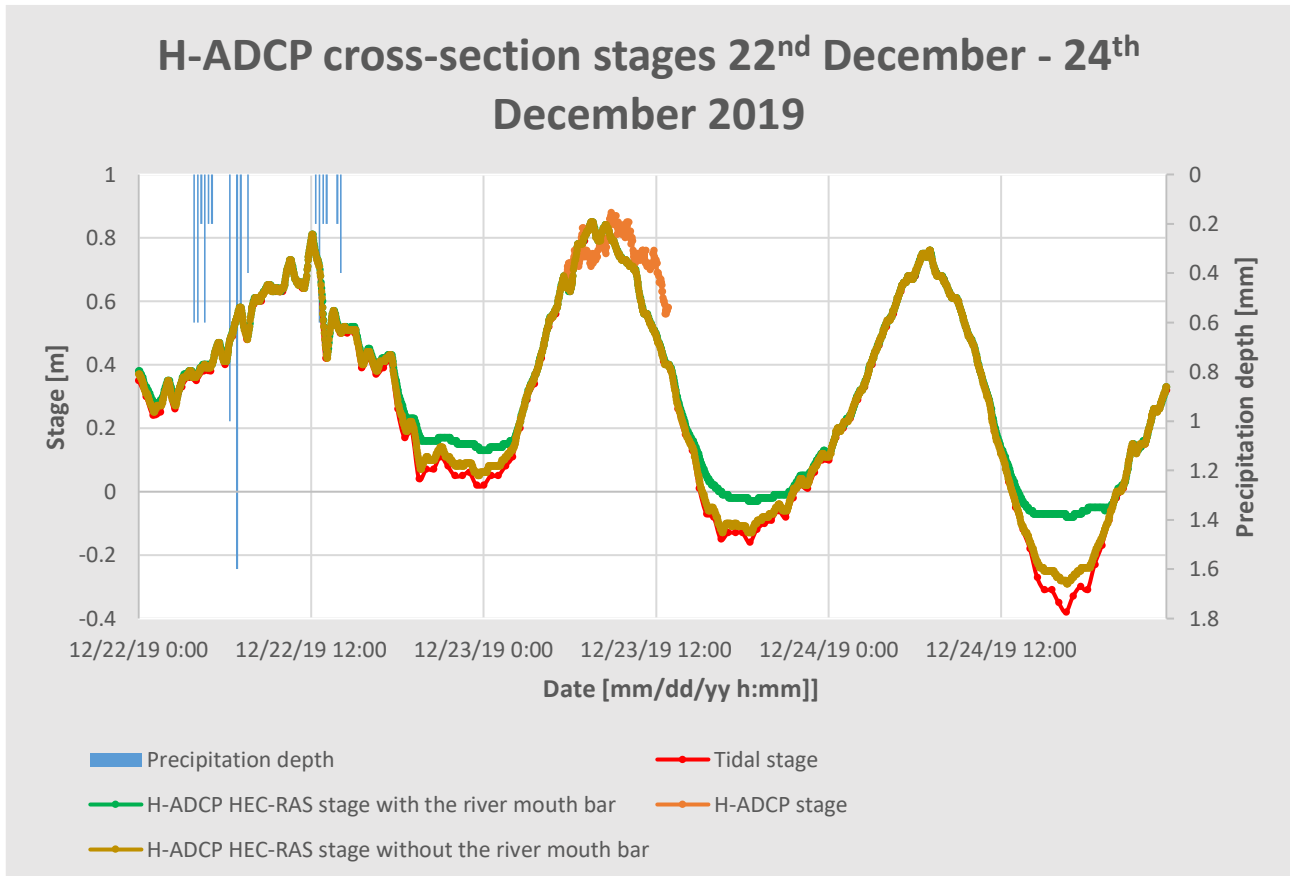


Figure 79. Simulation results at H-ADCP cross-section for the 22nd December – 24th December 2019 event

The plot showing the comparison of stages at Ponte Garibaldi cross-section reveals a little time shifting of the HEC-RAS results with respect to the SIRMIP measured stages (Figure 80). Nevertheless, the same considerations that have been previously done for the H-ADCP cross-section are valid for Ponte Garibaldi cross-section too.

Ponte Garibaldi cross-section stages 22nd December - 24th December 2019

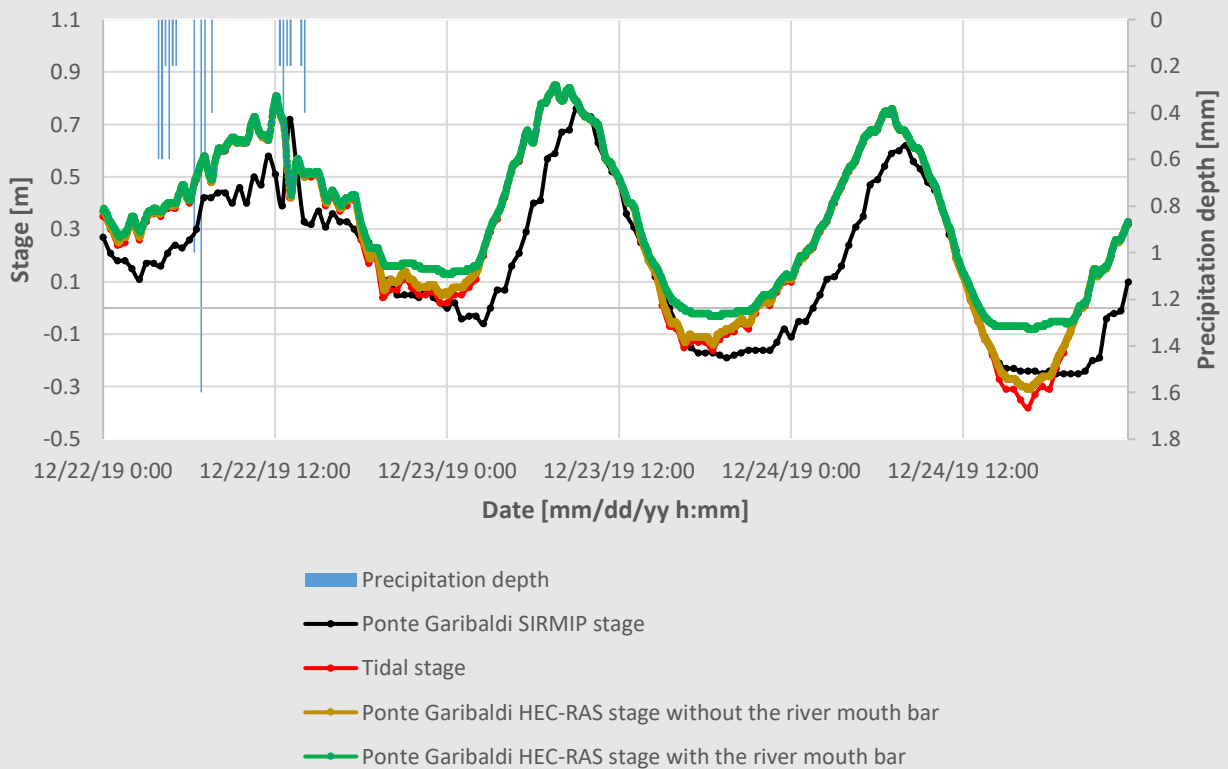


Figure 80. Simulation results at Ponte Garibaldi cross-section for the 22nd December – 24th December 2019 event

H-ADCP discharge data are mostly below both the HEC-RAS discharge curves (Figure 81), albeit differences in terms of discharge are quite low (less than 2 m³/s) probably due to the reduced portion of cross-section recorded by the H-ADCP.

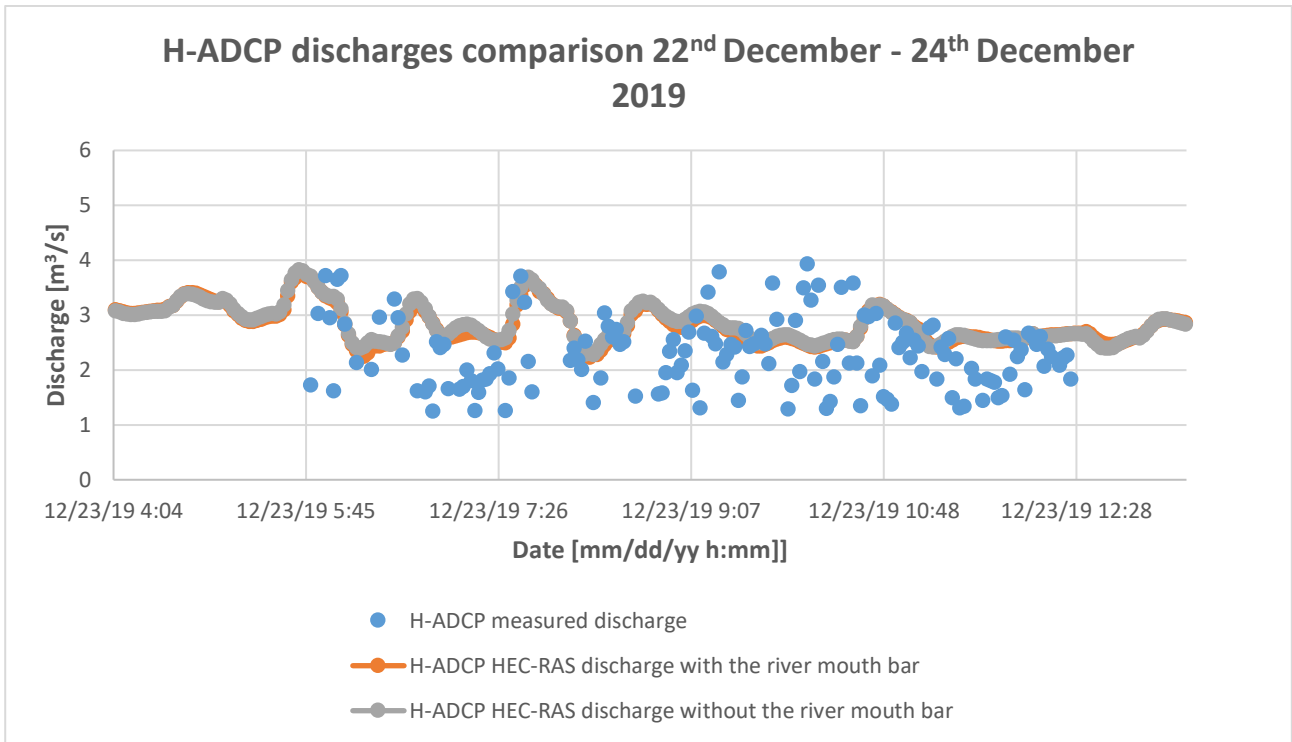


Figure 81. H-ADCP discharges comparison for the 22nd December – 24th December 2019 event

Observing both the discharges scatter plots, it turns out that the correlation between discharge data is poor, probably due to the fact the H-ADCP river gauge was not completely submerged during this event (Figure 82 and 83).

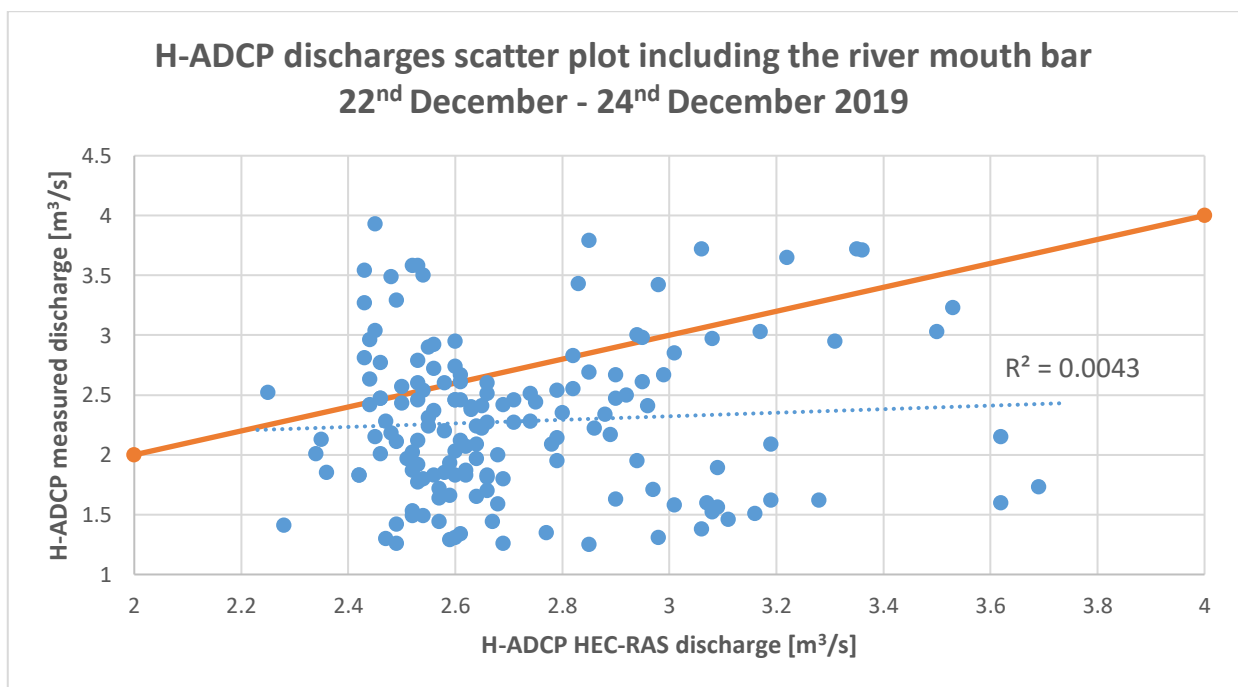


Figure 82. H-ADCP discharges scatter plot including the river mouth bar for the 22nd December – 24th December 2019 event

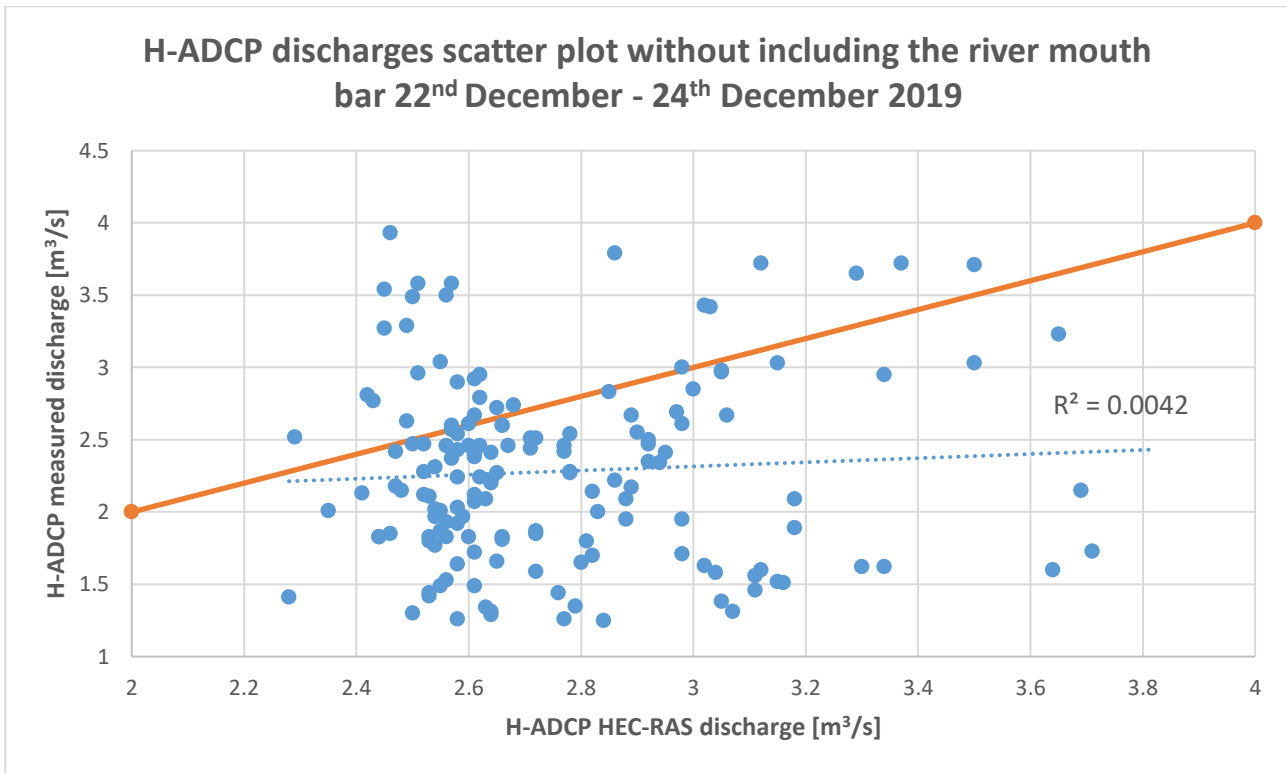


Figure 83. H-ADCP discharges scatter plot without including the river mouth bar for the 22nd December – 24th December 2019 event

As a reference, a photograph dating back to 2nd January 2020 showing an emerged bar owning a limited extension is reported in Figure 84.

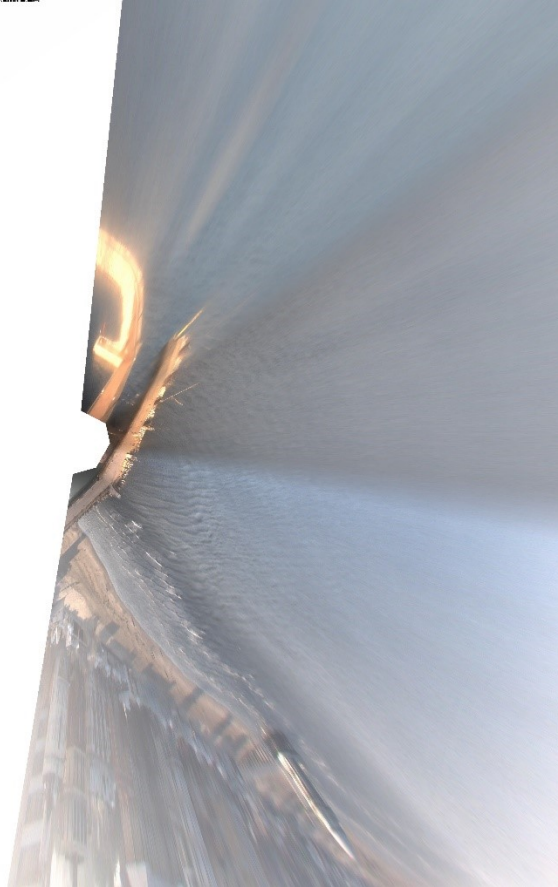


Figure 84. The Misa River mouth photograph taken by the SGS station on 2nd January 2020

HEC-RAS Mapper simulation result for this event illustrates a wider portion of the sandbar which is emerged because of the low river discharges approaching the river mouth (Figure 85).

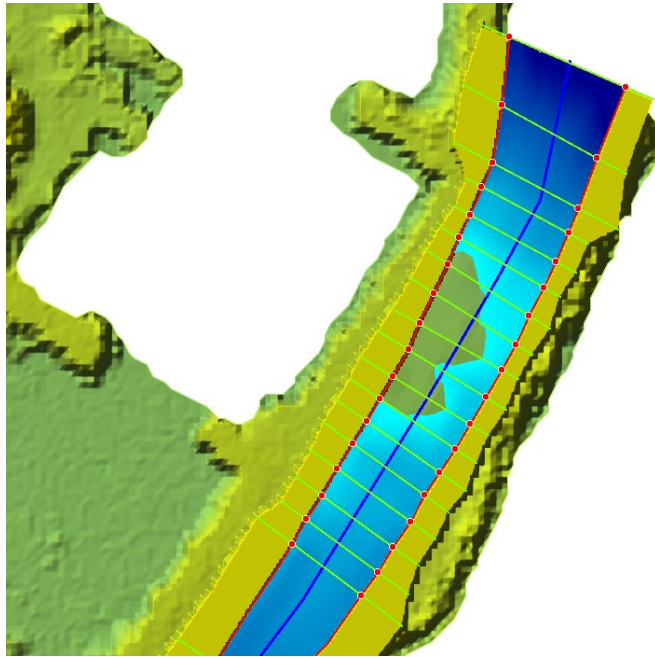


Figure 85. HEC-RAS Mapper simulation results displaying the river mouth bar under minimum flow conditions for the 22nd December –24th December 2019 event

3.3.2 2020 events

Following the analysis of the 2019 events, two events have been simulated for the 2020 year with the difference that tides measured by a tide gauge placed in Senigallia harbour have been employed. The first one concerns a time period which goes from the 27th March 2020 at 3:30 to 29th March 2020 at 23:30. In this event, the peak of the hydrograph is the zone where a better matching between the HEC-RAS stages and the Bettollelle SIRMIP ones exists when including the river mouth bar (Figure 86). On the other way around, the remaining portions of the hydrograph are characterized by a stage overestimation of maximum 10 cm.

When the river mouth bar is not included in the HEC-RAS model, the behaviour is the opposite of the case with the bar, thus, with a worse correspondence at the hydrograph peak and a better one in the remainder.

So, when lower discharges occur, the bar effect is felt less in the stages upstream of the bar, whereas at high discharges, the bar leads to higher stages upriver that overlap to the SIRMIP ones.

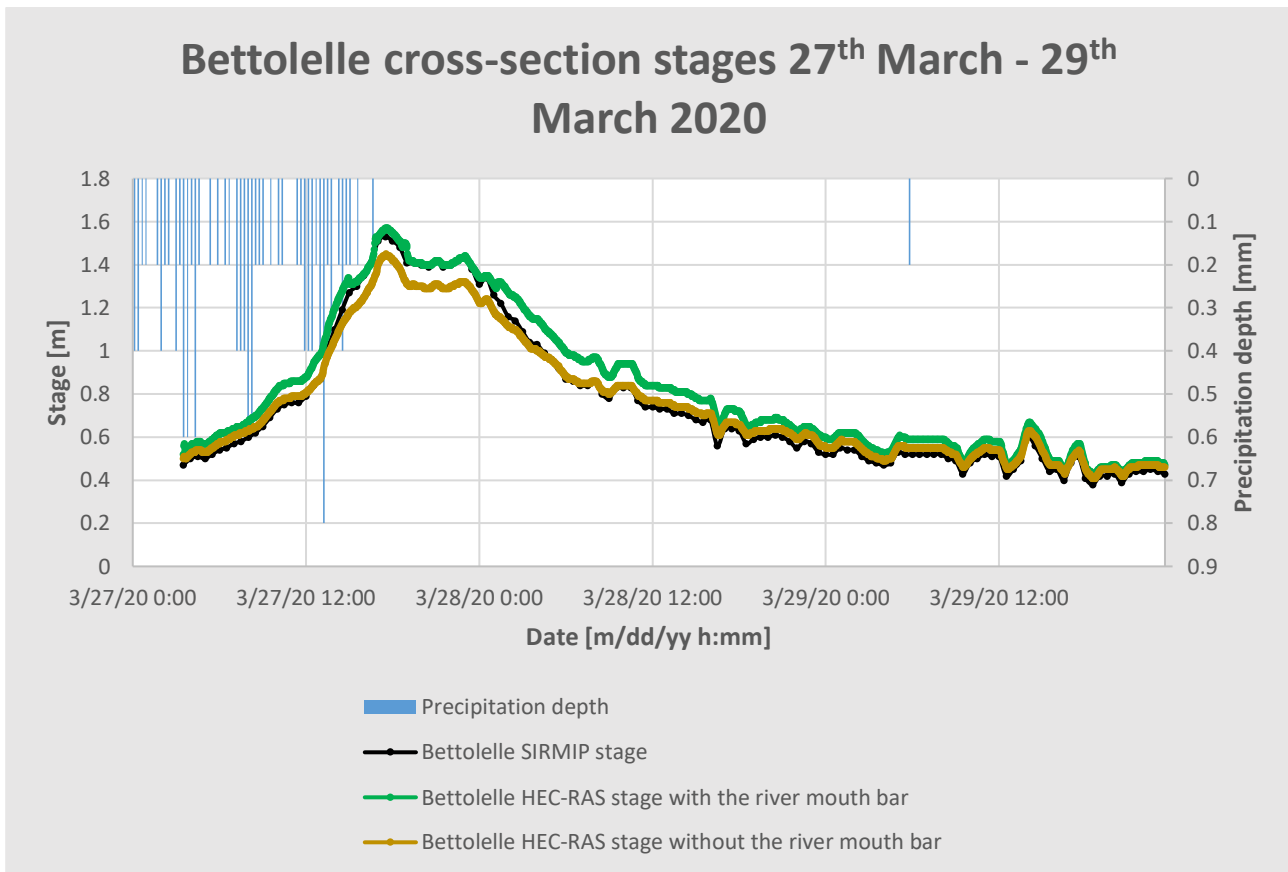


Figure 86. Simulation results at Bettolle cross-section for the 27th March – 29th March 2020 event

For what concerns the H-ADCP cross-section, the stages series that most approaches the one including the H-ADCP measured stages has been obtained by including the river mouth bar in the HEC-RAS model, thus confirming the presence of an emerged river mouth bar in correspondence of this event (Figure 87). The gap between these two stages is around 10 cm and can be due to the contribution of the runoff downstream of Bettolle, which is not considered in both HEC-RAS stages series. Besides, the dam effect exerted by the emerged bar prevails over the tide effects (measured by the tide gauge located in the Senigallia harbour), as confirmed by the almost total lack of correspondence between river stage and tide-gauge recording. Further, both HEC-RAS stages curves show a discrepancy at the peak zone since high river discharges (up to about 30 m³/s) dominates the tide excursions, whereas a good correlation of trends is found for lower discharges.

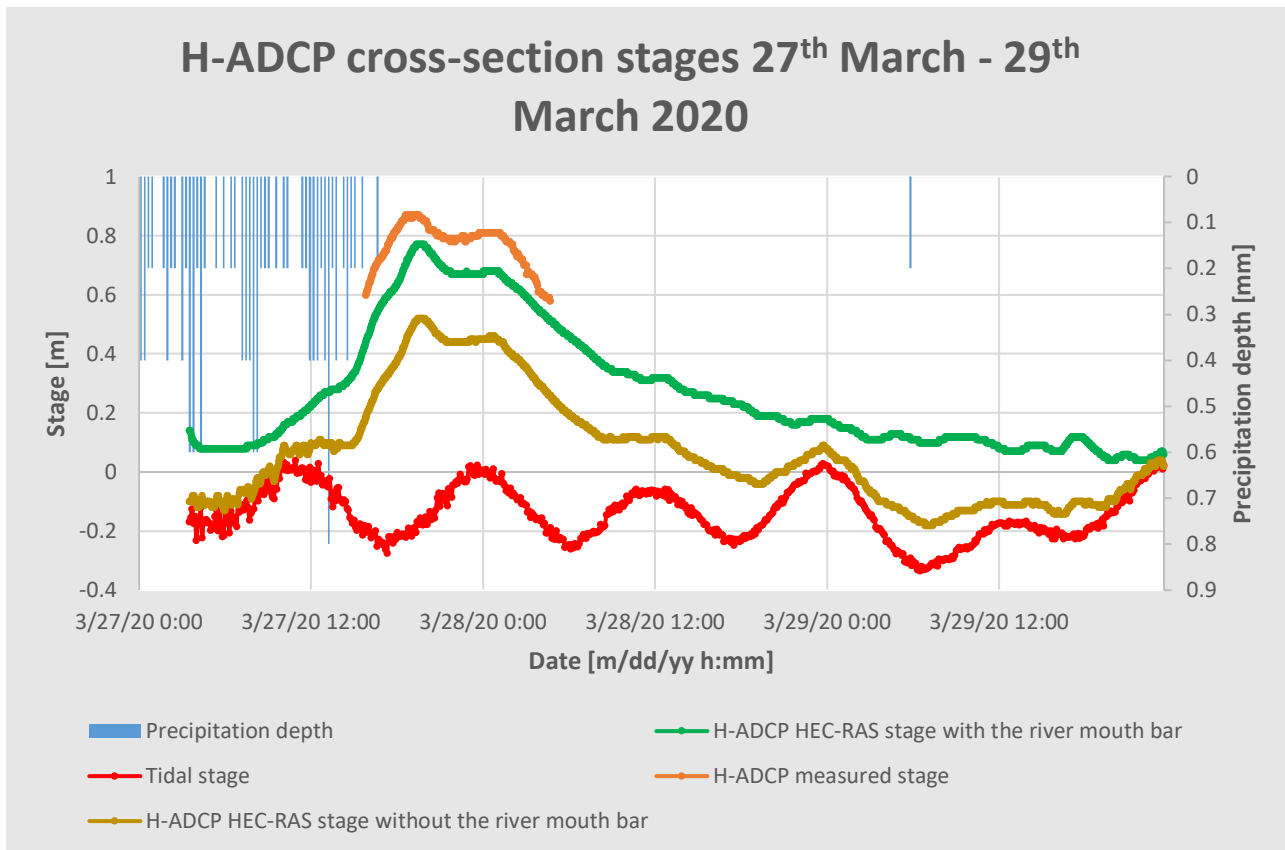


Figure 87. Simulation results at H-ADCP cross-section for the 27th March – 29th March 2020 event

In order to understand the variation of backwater occurring upstream of the river mouth bar, the HEC-RAS river profile downstream of the river mouth bar has been investigated: specifically, the last cross-section of the profile has been removed. As a result, a negligible difference of stages has turned out as shown in correspondence of the H-ADCP cross-section (Figure 88), hence, the variation in terms of stages is mainly attributed to the river mouth bar morphology.

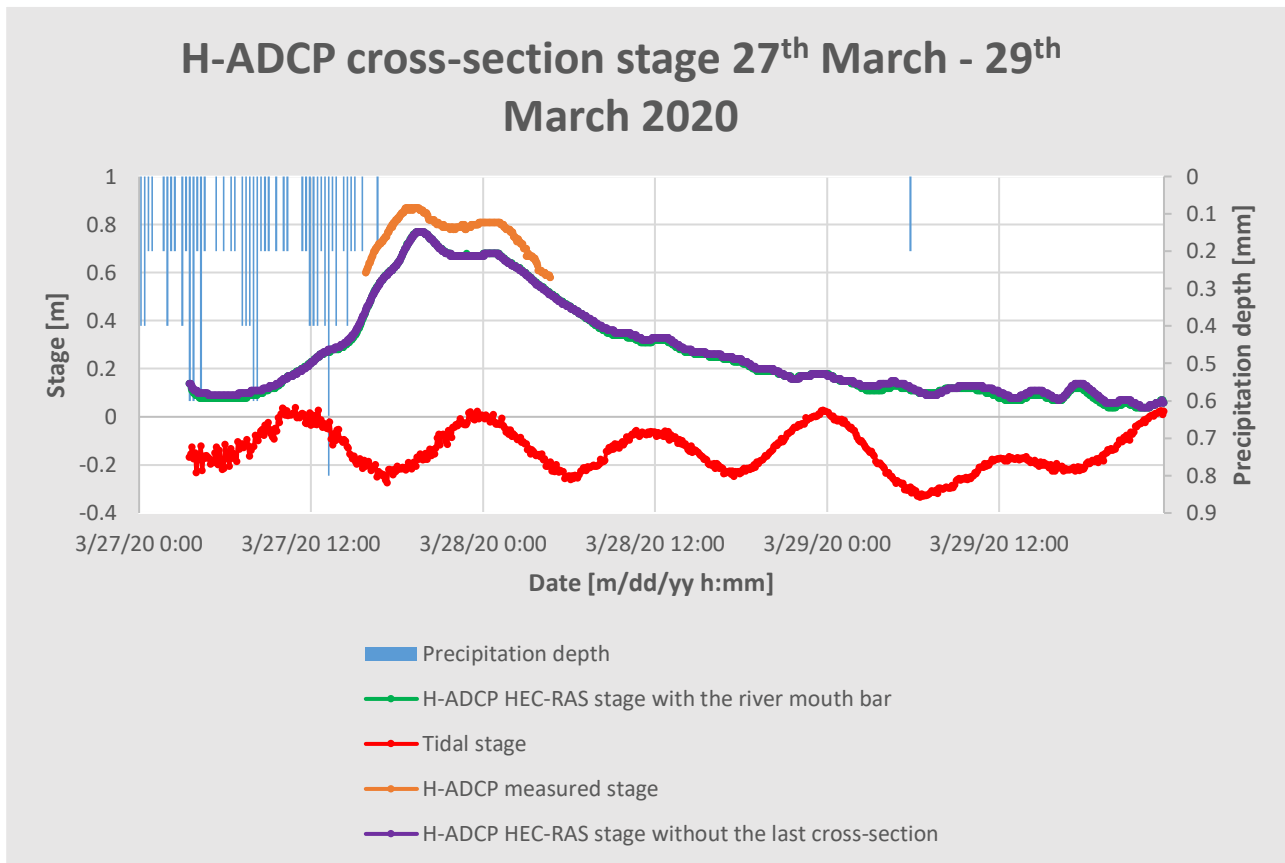


Figure 88. Simulation results at H-ADCP cross-section for the 27th March – 29th March 2020 event

By comparing the Ponte Garibaldi stages with the HEC-RAS results obtained including the river mouth bar, a good matching is observed before the hydrograph flood peak occurrence followed by an overestimation of stages onward (Figure 89). this trend may be due to the fact that the peak discharge dating back to the 27th of March at 17:30 has managed to erode the river mouth bar, thus reducing its height, and to drag it downriver. This is in agreement with the quite good matching between the Ponte Garibaldi SIRMIP stages series and the HEC-RAS one without including the bar in the descending part of the hydrograph. The consideration that has been made for tides at the H-ADCP cross-section is valid for Ponte Garibaldi one as well.

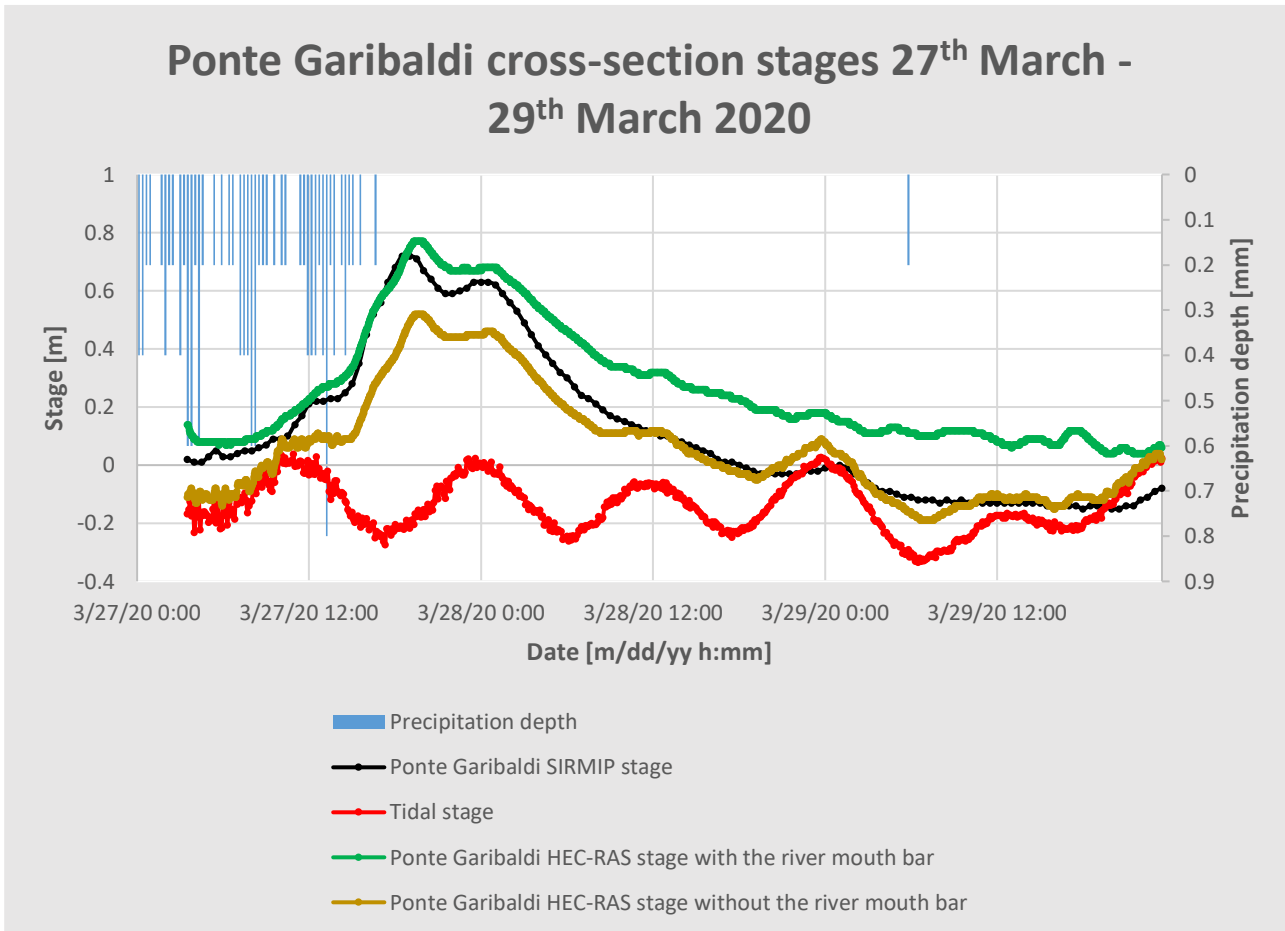


Figure 89. Simulation results at Ponte Garibaldi cross-section for the 27th March – 29th March 2020 event

Given the fact that the H-ADCP river gauge provided discharge outliers for the 27th March – 29th March 2020 event, the latter has been filtered out, even though the data analysis has shown a significant overestimation between the H-ADCP measured data and both simulations. However, the trend seems to be almost the same, hence the existing gap may be brought on by runoff contribution as well as some uncontrolled dumping that are discharged along the river (Figure 90).

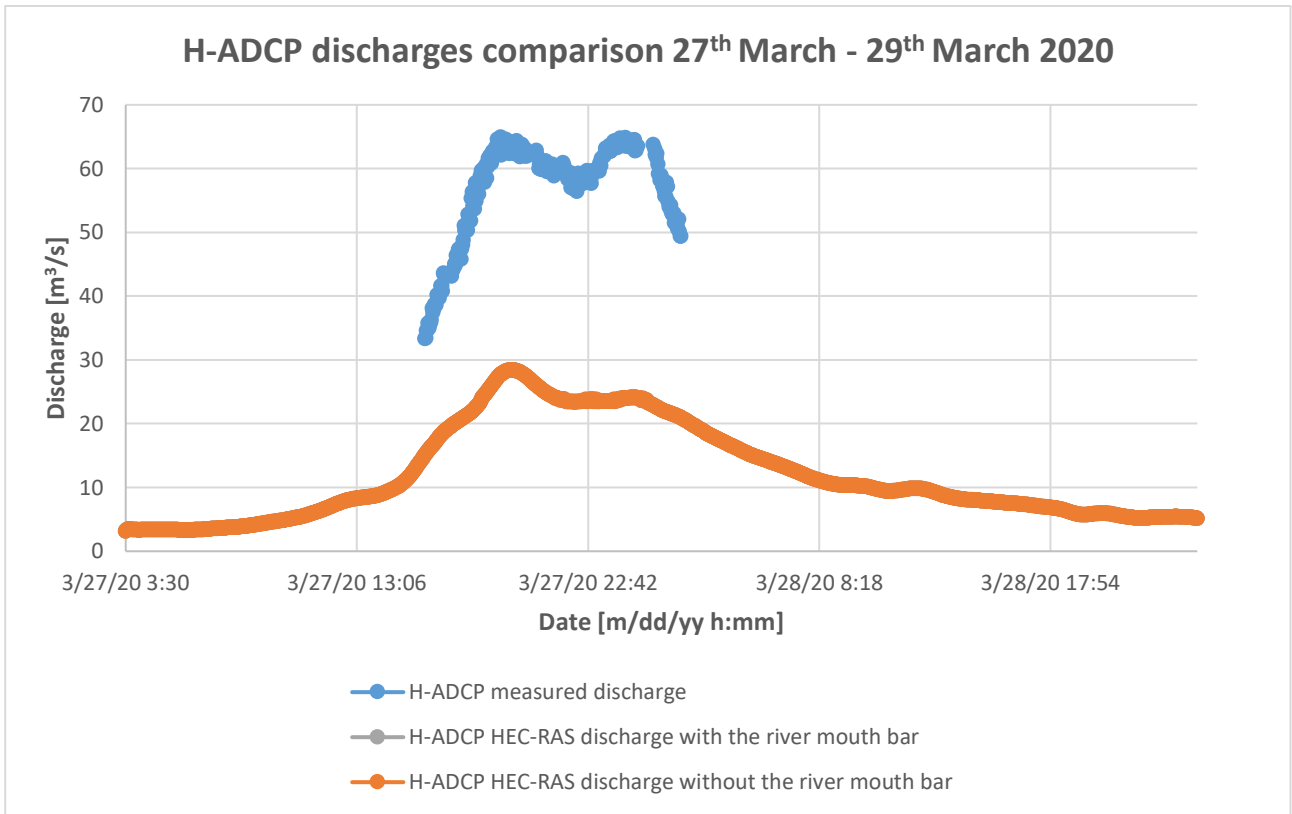


Figure 90. H-ADCP discharges comparison for the 27th March – 29th March 2020 event

The same is confirmed by looking at both the H-ADCP discharges scatter plot, where, additionally, R^2 confirms a good linear trend between simulated and recorded data (Figure 91 and 92).

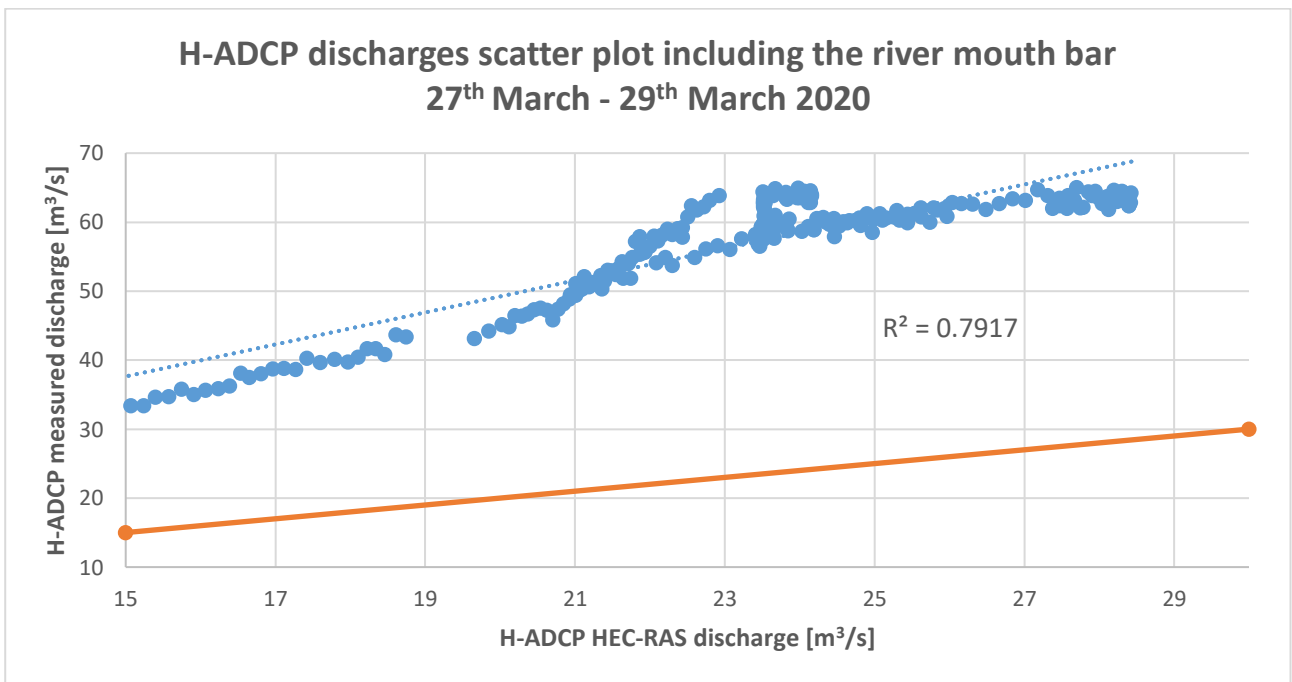


Figure 91. H-ADCP discharges scatter plot including the river mouth bar for the 27th March – 29th March 2020 event

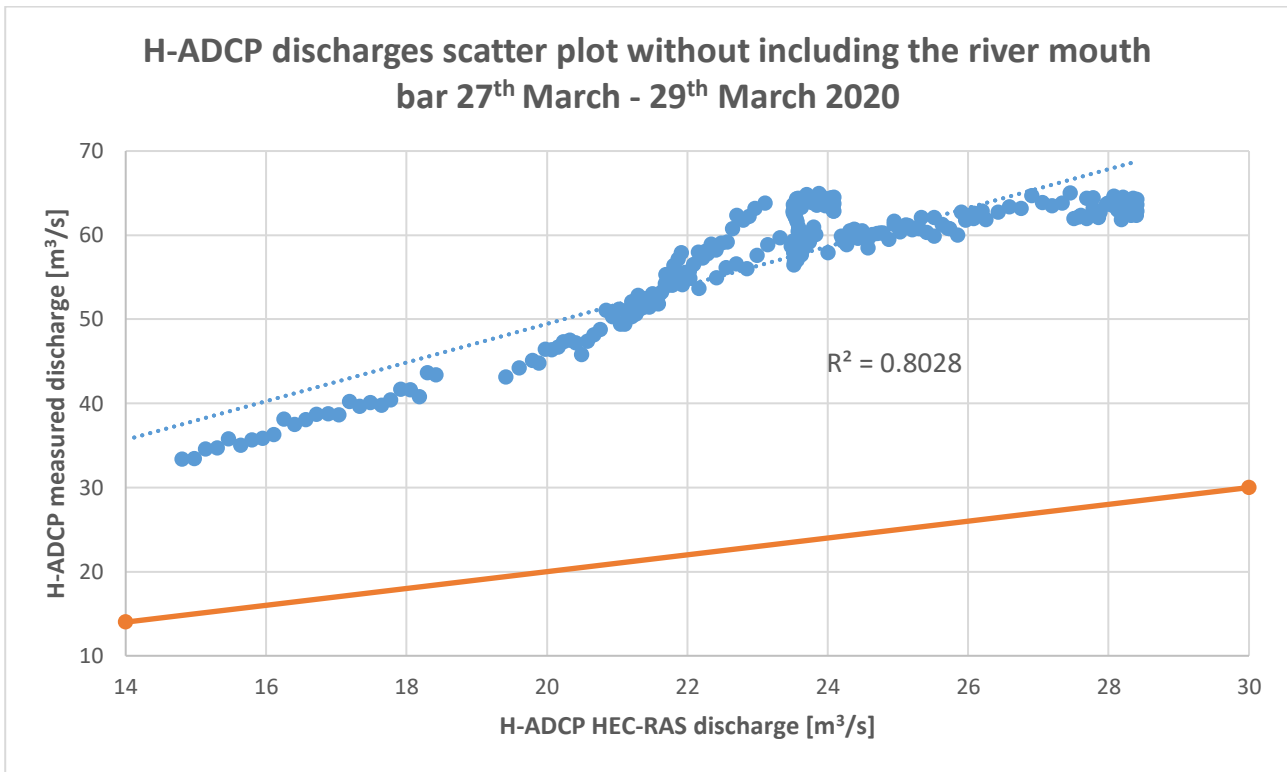


Figure 92. H-ADCP discharges scatter plot without including the river mouth bar for the 27th March – 29th March 2020 event

A photograph taken by the SGS video monitoring station the 20th March 2020 (i.e., a few days before the beginning of the considered event) gives the idea about the river mouth bar shape and extension (Figure 93): in particular the river mouth bar seems to appear emergent and rather extensive.

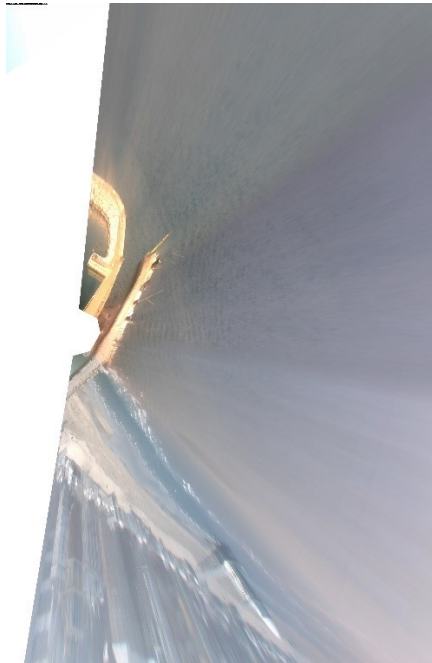


Figure 93. The Misa River mouth photograph taken by the SGS station on 20th March 2020

This river mouth bar morphology is displayed with a good approximation in the HEC-RAS Mapper results considering the minimum water level for the considered event (Figure 94).

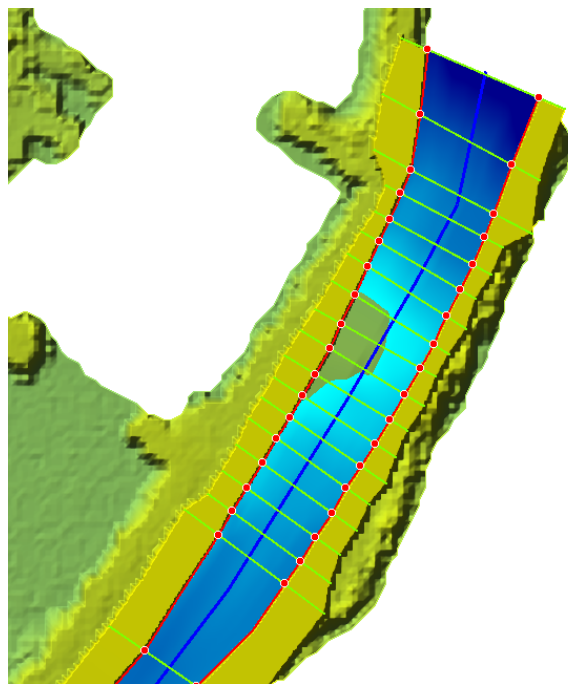


Figure 94. HEC-RAS Mapper simulation results displaying the river mouth bar under minimum flow conditions for the 27th March –29th March 2020 event

Always within the 2020 year, another event has been studied, which starts on 27th December 2020 at 00:00 and ends up on 31st December 2020 at 23:30. Also for this event, at Bettollelle cross-section the HEC-RAS stage series (with the addition of the river mouth bar) is always higher than the curve related to the SIRMIP measured stages, whereas an almost perfect overlapping is exhibited when considering the HEC-RAS simulation without the river mouth bar except for the peak zone where the difference in stages is increased (Figure 95).

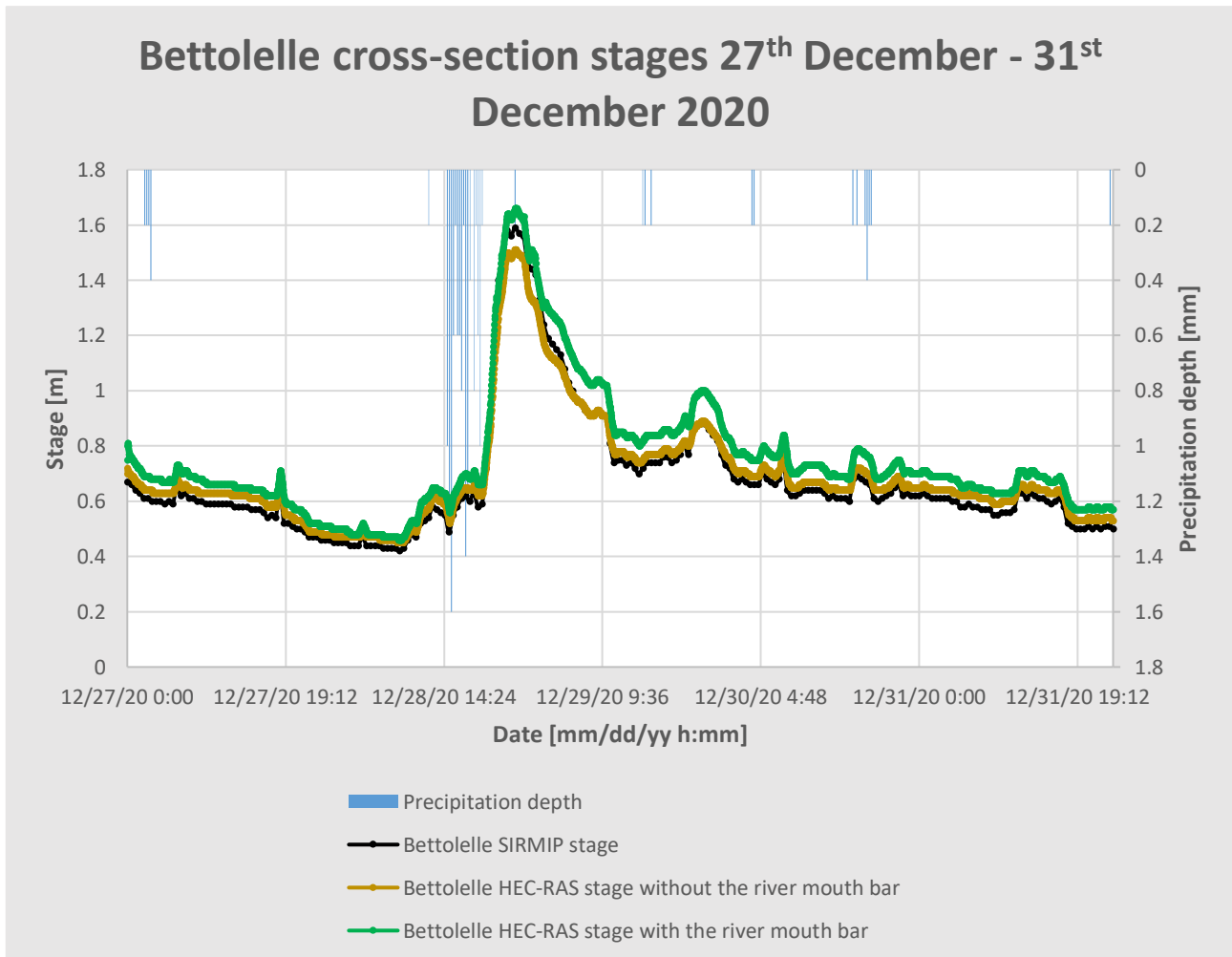


Figure 95. Simulation results at Bettollelle cross-section for the 27th December – 31st December 2020 event

From the H-ADCP measured stages, it turns out that the HEC-RAS curve that better approaches this series is that linked to the presence of the river mouth bar (with a difference of maximum 10 cm), while a higher gap is observed without considering the river mouth bar (Figure 96). Moreover, the green curve seems to overlap to the tidal stage one when high positive tides occur, whereas a significant overestimation of stages takes place in case of negative tides. While in the former case, the river bar effect is almost negligible, the high difference in terms of stages is due to the

backwater created by both the river mouth bar presence at negative tides occurrence, and the high discharges (in the hydrograph peak) that prevails over tides.

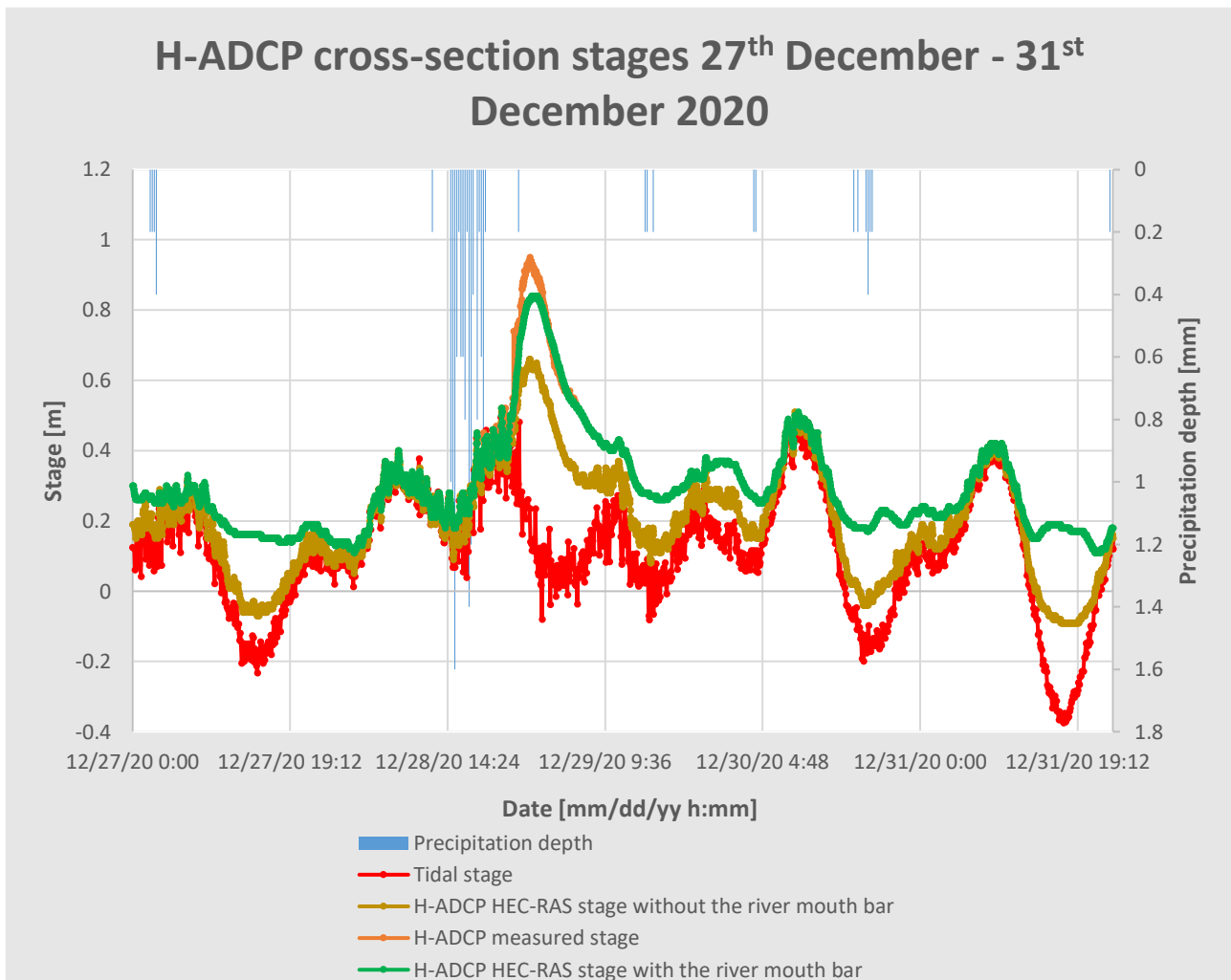


Figure 96. Simulation results at H-ADCP cross-section for the 27th December – 31st December 2020 event

The same is observed at Ponte Garibaldi cross-section, even though the HEC-RAS stage series comprising of the bar overlaps to the Ponte Garibaldi hydrometer one in correspondence of the main peak zone (Figure 97). Discrepancies exist between the HEC-RAS stages with the bar (solid green line) and SIRMIP measured stages (solid black line) in all the stage hydrograph except for the peak. This behaviour could be addressed to presence of the bar, which acts as a barrier towards the river flow, thus increasing the stages upstream of the bar itself. On the other hand, the presence of the bar allows for a better correspondence between simulated and measured stages in the peak.

Conversely, the absence of the bar gives back an underestimation of stages in correspondence of the peak, but a greater general matching. This behaviour can imply the presence of a not emerged bar in correspondence of this period of time although a submerged sediment deposit probably existed.

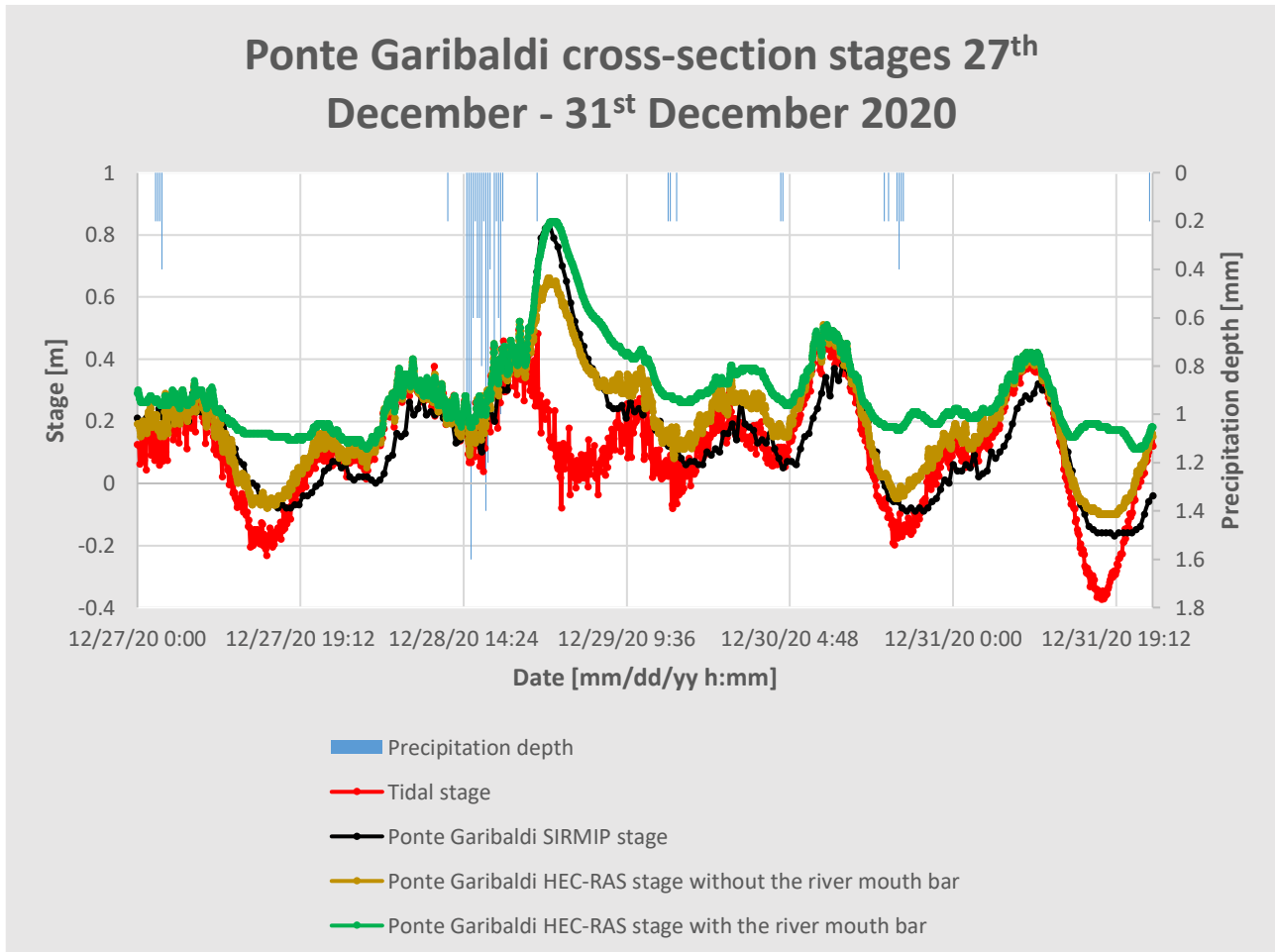


Figure 97. Simulation results at Ponte Garibaldi cross-section for the 27th December – 31st December 2020 event

Once again, the H-ADCP river gauge provided a discharge data series, which, resembles the HEC-RAS finding, although much larger than around the peak (Figure 98). This is also visible considering both the discharges scatter plots (Figure 99 and 100), in which determination coefficients R^2 close to 1 highlight the already observed linear trend between the simulated and recorded data.

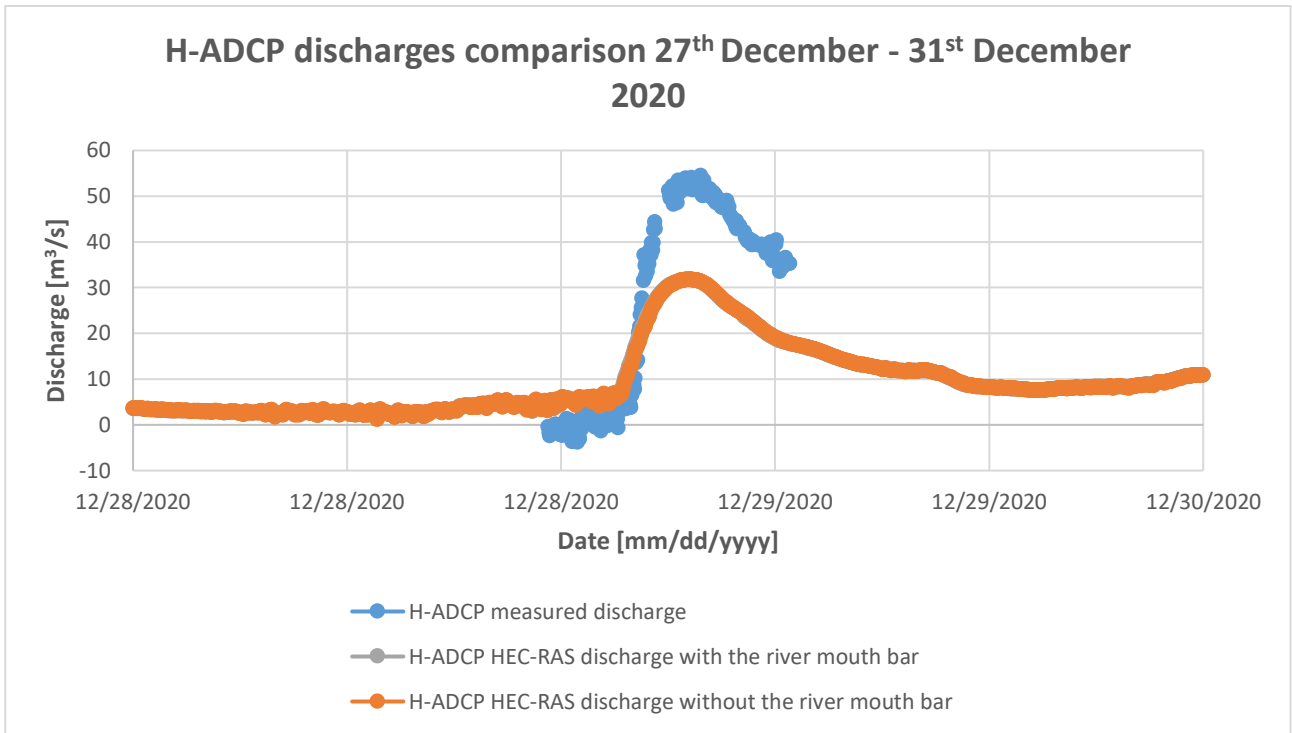


Figure 98. H-ADCP discharges comparison for the 27th December – 31st December 2020 event

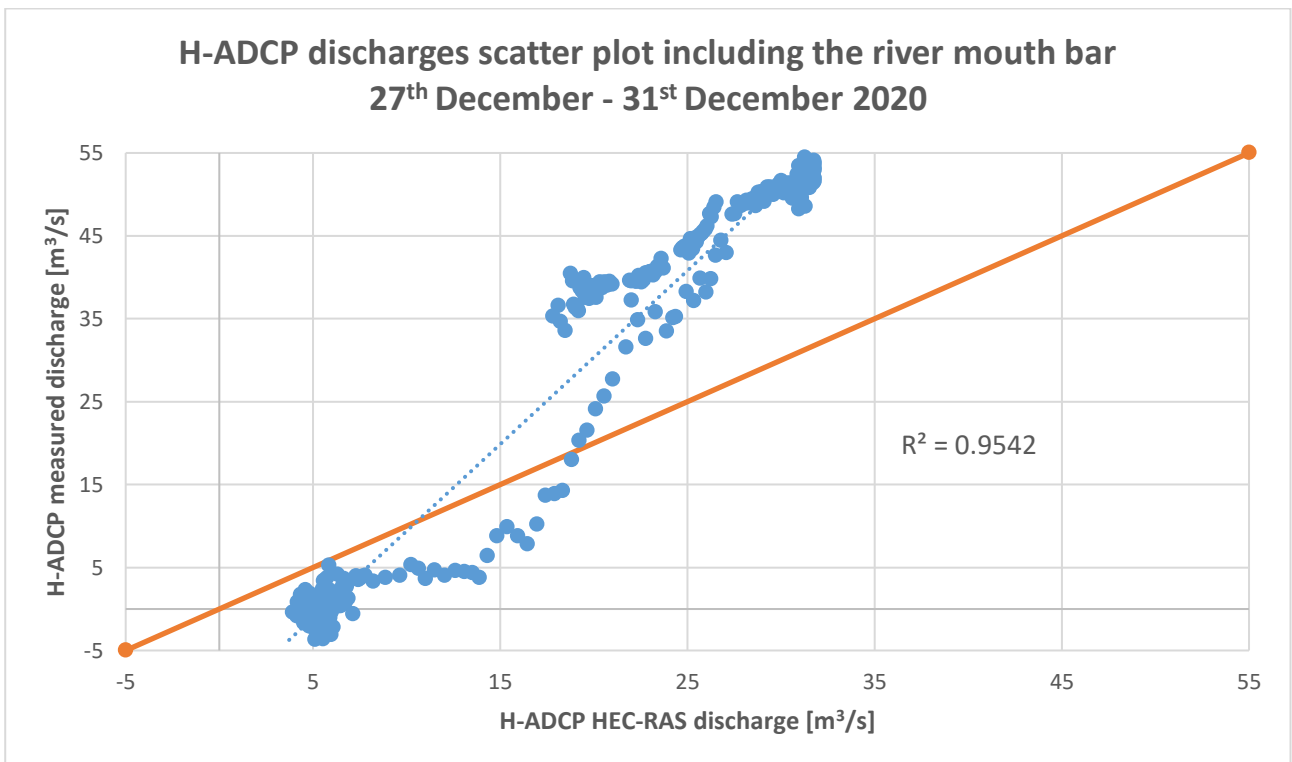


Figure 99. H-ADCP discharges scatter plot including the river mouth bar for the 27th December – 31st December 2020 event

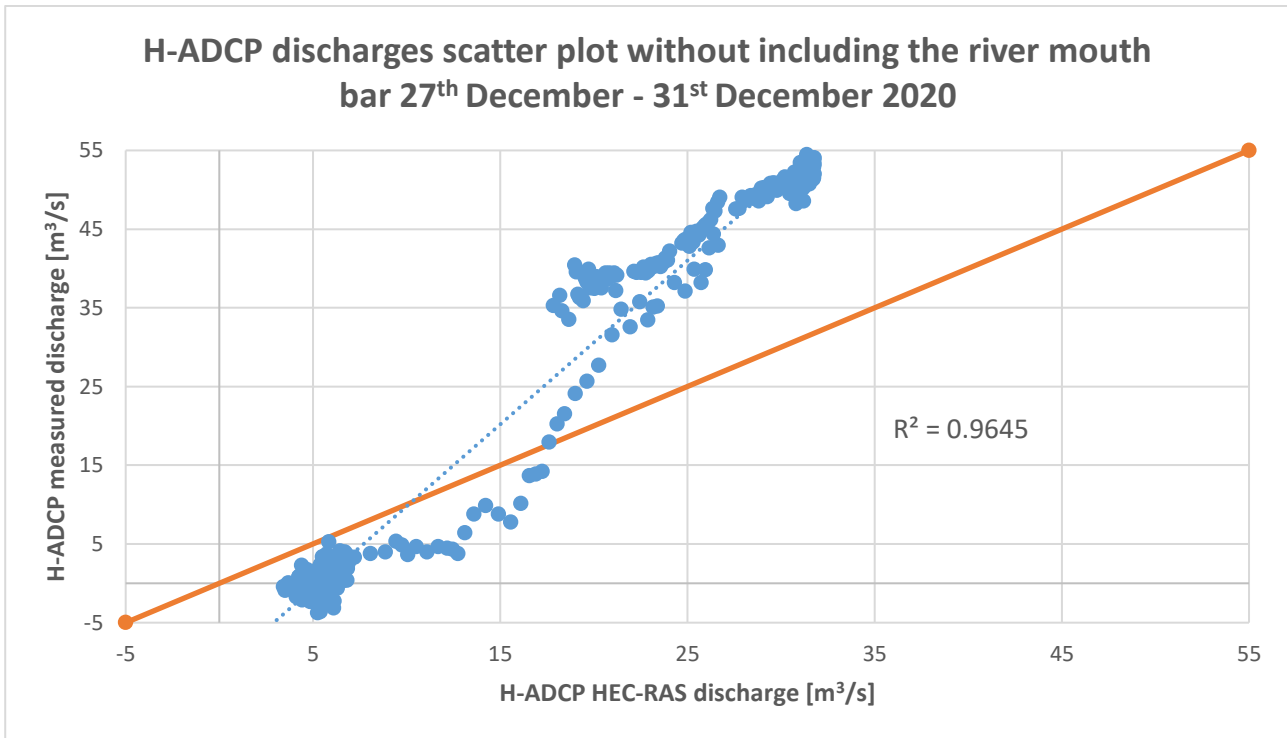


Figure 100. H-ADCP discharges scatter plot without including the river mouth bar for the 27th December – 31st December 2020 event

From 9th December 2020 onward, no photograph has been taken by the SGS video monitoring station. However, the river mouth bar was probably submerged with still a submerged accumulation of sediment.

Figure 101 displays the emerging portion of the river mouth bar considering the minimum water level for the considered event.

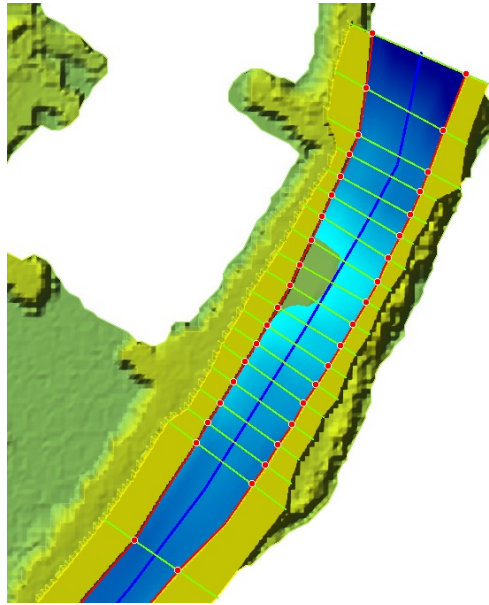


Figure 101. HEC-RAS Mapper simulation results displaying the river mouth bar under minimum flow conditions for the 27th December – 31st December 2020 event

The last event to be analysed occurred in 2021, in particular from 10th January 2021 at 8:30 to 13th January 2021 at 23:30. For this event, no H-ADCP data (stage and discharge values) are available since the river gauge was not completely submerged, thus providing distorted data. Therefore, a comparison between HEC-RAS stage series (considering the presence and the absence of the river mouth bar) has been carried out with the SIRMIP measured stage series for both Bettollelle and Ponte Garibaldi cross-section.

At Bettollelle cross-section, the HEC-RAS stage curve (including the river mouth bar) is always higher than the SIRMIP one, especially in the decreasing part of the main hydrograph, whereas this difference is almost null in the peak (Figure 102). The same occurs also when the bar is not modeled, except for an underestimation of the stages that occurs in correspondence of the peak.

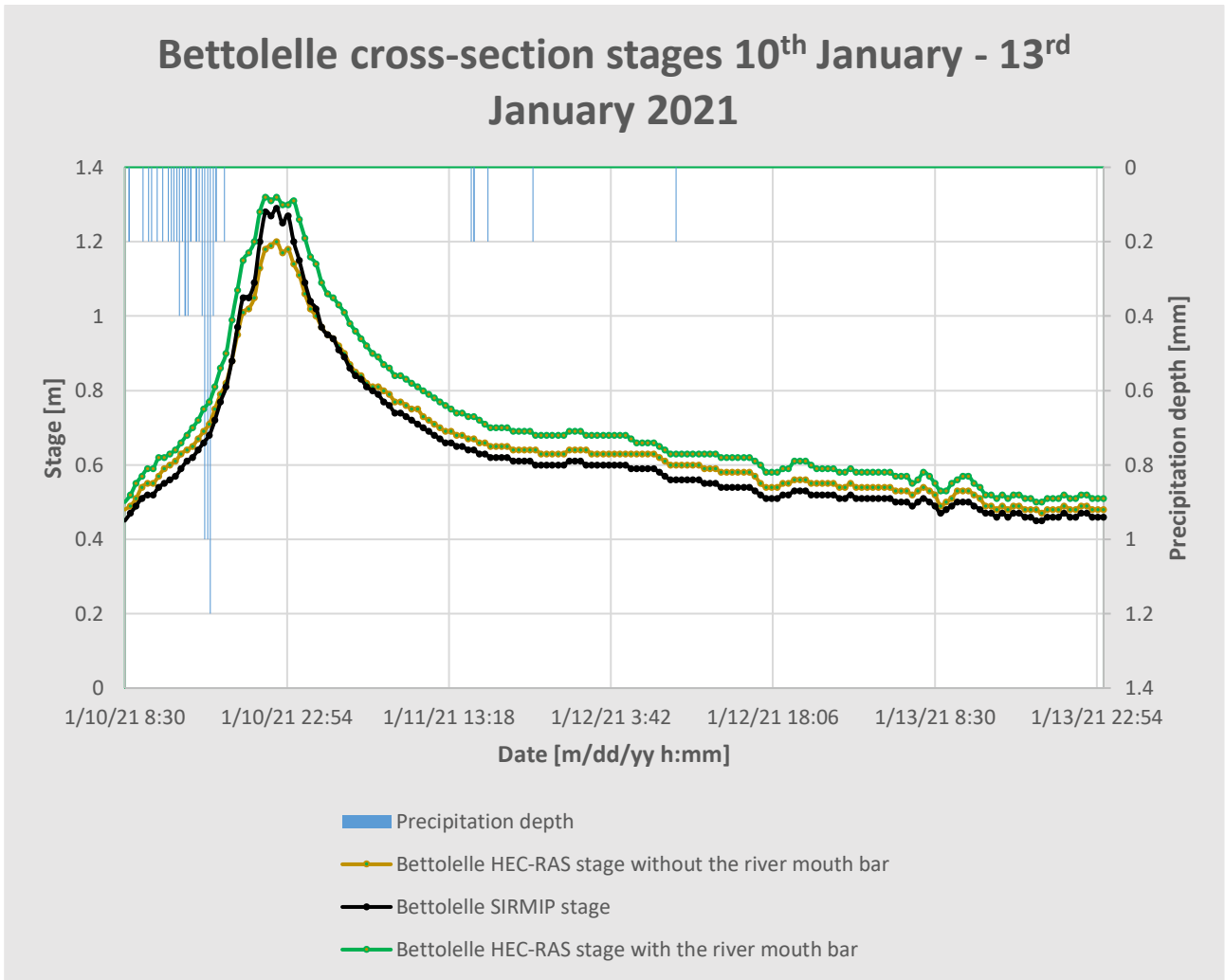


Figure 102. Simulation results at Bettollelle cross-section for the 10th January – 13rd January 2021 event

For what concerns the latter, the HEC-RAS stages curve where the bar is not included is the one that better matches the SIRMIP curve until 12th January 2021, particularly when lower stages (i.e., lower discharges) occur (Figure 103). On the other hand, the HEC-RAS stage curves are close each other in correspondence of higher stages and overestimate the stages after 12th January 2021.

Ponte Garibaldi cross-section stages 10th January - 13rd January 2021

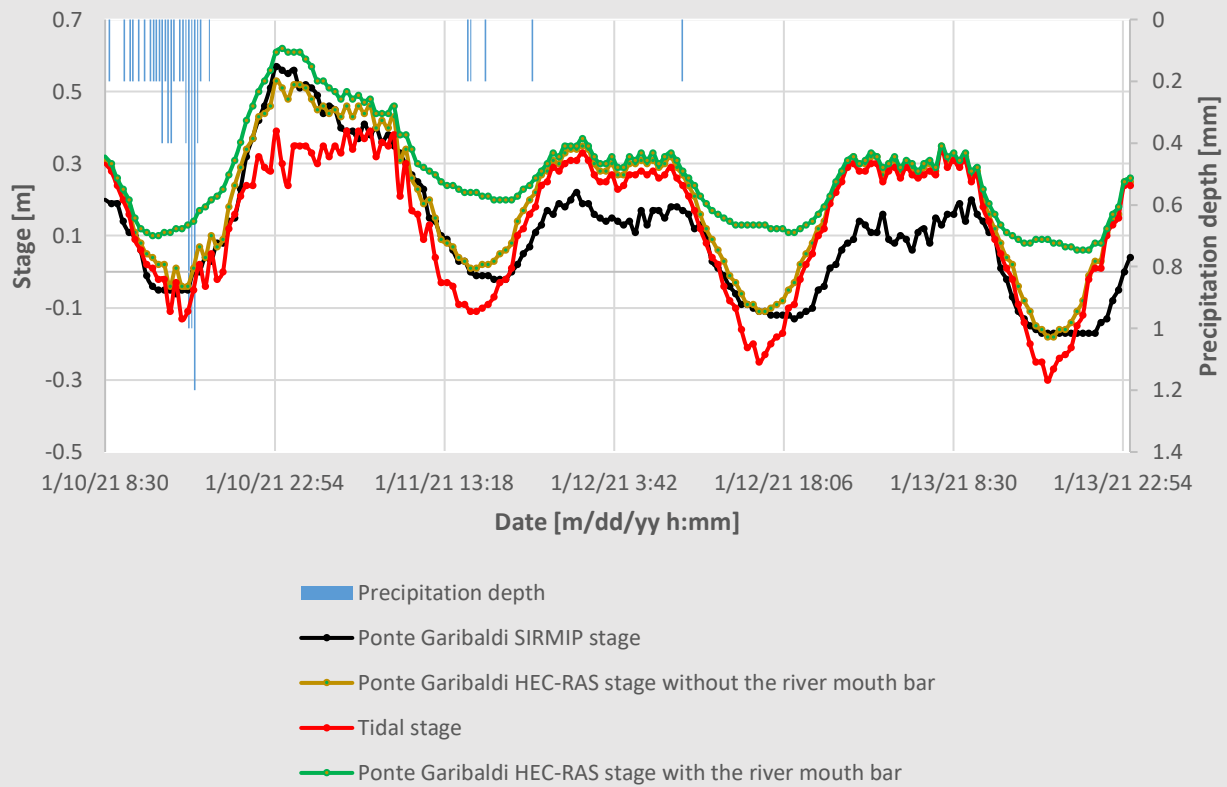


Figure 103. Simulation results at Ponte Garibaldi cross-section for the 10th January – 13rd January 2021 event

Figure 104 shows the minimum water height for the 2021 event, in which no portion of the river mouth bar results to be emerged.

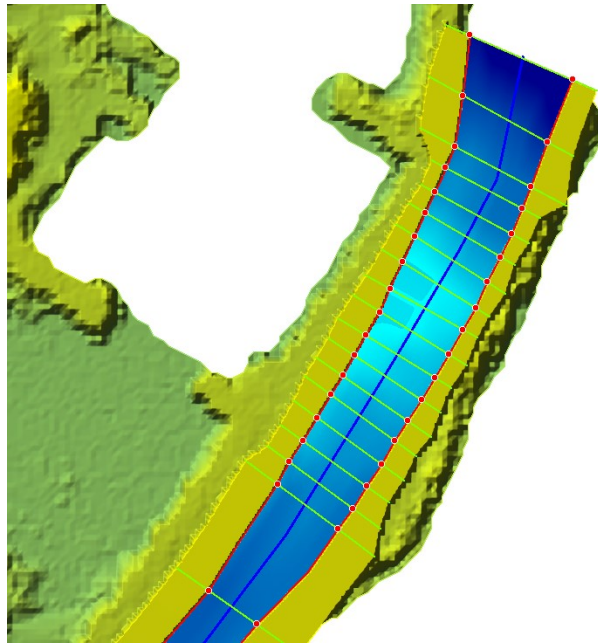


Figure 104. HEC-RAS Mapper simulation results displaying the river mouth bar under minimum flow conditions for the 10th January – 13rd January 2021 event

4 CONCLUSIONS

This thesis has attempted to look into and give answers to the influence of the sea and the riverbed patterns on the hydrodynamic modelling of the final stretch of the Misa River. As regards the characterization of estuaries as well as river bars, which are the result of the different hydrodynamic processes occurring in this environment, it turned out that microtidal environments, like the Misa River estuary, may lead to the generation of features, like river-mouth bars, whose geometry varies according to river discharge, tide and sea waves. Unsteady simulations have been performed using the HEC-RAS software and modelling the Misa River between the location of Bettolle (about 10 km from the estuary) and the river mouth. After the model calibration, the comparison between simulated stages and water elevations recorded during the EsCoSed field campaign has revealed a good correspondence in terms of trends, and the tide has been seen to propagate up to a distance from the mouth of 1.8 km even though translated of a certain amount due to tide gauges shifting as a result of a significant sea storm. A further comparison has been made between the stages measured by both Bettolle and Ponte Garibaldi hydrometers, and those modeled with and without the river mouth bar. The outcomes have pointed out that at low discharges and high tidal stages, the bar effect in terms of backwater is negligible in the upstream locations, whereas this effect is remarkable for high discharges and low tidal stages. Moreover, in the framework of the MORSE project, from the collection of the data supplied by the river gauge and following the removal of outliers for each of the considered events, an overall good matching in terms of stages has been found out. Conversely, a weaker comparison in terms of discharge values has been obtained, probably because of: i) the lack of runoff contribution between Bettolle and Ponte Garibaldi in the simulations, and ii) a rating curve does not properly represent high stage values.

5 REFERENCES

Maurizio Brocchini, Joseph Calantoni, Matteo Postacchini, Alex Sheremet, Tracy Staples, Joseph Smith, Allen H. Reed, Edward F. Braithwaite III, Carlo Lorenzoni, Aniello Russo, Sara Corvaro, Alessandro Mancinelli, Luciano Soldini. *Comparison between the wintertime and summertime dynamics of the Misa River estuary. Marine Geology 385 (2017) 27-40.*

Lorenzo Melito, Matteo Postacchini, Alex Sheremet, Joseph Calantoni, Gianluca Zitti, Giovanna Darvini, Pierluigi Penna, Maurizio Brocchini. *Hydrodynamics at a microtidal inlet: Analysis of propagation of the main wave components. Estuarine, Coastal and Shelf Science 235 (2020) 106603.*

Matteo Postacchini, Lorenzo Melito, Alex Sheremet, Joseph Calantoni, Giovanna Darvini, Sara Corvaro, Francesco Memmola, Pierluigi Penna, Maurizio Brocchini. *Upstream Propagating Long-Wave Modes at a Microtidal River Mouth. Environmental Sciences Proceedings (Published: 11 August 2011).*

Alessandra Crosato, Erik Mosselman. *An Integrated Review of River Bars Engineering, Management and Transdisciplinary Research. Water (Published: 21 February 2020).*

Sergio Fagherazzi, Douglas A. Edmonds, William Nardin, Nicoletta Leonardi, Alberto Canestrelli, Federico Falcini, Douglas J. Jerolmack, Giulio Mariotti, Joel C. Rowland, Rudy L. Slingerland. *Dynamics of river mouth deposits. AGU Publications (Published: 25 July 2015).*

Xiaodong Zhang, Daidu Fan, Zuosheng Yang, Shumei Xu, Wanqing Chi, Hongmin Wang. *Sustained growth of river-mouth bars in the vulnerable Changjiang Delta. Journal of Hydrology 590 (2020) 125450.*

Lorenzo Melito, Luca Parlagreco, Eleonora Perugini, Matteo Postacchini, Saverio Devoti, Luciano Soldini, Gianluca Zitti, Luca Liberti, Maurizio Brocchini. *Sandbar dynamics in microtidal*

environments: Migration patterns in unprotected and bounded beaches. Coastal Engineering 161 (2020) 103768.

Richard M. Warwick, James R. Tweedley, Ian C. Potter. *Microtidal estuaries warrant special management measures that recognise their critical vulnerability to pollution and climate change. Marine Pollution Bulletin 135 (2018) 41-46.*

Consorzio di Bonifica delle Marche. *Relazione bacino idrografico del fiume Misa. Dicembre 2019.*

Validazione Strumenti MORSE – River Gauge.

Il progetto MORSE a Senigallia: monitoraggio di lungo periodo della zona costiera-estuarina-fluviale. Newsletter Bimestrale Cluster BIG (8-10).

MORSE Project. Università Politecnica delle Marche and the U.S. Naval Research Laboratory.

Alessandra Crosato, Arthur Mynett, W. S. J. Uijttewaal, Meles S. Tewolde. *Effect of suspended sediments on river bars. June 2015.*

Bar (river morphology). WIKIPEDIA The Free Encyclopedia.

Jacopo Martinelli. *Hydrodynamic modeling of the final reach of the Misa River (Senigallia, Italy): model setup and calibration. A.A 2020/2021 Università Politecnica delle Marche.*

Laura Anitori. *Analysis of the Misa River watershed and numerical simulations of the river hydrodynamics during low- and high-flow conditions. A.A 2018/2019 Università Politecnica delle Marche.*

Regione Marche – Servizio Protezione Civile SIRMIP ON-LINE *Regione Marche - Sistema Informativo Regionale Meteo-Idro-Pluviometrico.* <http://app.protezionecivile.marche.it/sol/indexjs.php?lang=it>

US Army Corps of Engineers Institute for Water Resources Hydrologic Engineering Center. *HEC-RAS 5.0 User's Manual. Version 5.0 February 2016.*

US Army Corps of Engineers Institute for Water Resources Hydrologic Engineering Center.
Supplemental to HEC-RAS Version 5.0 User's Manual. Version 5.0.4 April 2018.

6 ACKNOWLEDGMENTS

My career as a university student is going to end up after almost 6 years since I have set foot for the first time in the Università Politecnica delle Marche, therefore, it is necessary to take stock of these years. I naturally had a little trouble especially at the beginning of my career, but I got lots of satisfactions, first of all the bachelor's degree obtained in December 2018. Before expressing my gratitude towards all the people have supported me in this long journey, I would like to devote this thesis to my grandfather Sante, who recently passed away and until the last moment he has never stopped spurring me to chase my dreams. So, the first two people that I would like to thank are my parents, i.e., Andrea and Lorella, who have always believed in me and my skills. Furthermore, a special thanks goes to my advisor Matteo Postacchini as well as my two co-advisors, i.e., Giovanna Darvini and Eleonora Perugini for the tips and the endorsement provided during these months. Among my university colleagues, I must thank Jacopo, with whom I shared all the work done to realize this thesis and I have a great relationship, as well as my other university colleagues. Moreover, I would like to thank my friends, including Michele (the human compass), Daniele (my personal IG manager), Antil (the Monarch), Margherita (the Monarch's wife), and Tronchetz (the King of the woods). The other group of friends that I would like to express my thanks comprises of Leonardo Staffo, Carla, Agnese, Luca, Sara, Leo Seba, Leo Gale, Caterina, Ugo e Serra. Finally, I would like to express my gratitude for the cooperation I have received with Viva Servizi S.p.A and in particular with its referent Maurizio Pieroni for supplying effluent discharge data of Senigallia wastewater treatment plant, with the Marche Civil Protection and their referents for the provision of Bettolle and Ponte Garibaldi data. A special word of thanks goes also to the EsCoSed project for providing data concerning the 2014 field campaign analysis within the Misa River estuary, and to the MORSE project for the supply of the H-ADCP river gauge data.